Improved Mitochondrial Stress Response in Long-Lived Snell Dwarf Mice

by

Varol Ulaş Özkurede

A dissertation submitted in partial fulfillment
of the requirements for the degree of
Doctor of Philosophy
(Molecular and Cellular Pathology)
in the University of Michigan
2018

Doctoral Committee:

Professor Richard A. Miller, Chair
Assistant Professor Michael Bachman
Professor Gregory Dressler
Associate Professor David O. Ferguson
Professor Jiandie Lin

V. Ulaş Özkurede

ozkurede@umich.edu

ORCID ID: 0000-0002-9058-2168

DEDICATION

To my grandfathers:

Bekir Soner,

who taught me the virtue of assiduousness

&

Mehmet Özkurede,

who taught me the virtue of integrity

TABLE OF CONTENTS

LIST OF FIGURES

LIST OF TABLES

LIST OF ABBREVIATIONS

ACTH	Adrenocorticotropic hormone
ADP	Adenosine diphosphate
AKT	Protein kinase B
ALKHB	Alpha-ketoglutarate-dependent dioxygenase alkB homolog
AMP	Adenosine monophosphate
ATP	Adenosine triphosphate
ATP6	ATP synthase F_o subunit 6
ATP8	ATP synthase F_o subunit 8
BP	Binding protein
BSA	Bovine serum albumin
CLK	Clock / CDC like kinase
CLPP	Clp protease
COX	Cytochrome c oxidase
CPN	Chaperonin
CR	Calorie restricted
CRH	Corticotropin-releasing hormone
CYTB	Cytochrome b
DAF	Abnormal dauer formation protein
DNA	Deoxyribonucleic acid
ER	Endoplasmic reticulum
ERα	Estrogen receptor alpha
ETC	Electron transport chain
FDA	Food and Drug Administration
FSH	Follicle-stimulating hormone

FTO	Fat mass and obesity associated protein
GH	Growth hormone
GHR	GH receptor
GHRH	GH releasing hormone
GHRHR	GHRH receptor
GnRH	Gonadotropin-releasing hormone
GTP	Guanosine triphosphate
HMG	High mobility group
HSC	Heat shock cognate protein
HSP	Heat shock protein
IGF-1	Insulin-like growth factor 1
IGF-1R	Insulin-like growth factor 1 receptor
IMS	Inter-membrane space
IRS1	Insulin receptor substrate 1
K	1000
kDa	Kilo Dalton
KO	Knock-out
LH	Luteinizing hormone
LONP1	Lon protease homolog, mitochondrial 1
LS	Laron syndrome
m^6A	N^6-methyladenosine
m^6A-CIT	m^6A-mediated cap-independent translation
m^7G	7-methylguanosine
METTL	Methyltransferase like
MPTP	1-methyl-4-phenyl-1,2,3,6-tetrahydropyridine
mRNA	Messenger ribonucleic acid
MSR	Mitochondrial stress response; Mitochondrial unfolded protein response
mtDNA	Mitochondrial DNA
mTOR	Mechanistic target of rapamycin
mTORC	Mechanistic target of rapamycin complex

mtUPR	Mitochondrial unfolded protein response; MSR
MTS	Matrix targeting sequence
NAD^+	Nicotinamide adenine dinucleotide in oxidized form
NADH	Nicotinamide adenine dinucleotide in reduced form
ND	NADH dehydrogenase
nDNA	Nuclear DNA
P_i	Inorganic phosphate group
PAPPA	Pregnancy-associated Plasma Protein A
PDK	Phosphoinositide 3 kinase dependent kinase
PGC-1α	Peroxisome proliferator-activated receptor gamma coactivator 1 alpha
PIT1	Pituitary-specific positive transcription factor 1
PI3K	Phosphoinositide 3 kinase
PKB	Protein kinase B
POLRMT	Mitochondrial ribonucleic acid polymerase
PPAR	Peroxisome proliferator-activated receptor
PRL	Prolactin
PROP1	Homeobox protein prophet of Pit-1
RAPTOR	Regulatory-associated protein of mTOR
RAR	Retinoic acid receptor
RHEB	Ras homolog enriched in brain
RICTOR	Rapamycin-sensitive companion of mTOR
RNA	Ribonucleic acid
ROS	Reactive oxygen species
rRNA	Ribosomal RNA
S6K	Ribosomal protein S6 kinase
SDH	Succinate dehydrogenase
SOD	Superoxide dismutase
TFAM	Mitochondrial transcription factor A
TFB2M	Mitochondrial transcription factor B2
TRH	Thyrotropin-releasing hormone

tRNA	Transfer RNA
Trp	Tryptophan
TRβ	Thyroid hormone receptor
TSC	Tuberous sclerosis complex
TSH	Thyroid-stimulating hormone
UCP	Uncoupler protein
UPR	Unfolded protein response
UTR	Untranslated region
UV	Ultraviolet
WTAP	Wilms tumor-1 associated protein
YTHDF	Yeast 30 kDa homolog domain containing family

Abstract

Upregulation of the mitochondrial unfolded protein response (mtUPR) as a result of alterations in mitochondrial protein stoichiometry has been proposed as a common pathway in longevity. While mtUPR upregulation correlates with lifespan extension in lower organisms, it is not known whether mtUPR is elevated in long-lived mice. We hypothesized that long-lived mutant mouse models would have enhanced mtUPR.

We found that Snell dwarf mice ("Snell mice"), one of the longest-lived mouse models with 30-40% lifespan extension, exhibit augmented mitochondrial stress response. Primary fibroblasts from Snell mice show elevated levels of the mitochondrial chaperone HSP60 and mitochondrial protease LONP1, two components of the mtUPR. In response to mitochondrial stress, the increase in the expression of *Tfam*, a regulator of mitochondrial transcription, is higher in Snell cells, while *Pgc-1α*, the main regulator of mitochondrial biogenesis, is upregulated only in Snell cells. Consistent with these differences, after exposure to mitochondrial stress by doxycycline treatment, oxidative respiration rate and cellular ATP content, indicators of mitochondrial function, are higher in Snell cells than those in normal cells. *In vivo*, Snell mice show robust mtUPR induction after mitochondrial stress exposure by doxycycline treatment, as demonstrated by a 40-50% increase in HSP60 and LONP1 protein levels in liver tissue samples. In contrast, normal mice fail to show such a response despite exhibiting aggravated disturbance of mitochondrial protein stoichiometry.

We noted elevated protein levels of LONP1 and TFAM in Snell liver without comparable increases in corresponding mRNA levels, suggesting an upregulation at the translational level. Based on recent findings showing that mRNA transcripts bearing 5'UTR N^6-methyladenosine

(m^6A) modifications are selectively translated by m^6A-mediated cap-independent translation (m^6A-CIT), we hypothesized that LONP1 and TFAM protein levels may be elevated through m^6A-CIT. Consistent with our hypothesis, *Lonp1*, *Tfam*, and *Pgc-1α* carry the consensus motif for m^6A modification, and are listed among putative targets of m^6A-CIT. We found that liver, kidney, and skeletal muscle of Snell mice have elevated protein levels of METTL3 and METTL14, which add m^6A marks to target mRNAs, and of YTHDF1 and YTHDF2, which promote translation of m^6A-tagged mRNAs. In contrast, ALKBH5 and FTO, which downregulate cap-independent translation of target transcripts by removing m^6A marks, are not upregulated. By knocking-down *METTL3* in HEK 293 cells, we demonstrated that protein levels of TFAM and PGC-1α, but not of LONP1, are regulated by m^6A-CIT. These findings support the hypothesis that the m^6A-CIT pathway is upregulated and might contribute to upregulation of TFAM and PGC-1α in Snell mice.

Our work demonstrates improved mitochondrial stress response in a long-lived mouse model, and provides a rationale for future mouse lifespan studies involving compounds that induce mtUPR. Our data indicating upregulation of the m^6A-CIT pathway in Snell mice support the hypothesis that m^6A-CIT may partially account for elevated protein levels of TFAM and PGC-1α.

Chapter 1 - Introduction

1.1 Aging

Aging can be defined as the process of progressive decline in the function and form of organisms starting at adulthood. It is generally thought to be driven by concurrent deterioration of multiple cellular structures and molecular pathways – a comprehensive understanding of this process is still lacking. Aging research investigates the molecular mechanisms underlying aging-associated deterioration with the aim of utilizing the ensuing insights to develop interventions to slow down the aging process and prolong lifespan *and* healthspan in mammals.

1.1.1 The idea of lifespan extension as a scientific query

Lifespan extension (and even immortality) has been sought by many throughout recorded history. However, the study of lifespan extension as a proper area of scientific research is very recent, and not yet complete. Historically, the pursuit of a longer lifetime has not been associated with science; to the contrary, it was considered to belong to the realm of the supernatural – or simply impossible. Until the late 20th century, a portion of the scientific community was quite confident that the laws of nature would not allow an expansion of the pre-determined limit on the time a living creature can spend on earth. This belief had to change

in the 21st century. Reports of lifespan extension in yeast (Fabrizio, Pozza, Pletcher, Gendron, & Longo, 2001), round worms (M. R. Klass, 1983), and fruit flies (Tatar et al., 2001), followed by those in naturally occurring mutant mice (Brown-Borg, Borg, Meliska, & Bartke, 1996; Flurkey, Papaconstantinou, Miller, & Harrison, 2001) firmly established that alteration of a single gene was sufficient to extend lifespan - even in mammals.

1.1.2 Lifespan extension across species

The first documented observation of lifespan extension by a genetic mutation took place only 35 years ago with the description of eight long-lived strains of the roundworm *C. elegans* by Klass (M. R. Klass, 1983). This early report provided insightful clues for aging research: (i) Two of the eight mutant strains entered a semi-quiescent nematode-specific developmental state named “dauer larva state”, which had been known to extend chronological lifespan (M. Klass & Hirsh, 1976). This early observation showed that future lifespan studies on *C. elegans* should watch for dauer formation and interpret the results accordingly. (ii) Five out of remaining six mutant strains of worms had partial paralysis of the pharynx resulting in decreased food (bacteria) ingestion. The last mutant strain showed a lack of interest in food, leading to reduced food intake. Moreover, among the five strains showing defective food ingestion, a direct correlation was noted between the amount of lifespan extension and the decrease in food intake. These findings supported the idea that restricted food intake may prolong lifespan in worms as had been suggested previously (M. R. Klass, 1977). Indeed, caloric restriction has

been proved to be a robust way of extending lifespan not only in worms, but also in higher organisms, including mammals (Flurkey, Astle, & Harrison, 2010).

1.1.3 Long-lived mutant mice I - Naturally occurring long-lived mice

Work published starting from the mid-1990s established that certain strains of dwarf mice had a striking phenotype: They showed retarded growth but lived longer their normal siblings.

1.1.3.1 Snell dwarf mice

Snell dwarf mice ("Snell mice") were first described by G.D. Snell in 1929 as naturally occurring mice exhibiting hereditary dwarfism as a recessive mendelian character (Snell, 1929). He also noted that these mice were "fairly healthy despite their greatly reduced size" (Snell, 1929). Seven decades after this report, a comprehensive lifespan study performed on two independent colonies located at two sites found that Snell mice show more than 40% increase in mean and maximum lifespan compared to normal littermates (Flurkey et al., 2001).

Snell mice were the first mutant mice described to show genetically transmitted dwarfism (S. Li et al., 1990). They carry an autosomal recessive mutation in the *Pit1* gene located on chromosome 16. PIT1 (pituitary-specific positive transcription factor 1) is a transcription factor required for proper development of anterior pituitary gland, a structure residing below the hypothalamus at the base of the brain (Fig. 1.1). In Snell mice, a single G-to-T point mutation in the *Pit1* gene results in the substitution of tryptophan (Trp261) with cysteine and renders the

transcription factor dysfunctional by abolishing its DNA binding (S. Li et al., 1990). Of note, the tryptophan residue found to be altered in Snell mice is conserved in PIT1 homologues from yeast to mammals, consistent with its functional role.

The anterior pituitary gland includes distinct cell populations for the synthesis and secretion of five hormones (Andersen et al., 1995). Pituitary cell types are listed below in the order they emerge during development:

• Adrenocorticotropic hormone (ACTH), β-lipotropin, and melanocyte-stimulating hormone are secreted by corticotropes under the control of corticotropin-releasing hormone (CRH) produced in the hypothalamus.

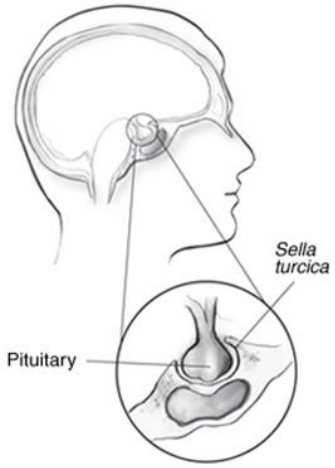

Figure 1.1 Pituitary gland.

Pituitary gland is located in a structure called *"sella turcica"* ("Turkish seat" in Latin) below the hypothalamus.

• Thyroid-stimulating hormone (TSH) is secreted by thyrotropes under the regulation of thyrotropin-releasing hormone (TRH) produced in the hypothalamus.

• Luteinizing hormone (LH) and follicle-stimulating hormone (FSH) are secreted by gonadotropes under the regulation of gonadotropin-releasing hormone (GnRH) produced in the hypothalamus.

• Growth hormone (GH) is secreted by somatotrope cells in response to growth hormone-releasing hormone (GHRH) produced in the arcuate nucleus of the hypothalamus. GH secretion can be inhibited by growth hormone-inhibiting hormone (GHIH), also produced in the hypothalamus.

• Prolactin (PRL) is released by lactotropes in response to multiple hormones produced in hypothalamus, including TRH.

Snell mice (*Pit1*$^{dw/dw}$) exhibit abnormal pituitary gland development. The *Pit1*$^{dw/dw}$ mutation primarily affects the anterior lobe of the pituitary gland (Carsner & Rennels, 1960). In normal mice, PIT1 protein expression can be detected in GH producing somatotrophs, PRL producing lactotrophs, and TSH producing thyrotropes (Simmons et al., 1990). As expected from the PIT1 expression pattern, no growth hormone (Wilson & Wyatt, 1986b), prolactin (Wilson & Wyatt, 1986b), or thyroid-stimulating hormone (Wilson & Wyatt, 1986a) can be detected in the pituitary of Snell mice.

Growth hormone stimulates hepatic production of insulin-like growth factor 1 (IGF-1), which mediates GH effects. Since Snell mice are deficient in GH (Sinha, Salocks, & Vanderlaan, 1975), they exhibit diminished levels of circulating insulin-like growth factor 1 (van Buul-Offers et al., 1994).

Lack of thyroid stimulating hormone leads to hypothyroidism in Snell mice. In rats, hypothyroidism is linked to decreased proton leakage in mitochondria (Brand, 1990), which is thought to stem from decreased conductance of mitochondrial inner membrane (Nobes, Brown, Olive, & Brand, 1990). Snell mice maintain a lower body core temperature compared to normal mice, probably due to hypothyroidism or GH deficiency, or to the requirements of maintaining temperature with a relatively high ratio of surface area to volume.

Snell mice develop normally until the 14th postnatal day, but some of them can be identified on the 12th day by their shorter noses and tails (Snell, 1929). Young adults are approximately one-third the weight of heterozygous or wild type littermates (Flurkey et al., 2001). Although they *may* have immunodeficiency of the thymus-dependent lymphoid system, which has been reported for the closely related Ames dwarf mice (Duquesnoy, 1972), Snell mice show partial protection from the age-associated decay in immune function (Flurkey et al., 2001).

1.1.3.2 Ames dwarf mice

Ames dwarf mice ("Ames mice"), first documented in 1961 in the University of Iowa (in Ames, Iowa), have a point mutation in the *Prop1* (homeobox protein prophet of Pit-1) gene located on

chromosome 11, the protein product of which is required for induction of Pit1 expression (Andersen et al., 1995). Ames mice (*Prop1*$^{df/df}$) closely resemble Snell mice (*Pit1*$^{dw/dw}$). They have smaller adult body size and an underdeveloped pituitary gland, leading to reduction in circulating levels of GH, TSH, and prolactin. Plasma IGF-1 levels are undetectably low in Ames mice (Chandrashekar & Bartke, 1993). Body core temperature average is 1.6 degree Celsius lower than normal mice (Hunter, Croson, Bartke, Gentry, & Meliska, 1999). Ames mice live longer than their normal littermates; the average lifespan increase is around 45% in males and 60% in females (Brown-Borg et al., 1996).

Ames mice show decreased levels of circulating glucose and insulin. Plasma glucose levels are ~20-30% lower in Ames mice, independent of sex (Borg, Brown-Borg, & Bartke, 1995). In normal mice, circulating insulin levels are ≥2-fold higher in males compared to females. However, Ames males, but not females, show lower insulin levels compared to normal sex-matched controls. As a result, the sex difference in insulin levels disappears in Ames mice (Borg et al., 1995). Ames mice are also insulin sensitive, which explains reduced blood levels of insulin.

The effects of the Ames mutation on plasma corticosterone concentration is in opposite directions in males and females. Corticosterone levels in normal males are only ~10-15% of those in normal females. While Ames males show 4-5 fold higher corticosterone levels compared to sex-matched controls, Ames females have 40-50% lower corticosterone (Borg et al., 1995). Ames mice show immunodeficiency of the thymus-dependent lymphoid system

(Duquesnoy, 1972), presumably as a consequence of thyroid dysfunction due to deficient TSH signaling.

1.1.3.3 Little mice

The “little” (lit) mutation was reported in 1976 as a new autosomal recessive mutation on chromosome 6, associated with dwarfism in mice (Eicher & Beamer, 1976). In the early 90s, the “little” mutation was identified as a missense mutation in the growth hormone releasing hormone receptor gene (*Ghrhr*$^{lit/lit}$) (Godfrey et al., 1993), providing another instance of naturally occurring mutation affecting the GH/IGF-1 signaling pathway.

GHRHR is expressed in the somatotrope cells of the pituitary gland and activated by the hypothalamic GHRH to stimulate GH synthesis and secretion (Godfrey et al., 1993). As opposed to Snell and Ames mutations, which lead to multiple hormone deficiencies, *Ghrhr*$^{lit/lit}$ mutation could be expected to lead to an isolated defect in GH/IGF-I signaling. However, the effect of the mutation is not restricted to GH signaling. Anterior pituitary glands of *Ghrhr*$^{lit/lit}$ mice show reduction in both GH and PRL (Eicher & Beamer, 1976), suggesting a possible effect of GH signaling pathway on the regulation of other pituitary hormones. Further research is needed to elucidate the inter-regulatory effects of distinct cell populations in the pituitary gland.

Little mice show prolonged lifespan. The increase in average lifespan is 23% in males, and 25% in females (Flurkey et al., 2001). They exhibit reduced growth. After 4 weeks of age their body weight is approximately half that of control mice (Eicher & Beamer, 1976). They are fertile but

show some reproductive deficiencies. Although females may lose their first litters due to failure of milk production, subsequent litters are raised normally. Males show reduced fertility; half of them produce only one litter, and only a few produce more than two litters (Eicher & Beamer, 1976).

1.1.4 Long-lived mutant mice II: Genetically engineered long-lived mice

Prolonged longevity observed in the naturally occurring mutants Ames dwarf and Snell dwarf which show impaired GH/IGF-1, TSH, and PRL signaling, and in *Ghrhr*$^{lit/lit}$ mice deficient in GH/IGF1 signaling, suggested a causative role for these pathways on mouse lifespan. With the aim of dissecting individual contributions of each pathway, multiple strains of genetically modified mice harboring defects in these pathways have been examined in the last 20 years.

1.1.4.1 Growth hormone receptor knockout mice

The first genetically modified mouse model with defective GH signaling was created in 1997 by replacing some portion of exon 4 and downstream intron sequence of growth hormone receptor (*Ghr*) gene with a *neo* cassette (Y. Zhou et al., 1997). The resulting mutants have been referred as “GHR-KO” or “GHR/BP disrupted” mice. GHR-KO mice have defective GH signaling and reduced levels of circulating IGF-1. However, they show elevated plasma levels of GH due to absence of a GHR-mediated negative feedback signal. Their body weight is comparable to normal mice at birth, but around 40% of normal controls at adulthood. In contrast to dwarf

mice, they are mostly fertile, but exhibit various reproductive defects (Bartke & Brown-Borg, 2004).

Up to 50% increase in lifespan is reported in GHR-KO mice colonies with multiple genetic backgrounds (Coschigano, Clemmons, Bellush, & Kopchick, 2000; Coschigano et al., 2003). The long-lived GHR-KO mice also show signs of partial resistance to age associated health deteriorations. The ability to acquire new information and to recall it at a later time is blunted by age. In tasks requiring retention of 4-week-old memories, normal old mice perform around 40% worse than young mice with the same genetic background. However, old GHR-KO mice perform as well as young controls, and exhibit a total rescue of the cognitive decay observed in old mice (Kinney, Coschigano, Kopchick, Steger, & Bartke, 2001). These observations in GHR-KO mice suggest that diminished GH/IGF-1 signaling may ameliorate the age-associated cognitive decline. Still, considering the highly elevated levels of circulating GH in these mice and the diminished PRL levels in the pituitary gland of *Ghrhr*$^{lit/lit}$ mice (Eicher & Beamer, 1976) indicating a possible of cross-talk between cell populations residing in the pituitary, it is necessary to perform further studies to rule out the potential effects of other hormones on the improved cognitive phenotype. Indeed, a follow-up study reported lower PRL receptor and elevated PRL levels in GHR-KO mice (Chandrashekar et al., 2007), making it harder to explain the GHR-KO phenotype solely by defective GH/IGF-1 signaling.

Despite having high fat to body weight ratio and obesity after adulthood, GHR-KO mice show improved insulin sensitivity (Masternak et al., 2012), which demonstrates that high fat deposition alone does not cause insulin resistance.

1.1.4.2 Growth hormone-releasing hormone knockout mice

The latest mouse model genetically modified to disrupt GH signaling was introduced in 2013 (L. Y. Sun et al., 2013). Growth hormone releasing hormone knock-out (GHRH-KO) mice are defective in GH/IGF-1 signaling and live more than 40% longer than normal siblings. They have reduced body weight and lower circulating IGF-1 levels, similar to other mouse models of disrupted GH signaling. Interestingly, despite exhibiting elevated adiponectin levels, increased insulin sensitivity, and lower plasma glucose concentration under fasting conditions, they have higher subcutaneous fat (both sexes) and perirenal fat (males only) to body weight ratio (L. Y. Sun et al., 2013).

1.1.4.3 Pregnancy-associated plasma protein-A knockout mice

Another model of disrupted GH/IGF-1 signaling is the pregnancy-associated plasma protein A knock-out (PAPPA KO) mouse (Conover & Bale, 2007). The mechanism and location of GH/IGF-1 disruption in PAPPA-KO mice differs from previous models which are defective either in secretion or recognition of GH. The *Pappa* gene encodes a zinc metalloproteinase which degrades certain proteins that inhibit IGF-1 signal transduction by binding to IGF-1. Degradation of these inhibitory factors facilitates IGF signaling. So, PAPPA knock-out results in the inhibition

of IGF-1 signal transduction, without directly altering the expression of IGF-1 or IGF-1 receptors. As opposed to GH or IGF-1, PAPPA acts locally to enhance IGF activity on the microenvironment it is expressed in.

PAPPA-KO mice live around 30% longer than normal controls (Conover et al., 2010). They exhibit normal serum levels of glucose, insulin, GH, and IGF-1. In old animals (23-38-month-old), tumor incidence and size are lower in PAPPA-KO mice (Conover & Bale, 2007).

1.1.5 Theories of longevity

Comparisons of young to old mice have revealed many effects of aging, but given little insight into factors that cause aging or regulate its rate. An alternative approach utilizes long-lived mouse models to identify characteristics found in these mice but not in their normal counterparts. This approach became possible only after the establishment of long-lived mutant mice strains and generation of genetically modified mice with extended lifespan.

1.1.5.1 GH and IGF-1 signaling pathways

Growth hormone (GH) and insulin-like growth factor 1 (IGF-1) promote organismal growth. GH/IGF-1 secretion decays gradually after adulthood, and partial reversal of this decay in elderly by recombinant human GH treatment has been shown to induce some positive effects on lean body mass, adipose mass, and skin thickness (Rudman et al., 1990), and initially led to consideration of GH and IGF-1 as candidate pro-longevity agents. Indeed, the alterations in

GH/IGF-1 pathway seem to be important for longevity, but not in the expected direction. Snell (*Pit1*$^{dw/dw}$), Ames (*Prop1*$^{dw/dw}$), *Ghrhr*$^{lit/lit}$, growth hormone receptor knock-out (GHR-KO), and growth hormone releasing-hormone knock-out (GHRH-KO) mice all have disrupted GH/IGF-1 signaling, and they exhibit lifespan extension (Coschigano et al., 2003; Flurkey et al., 2001; Sun et al., 2013).

Consistent with the idea that IGF-1 deficiency might lead to slower aging, mice lacking one copy of the IGF-1 receptor (*Igf-1r*$^{+/-}$ mice) live longer than wildtype controls (Holzenberger et al., 2003) with an average lifespan increase of ~30% in females and ~15% in males. Adult body size is 6-8% smaller than normal mice. IGF-1 expression in *Igf-1r*$^{+/-}$ mice as measured by ligand binding assay is around 50% less than wildtype levels. Blood IGF-1 levels are 25-40% higher, probably due to decreased levels of negative feedback signaling through IGF-1R. Unlike *Ghr* deletion (*Ghr*$^{-/-}$), which extends lifespan, homozygous deletion of *Igf-1r* (*Igf-1r*$^{-/-}$) is lethal.

The negative relationship between IGF-1 signaling and lifespan is not limited to mice. Mutations in the gene expressing IGF-1 receptor homolog DAF-2 in *C. elegans* result in increased lifespan and a delay in aging phenotype (Kenyon, Chang, Gensch, Rudner, & Tabtiang, 1993). Mutations that lead to GH/IGF-1 deficiencies and dwarfism have also been documented in humans.

GHRHR mutations in humans. A small population of ~100 people in Itabaianinha, Brazil carry a homozygous point mutation on *GHRHR* gene. Similar to *Ghrhr*$^{lit/lit}$ mice, affected people show GH/IGF-1 deficiency, have small body stature with adult heights in the range of 105-135 cm, and are fertile despite delayed onset of puberty (Salvatori et al., 1999). An analysis of limited

data on small number of subjects suggests no effect of lifespan, however, compared to unaffected heterozygous siblings, the frequency of deaths before the age of 20 is higher in affected females (Aguiar-Oliveira et al., 2010). Another cohort of 18 people with homozygous *GHRHR* mutation exhibiting dwarf phenotype is documented in Sindh, Pakistan. Emergence of affected population in this group is very recent. The oldest individual was 27 when the population was studied, so no lifespan data is available. Time of puberty was documented only in males, who show with 2-3 years delay in onset. However, no unusual pathology or early death is noted, and affected individuals present in good health and with normal intelligence (Maheshwari, Silverman, Dupuis, & Baumann, 1998).

GHR mutations in humans – Laron syndrome (LS). Laron syndrome is characterized by deficient GH signaling accompanied by high blood GH levels reflecting GH insensitivity (Laron, 2004). It is caused by various *GHR* mutations, including exon deletions and point mutations. Two groups of affected people, a ~60 patient cohort in Israel and a ~90 patient cohort from Ecuador, are documented. Adult height is in the range of 108-142 cm. No systematic analysis of longevity in either cohort is available since both populations are relatively young and some of the affected individuals receive replacement therapy with recombinant biosynthetic IGF-1. Nevertheless, Laron comments that LS patients live a long life and both cohorts include individuals at their 70s (Laron, 2004).

°°°

Expression levels of *Pgc-1α* ("Peroxisome proliferator-activated receptor gamma coactivator 1-alpha"; regulator of mitochondrial biogenesis. See section 1.2.5) are found to be elevated in epididymal adipose tissue (Masternak et al., 2012), skeletal muscle (assessed in females), and kidney (assessed in males) of GHR-KO mice, as well as in epididymal adipose tissue of Ames mice (assessed in males) (Menon et al., 2014), suggesting that diminished GH/IGF1 signaling may result in upregulation of the mitochondrial biogenesis pathway. PGC-1α protein expression data is available only for kidneys of GHR-KO males, and it is found to be ~50% higher (Gesing, Bartke, Wang, Karbownik-Lewinska, & Masternak, 2011). Assessment of PGC-1α levels in other tissues in both sexes, as well as TFAM ("Mitochondrial transcription factor A"; see section 1.2.5) expression, is needed to gain a better understanding on possible changes in mitochondrial biogenesis pathway in these mice. It would also be of interest to see whether Snell mice, which are also deficient in GH/IGF-1 signaling, have elevated expression genes involved in mitochondrial biogenesis.

While GH/IGF-1 signaling has been the main focus of attention, other hormonal pathways may also contribute to life extension in long-lived mutant mice. Supporting this possibility, growth hormone treatment before adulthood (between 4 and 15 weeks of age) does not diminish lifespan extension in Snell mice *unless* it is followed by lifelong thyroxin treatment (Vergara, Smith-Wheelock, Harper, Sigler, & Miller, 2004). Snell mice receiving additional thyroxin after 15 months of age show 17% decrease in mean lifespan, suggesting a possible prolongevity effect of thyroxin deficiency in Snell mice.

Although the specific mutations resulting in lifespan extension in Snell dwarf mice and in other long-lived mutant mice are well described and have major effects on GH/IGF1 signaling, how these alterations result in prolonged lifespan remains elusive. Modifications in a variety of cellular pathways have been proposed to play a causative role in longevity of these GH/IGF1 deficient mice, including diminished mTOR signaling (Dominick et al., 2015), increased autophagy (M. Wang & Miller, 2012b), and elevated proteasome activity (Drake, Miller, Miller, & Hamilton, 2015; Pickering, Lehr, & Miller, 2015).

1.1.5.2 mTOR as a regulator of cellular metabolism

"Mechanistic target of rapamycin" (mTOR) is a serine/threonine kinase initially identified in yeast by its inhibition by rapamycin (Heitman, Movva, & Hall, 1991). It forms two protein complexes "mTOR complex 1" (mTORC1) and "mTOR complex 2" (mTORC2), and through their activity it can regulate basic cellular functions including growth, maintenance, and translation. Given its involvement in such fundamental pathways, it is not surprising that mTOR activity is altered in several models of longevity. A brief summary of mTOR complexes, regulation of mTOR by GH/IGF-1 and intracellular signals, and their implications in lifespan extension is given in this section.

mTORC1 is composed of mTOR, regulatory-associated protein of mTOR (RAPTOR), and some other putative protein components (D. H. Kim et al., 2002). mTORC1 regulates protein synthesis according to extracellular signals from insulin and growth factors and intracellular signals reflecting nutrient, energy, and redox state of the cell. mTORC2 is primarily composed of mTOR

and rapamycin-insensitive companion of mTOR (RICTOR). Both mTORC1 and mTORC2 seem to be essential for mammalian development since knock-outs of their corresponding components Raptor and Rictor result in death at the embryonic stage.

Insulin and IGF-1 are well-established extracellular regulators of mTORC1. Insulin/IGF-1 signaling promotes mTORC1 activity through a signal transduction pathway involving AKT ("Protein kinase B"; also PKB). A brief summary of the mechanism of AKT-mediated mTOR regulation should be provided to understand how mutations in this pathway and deficient GH/IGF1 signaling affect mTOR activity and lifespan.

RHEB ("Ras homolog enriched in brain") is a GTP-binding protein, which, in its GTP-bound state (RHEB-GTP) activates mTORC1. TSC2 ("Tuberous sclerosis complex 2; tuberin", a GTPase activating protein) forms a complex (TSC) with TSC1 to hydrolyze GTP of the active Rheb-GTP complex and deactivate it, resulting in mTORC1 inhibition (Garami et al., 2003). Extracellular insulin, IGF-1, and IGF-2 are recognized by insulin receptor, IGF-1 receptor, and insulin/IGF1 receptor complexes. Their binding activates a signal cascade through PI3K ("Phosphoinositide 3-kinase") and PDK ("PI3-dependent kinase"), resulting in T308 phosphorylation of AKT (Garami et al., 2003). By inhibiting TSC formation, AKT relieves Rheb from deactivating activity of TCS, and promotes mTORC1 signaling.

AMP-activated protein kinase (AMPK) is an intracellular regulator of mTORC1 activity. AMPK is activated when the cellular AMP:ATP ratio increases, and it promotes catabolic metabolism to

increase cellular ATP levels. AMPK inhibits mTORC1 by stimulating TCS activity and also by phosphorylating Raptor (Gwinn et al., 2008).

Inhibition of mTORC1/2 signaling by genetic interventions or pharmacological approaches results in prolonged lifespan. The first study indicating a role for mTOR in longevity was in yeast, where deletion of *sch9* (yeast ortholog of *S6K* downstream of mTORC1), led to lifespan extension in *S. cerevisiae* (Fabrizio et al., 2001). Deficient expression of the Raptor homolog *daf-15*, mTOR homolog *let-363* (K. Jia, Chen, & Riddle, 2004), or the Rictor homolog *rict-1* (Soukas, Kane, Carr, Melo, & Ruvkun, 2009) extends lifespan in *C. elegans*. Downregulation of mTOR signaling by overexpression of either *tsc1* or *tsc2* in *D. melanogaster* also increases lifespan (Kapahi et al., 2004).

In mice, genetic modifications which disrupt mTOR signaling pathways, including deletion of downstream *S6k1* (females only)(Selman et al., 2009) or upstream *Irs1* (insulin receptor substrate 1) (Selman, Partridge, & Withers, 2011), heterozygous deletion of *Igf1r* (females only) (Bokov et al., 2011) or *Akt1* (Nojima et al., 2013), and partial disruption of *mTOR* (J. J. Wu et al., 2013), extend lifespan. Mouse lifespan can also be extended by pharmacological inhibition of mTOR by rapamycin treatment, even by rapamycin treatment late in life (Harrison, Strong, Fernandez, & Miller, 2009).

Rapamycin, isolated in 1972 from the bacterium *Streptomyces hygroscopicus* as an antifungal metabolite (Sehgal, Baker, & Vezina, 1975; Vezina, Kudelski, & Sehgal, 1975), is an FDA-approved compound for its use as an immunosuppressive and anti-cancer drug. Its prolongevity

effect is a more recent discovery and has been documented in *S. cerevisiae* (Powers, Kaeberlein, Caldwell, Kennedy, & Fields, 2006), *C. elegans* (Robida-Stubbs et al., 2012), *D. melanogaster* (Bjedov et al., 2010), and mice (Miller et al., 2011).

Supporting a prolongevity role for decreased mTOR signaling, long-lived Ames mice show downregulation in the PI3K/mTOR/Akt signal transduction pathway (Sharp & Bartke, 2005), presumably due to decreased IGF-1 signaling in dwarf mice. Reduced mTOR activity is also indicated in lifespan extension induced by calorie restriction. How reduced mTOR activity increases lifespan is not known.

1.1.5.3 Improved stress response

Increased ability to function under stress and to survive suboptimal conditions emerges as a common feature of long-lived nematodes, insects, and cells from long-lived mammals.

Long-lived *C. elegans* strains with mutations affecting insulin/IGF-1 signaling (*age-1*, *daf-2*, *daf-23* mutants) or mitochondrial metabolism (*clk1* mutant) show increased resistance to UV radiation (Murakami & Johnson, 1996). Compared to wildtype worms, *age-1* mutants also have higher survival rates after heat exposure (Lithgow, White, Hinerfeld, & Johnson, 1994) and after hydrogen peroxide treatment (Larsen, 1993). In addition, both *age-1* and *daf-2* mutants are better protected from death induced by cadmium and copper exposure (Barsyte, Lovejoy, & Lithgow, 2001).

In comparison to their normal counterparts, primary fibroblasts from long-lived Snell and Ames mice survive higher doses of UV radiation, hydrogen peroxide, paraquat, and cadmium exposure (Murakami, Salmon, & Miller, 2003; Salmon et al., 2005). Fibroblasts from GHR-KO mice show increased resistance to treatment with UV radiation, hydrogen peroxide, and paraquat, but not cadmium (Salmon et al., 2005). An indirect indication of protection from oxidative damage is also noted in Laron syndrome patients. Pre-exposure of human epithelial cells to serum from LS patients, but not from their unaffected siblings, results in increased protection from to H_2O_2-induced DNA breaks, but it also increases apoptosis (Guevara-Aguirre et al., 2011), which may be a protective mechanism by containing the damage and by preventing further mutations.

Mice deficient in IGF-1 signaling (*Igf-1r*$^{+/-}$ mice), which also live longer, survive intraperitoneal paraquat injection better than normal mice (Holzenberger et al., 2003). Also, as reported for other long-lived mutants, ex-vivo analyses of primary cells isolated from IGF-1 deficient mice indicate increased resistance to hydrogen peroxide-induced cell death (Holzenberger et al., 2003). As a side note, this study evaluates hydrogen peroxide resistance as the ratio of surviving cells after exposure to a certain dose of peroxide. This approach differs from widely used "lethal dose 50 (LD50)" analysis wherein the cells are exposed to a range of different doses to calculate the dose that kills 50% percent of the initial population.

1.2 Mitochondria

Mitochondria were first recognized as distinct organelles in 1890 by Altman who observed these intracellular structures and called them "Bioblasts" (Altmann, 1890). He thought that these structures comprised the morphological unit of living matter ("*Im Bioblast scheint jene morphologische Einheit der lebenden Ma terie gefunden zu sein.*"). The use of the name "mitochondrion" started around 1900 due to the resemblance of these structures to threads ("mitos" in Greek) made of small compact particles ("chondro" in Greek) during spermatogenesis (Ernster & Schatz, 1981)(Pagliarini & Rutter, 2013). For the next fifty years following their discovery, mitochondria were recognized by their specific staining with the redox dye Janus Green B, with no mechanistic understanding of the specificity of this dye for mitochondria.

Mitochondrial research during the first half of the 20th century resulted in important developments around 1950, mostly stemming from the successful isolation of mitochondria by fractionation and the development of electron microscopy.

1.2.1 Mitochondrial DNA

Mitochondria contain their own DNA called "mitochondrial DNA" (mtDNA) (Schatz, Haslbrunner, & Tuppy, 1964). Depending on the species and tissue type, each cell may have hundreds to thousands of mtDNA molecules. mtDNA is a circular double-stranded DNA comprised of 16-17K base pairs in mammals; 16295 base pairs in mice (Bibb, Van Etten, Wright,

Walberg, & Clayton, 1981) and 16569 base pairs in humans (Anderson et al., 1981). It encodes 13 peptides, which are subunits of electron transport chain (ETC) complexes, 2 mitochondrial rRNAs, 22 mitochondrial tRNAs, and some putative peptides with elusive expression and function including Humanin and MOTS-c (Shokolenko & Alexeyev, 2017) (Table 1).

The mitochondrial genome is mostly comprised of coding sequences as opposed to intron-rich nuclear genome (Gustafsson, Falkenberg, & Larsson, 2016). Mitochondrial DNA is so compact that it hosts rare instances of "overlapping gene" sequences in humans. *ATP6* and *ATP8*, which encode subunits of ATP Synthase (ETC complex V), as well as *ND4* and *ND4L*, which encode subunits of NADH-ubiquinone oxidoreductase (ETC complex I), share overlapping nucleotide sequence encoded in alternate reading frames producing distinct peptide sequences. Strands of mtDNA are named according to their relative guanine content as heavy (contains more guanine) and light strands.

Mitochondria carry out vital cellular functions including ATP production by oxidative phosphorylation and heme biosynthesis. They also regulate intracellular calcium concentration, function in thermogenesis, and can initiate apoptosis by cytochrome c release. Production of reactive oxygen species (ROS) is also listed among the functions of mitochondria by some researchers, although ROS can also be considered a byproduct of metabolism as will be discussed later.

Gene product	Component of	Mouse gene	mtDNA strand
NADH dehydrogenase 1 (ND1)	ETC complex I	*Nd1*	Heavy
ND2	ETC complex I	*Nd2*	Heavy
ND3	ETC complex I	*Nd3*	Heavy
ND4	ETC complex I	*Nd4*	Heavy
ND4L	ETC complex I	*Nd4l*	Heavy
ND5	ETC complex I	*Nd5*	Heavy
ND6	ETC complex I	*Nd6*	Light
Cytochrome b	ETC complex III	*Cytb*	Heavy
Cytochrome c oxidase 1 (COXI)	ETC complex IV	*CoxI* or *co1*	Heavy
COX2	ETC complex IV	*Cox2* or *co2*	Heavy
COX3	ETC complex IV	*Cox3* or *co3*	Heavy
ATP6	ATP Synthase (ETC complex V)	*Atp6*	Heavy
ATP8	ATP Synthase (ETC complex V)	*Atp8*	Heavy
Ribosomal RNA small subunit 12S	Mitochondrial ribosome	*Mt-rnr1*	Heavy
Ribosomal RNA large subunit 16S	Mitochondrial ribosome	*Mt-rnr2*	Heavy
22 Transfer RNAs (tRNAs)	Mitochondrial translation machinery	*Mt-trn*[*] [*] = *A, R, N, D, C, E, Q, G, H, I, L1, L2, K, M, F, P, S1, S2, T, W, Y, or V.*	Heavy (14) and Light (8)

Table 1 Peptides and RNAs encoded in mtDNA

1.2.2 Oxidative phosphorylation

By mid-20th century, it was known that ATP production by aerobic respiration took place in the mitochondria (Kennedy & Lehninger, 1949). However, the development of a viable theory for the underlying mechanism required diligent research for the next 20 years.

In 1961, Peter Mitchell proposed a model to explain coupling of electron transfer and phosphorylation (Mitchell, 1961). The "chemiosmotic hypothesis" is explained in great detail in Mitchell's brilliantly written book "Chemiosmotic coupling and energy transduction" (Mitchell, 1968). Briefly, he proposed that oxido-reduction reactions carried out by ETC complexes create a protein gradient through the inner mitochondrial membrane by moving hydrogen ions (protons) from matrix to the intermembrane space (IMS). Once the proton gradient is present, a proton-translocating ATPase located on the inner membrane works in reverse direction to synthesize ATP from ADP and P_i using the energy generated by the flow of protons from the intermembrane space to the matrix. Mitchell's model not only provided a mechanism for the conservation of energy generated in distinct steps, but also implied the presence of an ion-impermeable inner membrane, which would explain the uncoupling effect of membrane-permeabilizing agents. Most importantly, it elaborated a hitherto unknown biological mechanism for energy conversion and transduction where molecular concentration gradients (potential energy) between separated compartments are created and utilized to carry out a chemical reaction which is coupled to the controlled flow of molecules down the concentration gradient.

Electron transfer	→	Proton gradient	→	Phosphorylation
(chemical energy)		(potential energy)		(chemical energy)

Oxidative respiration is carried out by electron transport chain (ETC) complexes located on the inner mitochondrial membrane: the proton gradient is generated by ETC complexes I-IV, while ATP synthesis by phosphorylation is performed by ATP synthase (also called "ETC complex V"), as discussed in the next section.

1.2.3 Respiratory chain

The respiratory chain, also named electron transport chain (ETC), comprises five multiple-subunit protein complexes located in the inner mitochondrial membrane. Each complex, except complex II, is formed by coordinated assembly of nuclear-DNA-encoded and mitochondrial-DNA-encoded peptides in a precise stoichiometry (Table 2).

Complex	Common name	nDNA-encoded subunits	mtDNA-encoded subunits	Total
I	NADH-ubiquinone oxidoreductase	37	7	44
II	Succinate-ubiquinone oxidoreductase	4	-	4
III	Ubiquinone-cytochrome c oxidoreductase	10	1	11
IV	Cytochrome c oxidase	11	3	14
V	ATP synthase	12	2	14
Total	Electron transport chain	74	13	87

Table 2 Electron transport chain complexes in mammalian mitochondria

ETC complex I is called NADH-ubiquinone oxidoreductase. In mammals, it is a ~1000 kDa, 44-subunit protein complex. Seven core peptides, named ND1 to ND6 and ND4L, are encoded in the mtDNA. The remaining 37 peptides are encoded in the nDNA, translated in the cytosol, transported to the mitochondria, folded into their native structure in the mitochondrial matrix, and amalgamated with the mtDNA-encoded core peptides to form the complex I assembly. As will be explained later, the formation of ETC complexes comprised of peptides encoded both in the nuclear and the mitochondrial DNA requires strict regulation and communication between cellular and mitochondrial transcription. As the name implies, NADH-ubiquinone oxidoreductase oxidizes NADH and reduces ubiquinone (Q) with the overall reaction shown below:

$$NADH + Q + 5H^+ \rightarrow NAD^+ + QH_2 + 4H^+$$

Importantly, the five protons entering the reaction are taken from the matrix, and the four protons on the right-hand side of the reaction are released to the intermembrane space, resulting in the transfer of four protons from the matrix to the intermembrane space. The "pumping" of the protons through the inner membrane creates a proton gradient which is utilized to generate the electromotive force required for ATP production by complex V (ATP synthase).

Complex I activity can be inhibited by multiple compounds including MPTP (1-methyl-4-phenyl-1,2,3,6-tetrahydropyridine), phenoxan, piericidin A, annonin VI, amytal, and rotenone. Among

those, rotenone is regularly used in mitochondrial research, as it is used in this work for the analysis of individual components of oxygen consumption.

° ° °

Complex II, succinate-ubiquinone oxidoreductase, is the smallest of the five complexes – it consists of four subunits. It also differs from other complexes in that it is not buried in the inner membrane but attached to the inner mitochondrial membrane on the matrix side through its interaction with the integral membrane proteins. In addition to the four subunits complex II also contains cofactors and metal ions. The largest peptide of the complex is covalently bound to a flavin to form flavoprotein subunit (Fp) (Walker & Singer, 1970). Another smaller subunit, called iron-protein subunit (Ip), contains nine iron atoms in three Fe-S centers. The Ip and Fp subunits together constitute the enzyme succinate dehydrogenase (SDH).

Complex II is the only ETC complex that is composed of nuclear-DNA-encoded subunits with no contribution from mtDNA in mammals. As complex II oxidizes succinate to fumarate in the Krebs cycle, it reduces ubiquinone to QH_2 in the ETC, linking the two pathways:

$$\text{Succinate} + Q \rightarrow \text{Fumarate} + QH_2$$

As in the case of complex I, inhibitors specific to complex II are utilized in biochemical analysis of the electron transport chain. The succinate analog malonate binds to complex II, competing with and inhibiting succinate binding, and is therefore utilized to block succinate : ubiquinone oxidoreductase activity.

° ° °

Complex III, ubiquinol-cytochrome c oxidoreductase, is also called “cytochrome c reductase” or “bc_1 complex” referring to its components cytochrome b and cytochrome c_1. It reduces cytochrome c and pumps 4 protons from matrix to IMS.

$$QH_2 + 2\ Fe^{+3}\ \text{cyt c} + 2\ H^{+}_{(Matrix)} \rightarrow\ Q + 2\ Fe^{2+}\ \text{cyt c} + 4\ H^{+}_{(IMS)}$$

Complex III is composed of 11 peptides in mammals and 9 peptides in yeast. Only one of these peptides, cytochrome b, is encoded in the mtDNA. The remaining subunits are encoded in the nuclear DNA.

Specific inhibition of complex III can be achieved by the antibiotic antimycin A. Assays of oxidative respiration make use of antimycin A to dissect mitochondrial versus cytosolic portions of total oxygen consumption. In our work, we use a modified protocol which includes inhibition of antimycin A-mediated inhibition of complex III to analyze oxidative respiration after mitochondrial stress exposure.

° ° °

Complex IV, also referred as “cytochrome c oxidase”, catalyzes the overall reaction where O_2 consumption takes place and H_2O is produced; molecular oxygen receives the electrons, cytochrome c is reoxidized, and 4 protons are pumped from the matrix to intermembrane space.

$$4\ Fe^{2+}\ cyt\ c + 8\ H^{+}_{(Matrix)} + O_{2\ (Matrix)} \rightarrow 4\ Fe^{3+}\ cyt\ c + 4\ H^{+}_{(IMS)} + 2\ H_2O_{(Matrix)}$$

The mammalian complex IV is composed of 13 protein subunits. In addition, it contains the two heme groups (heme a and a_3), and three copper atoms (2 Cu_A and Cu_B) required for separation of the oxygen atoms in the O_2 molecule to form H_2O. The largest subunits, COXI, COXII, and COXIII are encoded in the mtDNA and synthesized in the mitochondrial matrix. The remaining ten subunits of the mammalian complex IV are COXIV, COXVa-b, COXVIa-c, COXVIIa-c, and COXVIII.

Complex IV catalyzes a critical process where partially reduced oxygen may be released and produce the superoxide radical $^{\bullet}O_2^-$, which can lead to production of hydrogen peroxide (H_2O_2) or hydroxyl radical ($^{\bullet}OH$). However, it is not clear whether mitochondrial reactive oxygen species are produced as a result of incomplete oxygen reduction in complex IV or generated independent of oxygen reduction reactions.

° ° °

Complex V is the ATP synthase, and is considered part of the ETC complexes. In principle this perception is not correct since ATP synthase is not an electron transporter. It functions independent of the complexes I-IV by using the proton gradient generated by ETC complexes I-IV as energy source to produce ATP. Complex V can be inhibited by oligomycin. Analysis of respiration rate when ATP synthase is blocked allows assessment of the amount of respiration directly utilized in ATP production.

1.2.4 Thermogenesis

Brown fat utilizes the proton gradient created by mitochondrial respiration chain for a different purpose; it generates heat for non-shivering thermogenesis. Interestingly, this is achieved by a mechanism that counters ATP production. Initially it was believed that brown fat generated heat by rapid production and consumption of ATP. However, this idea conflicted with findings indicating the presence of low levels of ATP synthetase and the absence of electron-transport coupled phosphorylation in brown fat mitochondria (Lindberg, de Pierre, Rylander, & Afzelius, 1967) despite the higher density of mitochondria present in this tissue. Analysis of mitochondria isolated from guinea pig brown adipose tissue led to the discovered that a 32 KDa ion uniport protein localized to the inner mitochondrial membrane acting as mitochondrial uncoupler was responsible for the heat generation during thermodynamic adaptation (Heaton, Wagenvoord, Kemp, & Nicholls, 1978). The uniporter protein was purified (Lin, Hackenberg, & Klingenberg, 1980), sequenced (Aquila, Misra, Eulitz, & Klingenberg, 1982), and a decade after its association with thermogenesis, it was cloned and named “Uncoupler Protein (UCP)”. Since the identification of its homologue “Uncoupler Protein 2 (UCP2)” in 1997 (Fleury et al., 1997; Gimeno et al., 1997), it has been known as “Uncoupler Protein 1 (UCP1)” or “Thermogenin”.

Thermogenesis demonstrates how mitochondrial protein gradient can be regulated according to tissues-specific functions. While it is utilized for ATP synthesis in other tissues, in brown fat the protons are allowed to flow though the inner membrane in order to produce heat by burning maximum amount of oxygen.

1.2.5 Mitochondrial biogenesis

Mitochondria are produced by growth and division of pre-existing mitochondria as opposed to *de novo* generation (Schatz et al., 1964). Mitochondria have their own transcription machinery, which is distinct from its counterparts residing in the nucleus as well as in the bacteria. Nevertheless, mitochondrial biogenesis is not autonomous but regulated by nuclear-DNA-encoded proteins. *In vitro*, efficient mitochondrial transcription requires only three proteins (Shutt, Lodeiro, Cotney, Cameron, & Shadel, 2010). Mitochondrial RNA polymerase (POLRMT) is a single subunit protein homologous to RNA polymerase found in T3 and T7 bacteriophages (Masters, Stohl, & Clayton, 1987). While no transcription factor is necessary for phage polymerase activity, POLRMT requires mitochondrial transcription factors A (TFAM) and B2 (TFB2M).

The mitochondrial transcription process is not fully understood, and less is known about mitochondrial translation events. So far, *in vitro* reconstitution of mitochondrial translation has not been achieved.

1.2.5.1 Mitochondrial transcription factor A

The first component of the mitochondrial transcription machinery to be purified was mitochondrial transcription factor A (TFAM), initially referred as “mitochondrial transcription factor 1” (Fisher & Clayton, 1988). It contains a matrix targeting sequence (MTS) and two HMG

DNA binding domains (HMG1 and HMG2), which can bind the DNA in minor groove to bend and unwind it. In contrast to nuclear transcription factors, TFAM is not gene-specific.

TFAM binds to mtDNA at 10-40 nucleotides upstream of promoter regions (Fisher, Topper, & Clayton, 1987) and bends the mtDNA (Ngo, Kaiser, & Chan, 2011; Rubio-Cosials et al., 2011). DNA-bound TFAM recruits POLRMT to form pre-initiation complex (Morozov et al., 2014), which recruits TFB2M to initiate translation (Sologub, Litonin, Anikin, Mustaev, & Temiakov, 2009). Mitochondrial transcription produces polycistronic transcripts which are spliced into individual mRNAs. Mitochondrial transcripts have no 5'methyladenosine caps and very short poly(A) regions – if any.

Mice heterozygous for *Tfam* gene disruption ($Tfam^{+/-}$) are viable but show respiration chain deficiency and low mtDNA content, whereas TFAM knock-out ($Tfam^{-/-}$) mice die before embryonic day 11 (Larsson et al., 1998). Consistent with its function in mitochondrial transcription and mtDNA replication, deletion of *Tfam* in cardiomyocytes (H. Li et al., 2000), skeletal muscle (Wredenberg et al., 2002), pancreatic beta-cells (Silva et al., 2000), or forebrain neurons (Sorensen et al., 2001) results in depletion of mitochondrial transcripts and electron transport chain proteins in corresponding tissues. Cardiac-specific *Tfam* knock-out mice show severe defects in heart starting at 2 weeks of age including mtDNA depletion, impaired ETC function, reduced ATP levels, and progressive cardiomyopathy (Hansson et al., 2004).

1.2.5.2 Peroxisome proliferator-activated receptor gamma coactivator 1 alpha

Peroxisome proliferator-activated receptor gamma (PPARγ) coactivator 1-alpha (PGC-1α) was isolated from brown fat cells through its interaction with PPARγ (Puigserver et al., 1998). PGC-1α does not directly bind to DNA, but it binds to various transcription factors and activates them. In addition to PPARγ, it interacts with thyroid hormone receptor β (TRβ), retinoic acid receptor alpha (RARα), and estrogen receptor alpha (ERα).

As soon as *Pgc-1α* had been isolated, it was observed that *Pgc-1α* induction was accompanied by elevated mtDNA abundance and upregulation of mtDNA-encoded genes including subunits of cytochrome c oxidase and ATPase, providing an early sign for its role in mitochondrial biogenesis (Puigserver et al., 1998). Follow-up studies established that, PGC-1α directly induces mitochondrial biogenesis by co-activating nuclear respiratory factors to upregulate TFAM which regulates both mtDNA replication and mitochondrial transcription (Z. Wu et al., 1999).

Ectopic Pgc-1α expression increases mitochondrial biogenesis and oxidative respiration in skeletal muscle cells and in cardiac muscle cells (Lehman et al., 2000). *In vivo*, Pgc-1α overexpression in type II skeletal muscle fibers increases mitochondrial mass, and induces fiber type switch from glycolytic type IIb fibers to more oxidative type I and IIa fibers (J. Lin et al., 2002). Similarly, cardiac-specific Pgc-1α overexpression induces extensive mitochondrial proliferation in heart disturbing sarcomere structure (Lehman et al., 2000). Effects of artificially upregulated Pgc-1α expression suggest that Pgc-1α can induce mitochondrial biogenesis and

increase oxidative respiration both in cell culture and *in vivo* - at least in skeletal and heart muscle.

In addition to transgenic mice, studies on *Pgc-1α*-deficient mice have provided key findings on the critical role of Pgc-1α on mitochondrial biogenesis and function. Somewhat unexpectedly, by 3 months of age, PGC-1α KO mice show no structural defects in heart or in skeletal muscle fibers, two tissues with high energy demand. Mitochondrial content in heart is also comparable between *Pgc-1α*$^{-/-}$ and normal mice. At first, the healthy looking phenotype of 3-month old PGC-1α KO mice may seem to be in contradiction with proposed function of Pgc-1α in mitochondrial biogenesis. In fact, it underlies two important qualities of mitochondrial biology highly relevant to our work:

(i) Comparable mitochondrial content does not imply comparable mitochondrial function, i.e. in the case of mitochondria, functionality cannot be deduced from abundance.

Although they exhibit no abnormality in mitochondrial content or morphology, both heart and skeletal muscle of PGC-1α KO mice have reduced expression of ETC complex subunits, including those of ATP synthase and cytochrome c oxidase which are required for oxidative respiration (Arany et al., 2005). In addition, expression of *Tfam*, which is required for mitochondrial transcription, is also reduced in PGC-1α deficient mice. Consistent with reduced expression of respiration chain components, ATP content in heart of PGC-1α KO mice is 20% lower than normal despite comparable mitochondrial content. Of note, 20% reduction in cardiac ATP content is of physiologic importance since ~30% decrease in ATP content is associated with

terminal heart failure (Bashore, Magorien, Letterio, Shaffer, & Unverferth, 1987; Starling, Hammer, & Altschuld, 1998). PGC-1α KO mice also show defective cardiac function with more than 50% decrease in contractile performance (Arany et al., 2005).

(ii) Defects in mitochondrial biology become more apparent as the organism gets older due to cumulative effects of mitochondrial damage accumulation and impaired mitochondrial stress response.

No structural abnormality or morphological signs of cardiac defects are observed in *Pgc-1α*$^{-/-}$ mice at 3 months of age. However, as early as 8 months of age, which corresponds to adulthood period, symptoms of cardiac dysfunction become apparent (Arany et al., 2005). Left ventricular chamber size gets more dilated, and the contraction-induced change in internal diameter gets smaller, indicating impaired cardiac contraction. Also, upregulated expression of certain genes, which is used as a molecular marker of cardiac stress, can be detected in hearts of adult *Pgc-1α* deficient mice (Arany et al., 2005). Development of cardiac dysfunction only after adulthood exemplifies the aging-associated gradual development of mitochondrial pathologies caused by mitochondrial maintenance defects.

In mice, *Pgc-1α* mRNA can be detected by northern blot analysis in brown fat, heart, kidney, and brain, but not in white fat, lung, skeletal muscle, liver, testes, or spleen (Puigserver et al., 1998). Upon cold exposure (4 °C for 12 hours), *Pgc-1α* expression is robustly induced in brown fat and skeletal muscle, while heart, kidney, white fat, and liver are not affected.

1.2.6 Mitochondrial stress response

1.2.6.1 Cellular protein homeostasis

Proteostasis is an auto-regulation process through which a biological system reacts to competing intrinsic factors and environmental changes to keep the proteome in a stable, functional state. Cellular mechanisms regulating proteostasis can be summarized in three main groups: protein biogenesis, folding and conformational maintenance, and degradation. It is estimated that, in mammalian cells, there are around 400 proteins functioning in protein biogenesis, 300 in folding and maintenance, and 700 in degradation, some falling in more than one group (Y. E. Kim, Hipp, Bracher, Hayer-Hartl, & Hartl, 2013).

Protein folding can be defined as the process through which a linear polypeptide reaches its well-defined three-dimensional conformation, forming the functional protein (Hartl, 1996). In the 1950s, multiple researchers reported that they were able to observe denatured proteins fold into their native state spontaneously *in vitro* (Anfinsen, 1973). These observations led to the "thermodynamic hypothesis" which stated that the native three dimensional state of the protein in physiological environment has lower entropy, so a polypeptide chain folds into the correct conformation spontaneously, and the native conformation of a protein is totally determined by its amino acid sequence (R. J. Ellis & Minton, 2006). As the thermodynamic hypothesis gained support, the general belief in 1970s was that folding of proteins and their assembly into oligomers could take place in cells *in vivo* without a need for molecular catalysts or energy consumption (Anfinsen, 1973).

This view started to be challenged by the new findings in the 1990s (Hartl, 1996). Cytosol, as opposed to the conditions set *in vitro*, is a crowded medium with an estimated macromolecule density of 300 mg/ml (R. J. Ellis & Minton, 2006). Newly synthesized peptides are prone to interactions with proteins and other molecules present in the cytosol which can interfere with their folding. Moreover, some peptides should be maintained in an unfolded state until they are transported to a specific location in the cell, such as mitochondria, where they are folded into their functional structure. Premature folding or misfolding during transport would render the peptides unsuitable to pass through membranes enclosing the target compartment. Proper translocation and folding of many proteins require regulated interactions with specific proteins called molecular chaperons.

1.2.6.1.1 Chaperons

The term "molecular chaperons" was proposed in 1987 by John Ellis to describe "a class of cellular proteins whose function is to ensure that the folding of certain other polypeptide chains and their assembly into oligomeric structures occur correctly" (J. Ellis, 1987). The existence of such a group of proteins was suggested a year earlier by Hugh Pelham, who, commenting on the presence of proteins related to Hsp70 and Hsp90 in both ER and cytoplasm of unstressed cells, speculated that they may play a role in protein folding and assembly occurring in both cellular compartments (Pelham, 1986). Incorporating our current understanding in Ellis's initial description, molecular chaperons can be described as proteins that interact with nascent peptides and with structurally unstable proteins to prevent their

misfolding, maintain them in an unfolded state during transportation, help them fold into native protein structure and assemble into oligomers, and facilitate their degradation (Hartl, 1996; Hendrick & Hartl, 1993; Y. E. Kim et al., 2013).

Most of the chaperons are "heat shock proteins" (HSPs). They were named HSPs because either (i) their expression was found to be upregulated in response to heat stress, or (ii) they share homolog sequences with other HSPs. HSPs are generally considered as stress-response proteins, but this categorization may be misleading. Although some of them are upregulated in response to stress (such as heat), many are not. Most are essential for cell function and indispensable under normal growth conditions. In fact, by 1996, years after their role in protein folding was established, it was not known whether Hsp70s had any protective function under stress conditions, including exposure to high temperature (Hartl, 1996). Accordingly, HSPs can be described as molecular chaperons which interact with structurally unstable peptides for their folding, assembly, transport, or degradation (Hendrick & Hartl, 1993) – with no requirement of heat-inducibility.

There are two essential qualities of molecular chaperons involved in protein folding: (i) reusability; they do not take part in the final assembly. (ii) unspecificity; they do not carry any steric information for any specific protein.

Chaperons are historically named according to their molecular weight: Hsp40s, Hsp60s, Hsp70s, Hsp90s, Hsp100s, and small Hsps, independent of their function or cellular localization. Heat shock protein 70 family proteins (Hsp70s), partnering with Hsp40s, bind to nascent and newly

translated polypeptide chains, maintain them in an unfolded soluble state, and release them still in unfolded conformation (Hartl, 1996). The Hsp70/Hsp40 complex requires ATP to perform its function.

1.2.6.1.2 Chaperonins

Chaperonins are multi-subunit double-ring protein complexes that form cavities to provide isolated spaces for proper folding of peptides into their 3D structure. In contrast to chaperons which release the peptides in unfolded state, chaperonins release peptides in folded tertiary conformation (Hartl, 1996). Chaperonins use an ATP-dependent mechanism to facilitate folding of the substrate proteins. The HSP60/HSP10 chaperonin is the key component of mitochondrial stress response, which is discussed next.

1.2.6.2 A mitochondria-specific stress response

A mitochondria specific stress response was first described in mammalian cells by Martinus *et al.* in 1996 (Martinus et al., 1996). By growing rat hepatoma cells in media containing ethidium bromide (EtBr) for 10 generations, the Hoogenraad group generated "ρ^0 cells", which means cells devoid of mitochondria DNA. Cells lacking mtDNA cannot synthesize the 13 peptides encoded in the mitochondrial genome, hence cannot perform oxidative respiration. Once mtDNA depletion is achieved, ρ^0 cells are cultured in EtBr-free media supplemented with pyruvate and uridine. Cells devoid of mtDNA can be propagated at least a year and show growth characteristics similar to those of normal cells.

Although they lack mtDNA encoded ETC subunits, ρ^o cells still express ETC subunits encoded in the nuclear genome. Under these conditions, the mitochondria not only have impaired respiration but also accumulate unassembled nuclear-encoded ETC subunits which are prone to unfolding and aggregation, and induce a proteostatic stress load specifically in the mitochondria. It is found that the mitochondrial stress load in ρ^o cells induces a corresponding stress response specific for mitochondria, an organelle-specific protective mechanism similar to the previously discovered endoplasmic reticulum (ER)-specific unfolded protein response (UPR^{ER}). ρ^o cells show 2.5-fold higher protein levels of HSP60 and HSP10, which form the mitochondrial HSP60/HSP10 chaperonin. Protein levels of mitochondrial chaperon mtHSP70, constitutively expressed cytosolic chaperon HSP73, and stress-inducible cytosolic chaperon HSP72 are not altered, demonstrating that (i) not all mitochondrial chaperons and (ii) not all stress-inducible chaperons are upregulated in ρ^o cells. These observations indicate that HSP60/HSP10 upregulation is a major component of the mitochondrial stress response (MSR), which is lately referred as “mitochondrial unfolded protein response” (mtUPR; occasionally abbreviated UPR^{mt}).

Another study in COS-7 cells (a cell line derived from monkey kidney cells) showed that ectopic expression of truncated form of mitochondrial protein ornithine transcarbamylase (OTCΔ), which forms insoluble aggregates in the mitochondrial matrix, induces transcriptional upregulation of mitochondrial chaperonin components *Hsp60* and *Hsp10* (Zhao et al., 2002). Upregulation of HSP60 and HSP10 protein levels, previously reported in ρ^o cells, is also detected. In addition, an increase in transcript levels of *mtDnaJ*, *Clpp*, and *Lonp1* is detected

upon ΔOTC expression, while transcript levels of mitochondrial chaperon *mtHsp70*, cytoplasmic chaperons *Hsp72*, *Hsp73*, and ER chaperon *Bip* are not affected.

In worms, RNAi-mediated silencing of almost any protein which either takes part in the assembly of ETC complexes or functions in mitochondrial protein synthesis results in mtUPR induction (Yoneda et al., 2004). Loss of the mitochondrial protein gradient (ΔΨ), which diminishes oxidative respiration, however, does not induce mtUPR (Yoneda et al., 2004). Together, these observations suggest that disturbance of the fixed ratio of nuclear and mitochondrial encoded subunits ("mito-nuclear protein imbalance") interferes with complex assembly and results in accumulation of unassembled subunits in the mitochondrial matrix, and, in turn induces mtUPR (Houtkooper, Mouchiroud, Knott, Williams, & Auwerx, 2013).

HSP60 and HSP10 are upregulated in both the mRNA and protein level as part of the mitochondrial stress response (Martinus et al., 1996; Zhao et al., 2002). When the chaperonin activity is not sufficient, polypeptides can form terminally misfolded protein structures in the mitochondrial matrix. During the initial phase, these misfolded proteins can be degraded and recycled by the mitochondrial protease LONP1, which is also upregulated in response to mitochondrial stress (Zhao et al., 2002).

Upregulation of HSP60, or its orthologs in lower organisms, is used as the key indicator of mtUPR induction (Durieux, Wolff, & Dillin, 2011; Houtkooper et al., 2013; H. Zhang, Ryu, Menzies, & Auwerx, 2016). CLPP or LONP1 upregulation is also utilized as an additional mtUPR marker by some researchers. However, their use is not consistent, which may be due to

variability in expression and response patterns depending on the type of cell/tissue, model organism, or method of stress exposure.

Under normal conditions where no mitochondrial stress is present, HSP60/HSP10 chaperonin function is required for proper folding of newly synthesized nuclear-DNA-encoded mitochondrial proteins imported into the matrix. Accordingly HSP60 is required during development – *Hsp60* deletion is lethal (Yoneda et al., 2004). HSP60 and HSP10 also function in the re-folding of structurally unstable proteins prone to aggregation. The role of mtUPR and other aspects of mitochondrial homeostasis in aging will be discussed in the next section.

1.2.7 Mitochondria in aging and longevity

Mitochondria accumulate multiple forms of damage during aging. Importantly, prevention or partial reversal of mitochondrial damage though genetic and pharmaceutical interventions can improve mitochondrial function and extend lifespan. Some of the aging-associated mitochondrial defects and animal models resistant to such deterioration will be introduced in the following sections.

1.2.7.1 Accumulation of mtDNA damage with age

In humans, mtDNA deletions increase with age in multiple tissues including diaphragm muscle (Hayakawa, Torii, Sugiyama, Tanaka, & Ozawa, 1991), brain (Corral-Debrinski et al., 1992; Cortopassi & Arnheim, 1990; Soong, Hinton, Cortopassi, & Arnheim, 1992), and heart

(Cortopassi & Arnheim, 1990). Mouse liver also shows accumulation of mtDNA deletions during aging (Piko, Hougham, & Bulpitt, 1988). An increase in mtDNA point mutations by age is detected in extraocular muscle of the human eye (Munscher, Muller-Hocker, & Kadenbach, 1993; Munscher, Rieger, Muller-Hocker, & Kadenbach, 1993).

Mitochondrial DNA is subject to oxidative damage at least 10-15 times more than nuclear DNA (Mecocci et al., 1993; Richter, Park, & Ames, 1988). Oxidative damage in mtDNA increases with age in human brain (Mecocci et al., 1993) and diaphragm muscle (Hayakawa et al., 1991), as well as in rat liver (Ames, Shigenaga, & Hagen, 1993). Age-associated escalation of oxidative damage is also detected in mitochondrial proteins (Sohal & Dubey, 1994).

Another abnormality of mtDNA is occurrence of catenated mtDNA dimers, which indicates impaired separation of mtDNA molecules during replication. Abundance of catenated DNA increases by age in heart and brain tissues of mice (Piko, Bulpitt, & Meyer, 1984) (Bulpitt & Piko, 1984). A similar age-associated increase in catenated DNA also takes place in rat heart and kidney (Piko et al., 1984).

mtDNA mutator mice

Although the correlation between aging and increase in mtDNA mutations was established by the end of 90s, it was not known whether the mtDNA mutations were driving the aging process or *vice versa.* In order to assess the effects of mtDNA mutations in mice, a mouse model exhibiting accelerated accumulation of mtDNA alterations was generated by adding a defective

copy of mitochondrial DNA polymerase in mouse genome (Trifunovic et al., 2004). The "mtDNA-mutator" (*PolgA*$^{mut/mut}$) mice generate new mtDNA mutations resulting in 3 to 5-fold increase in point mutations and higher frequency of deletions at each mtDNA replication. Mutator mice demonstrated that increase in mtDNA mutations beyond physiologic levels induce severe pathology and mortality with maximum lifespan of ~15 months (Trifunovic et al., 2004). Males start losing weight around 4-5 months of age, while weight loss in females is observed after ~6 months of age. As a reference point, decrease in body weight does not start before ~18 months of age in normal (B6;129) mice (Haines, Chattopadhyay, & Ward, 2001). Health defects in mtDNA-mutator mice are observed only after 25 weeks of age and gradually increase, suggesting an age-associated effect which requires accumulation of mtDNA mutations.

However, accelerated health deterioration in mtDNA-mutator mice was *not* due to oxidative damage (Kujoth et al., 2005). As opposed to the view suggesting that accumulation of mtDNA mutations promotes aging by increasing free-radical production and oxidative damage, the mtDNA-mutator mice does not show any indication of increase in oxidative damage or reactive oxygen species despite highly elevated levels of mtDNA mutations and compromised mitochondrial function (Kujoth et al., 2005; Trifunovic et al., 2005; Trifunovic et al., 2004).

These observations demonstrate that, in contrast to earlier assumptions, mtDNA alterations alone do *not* increase reactive oxygen species or oxidative damage. Importantly, the same results also demonstrate that loss of mtDNA integrity is sufficient to induce detrimental pathology and early mortality - but not through oxidative damage. How mtDNA mutations

cause deleterious effects is not known. Health defects in mtDNA-mutator mice are observed only after 25 weeks of age and gradually increased, suggesting an age-associated effect requiring accumulation of mtDNA mutations.

1.2.7.2 Increase in mitochondrial oxidants and oxidative damage

Oxidants are continuously produced as a part of metabolism. Highly reactive oxidants containing oxygen are called "reactive oxygen species (ROS)". Molecular oxygen (O_2) is an abundant oxidant in mitochondria. When reduced by gaining an extra electron it forms a reactive oxygen species, superoxide ($^{\bullet}O_2^-$). Superoxide interacts with protons (H^+) to produce hydrogen peroxide (H_2O_2). Hydrogen peroxide reacts with two protons and two electrons to form water (H_2O). However, hydrogen peroxide can also react with a single electron. This "partial reduction" of hydrogen peroxide produces another reactive oxygen species, hydroxyl radical ($^{\bullet}OH$). Reactive oxygen species can interact with and modify almost any macromolecule including proteins, lipids, and nucleic acids. The damaging activity of reactive oxygen species on cellular structures is referred as "oxidative stress". Excessive oxidative damage in mitochondria can lead to cytochrome c release and apoptosis (Perier et al., 2005).

During mitochondrial respiration, oxygen is normally reduced to water (discussed in section 1.2.3). However, oxygen reduction does not always reach completion. Although with low frequency, incomplete oxygen reduction can produce superoxide radical and hydrogen peroxide, which may induce oxidative damage. Antioxidant enzymes protect the cell from the deleterious effects of the two species by facilitating their conversion into non-reactive

molecules. Superoxide dismutase converts superoxide into oxygen and hydrogen peroxide, which is converted to water by catalase.

In rats, the rate of superoxide and hydrogen peroxide production in heart mitochondria increases with age despite comparable superoxide dismutase activity in young and old rats (Nohl & Hegner, 1978). Organic peroxide content in the mitochondrial membranes is also higher in old rats, suggesting an increase in oxidative damage by age.

Oxidative damage is thought to contribute to aging, and it is suggested that reversal or protection from oxidative damage could lead to prolonged lifespan (Harman, 1956). Consistent with this view, resistance to oxidative damage in primary fibroblasts correlates with maximum lifespan in rodent and primate species (Pickering, Lehr, Kohler, Han, & Miller, 2014). Also, cross-species studies of mammals indicate a negative correlation between maximum life span and rate of mitochondrial superoxide production and H_2O_2 release in liver, kidney, and heart (Ku, Brunk, & Sohal, 1993; Sohal, Svensson, & Brunk, 1990; Sohal, Svensson, Sohal, & Brunk, 1989). In flies, hydrogen peroxide release as well as oxidative protein damage in flight muscle mitochondria increases with age (Sohal & Dubey, 1994; Sohal & Sohal, 1991).

Thioredoxin reductase 2 (TXNRD2) facilitates reduction of hydrogen peroxide; inhibition of TXNRD2 increases hydrogen peroxide release from mitochondria (Stanley et al., 2011). Activity of mitochondrial thioredoxin reductase (TXNRD2), but not of cytosolic thioredoxin reductases (TXNRD1 and TXNRD3), is elevated in cells from long-lived species of rodents, primates, and birds (Pickering, Lehr, Gendron, Pletcher, & Miller, 2017). Association of mitochondrial form of

thioredoxin reductase with longer lifespan is not limited to mammals and birds. Overexpression of mitochondrial Trxr-2 (TXNRD2 ortholog), but not of Trxr-1 (TXNRD1 ortholog), extends median lifespan in fruit flies (Pickering et al., 2017).

Overexpression of mitochondrial superoxide dismutase (SOD-2; also Mn-SOD) (Hu et al., 2007) and mitochondria-targeted overexpression of catalase (Schriner et al., 2005) are found to extend mouse lifespan. However, there are also reports suggesting negative health effects (Levin et al., 1998) and no longevity effect of antioxidant overexpression in mice (Jang et al., 2009; Levin, Christopher, & Crapo, 2005). Interestingly, young adult mice overexpressing extracellular superoxide dismutase show learning impairments (Levin et al., 1998). However, the same mice perform better than normal controls in learning and memory tasks if they are tested at old age (Levin et al., 2005; Levin et al., 2002). No effect on lifespan is detected in these mice (Levin et al., 2005). Previously reported lifespan extension in mice overexpressing SOD2 has been questioned in later studies; although partial reversal of age-associated decline in ATP production is observed SOD2-overexpressing mice, no effect on lifespan was detected (Jang et al., 2009). Therefore, the prolongevity effect of antioxidant overexpression is not decisively established yet.

1.2.7.3 Decline in ETC protein levels and respiratory function

Enzymatic activity assays show that mitochondrial ETC complex I and IV content per total mitochondrial protein mass decrease with age in human skeletal muscle (Boffoli et al., 1994), rat diaphragm (Torii, Sugiyama, Takagi, Satake, & Ozawa, 1992), and rhesus monkey neocortex

(Bowling et al., 1993). A similar age-associated decrease is observed for ETC complex IV in human diaphragm (Muller-Hocker, 1990) and extraocular muscle (Muller-Hocker, Schneiderbanger, Stefani, & Kadenbach, 1992). In rats, cardiac protein levels of cytochrome c subunits Va, Vb, VIc, and ATP synthase subunit beta decrease 20-40% with age, while enzymatic activities of NADH-ubiquinone oxidoreductase and ATP synthase are reduced 46% and 25%, respectively (Preston et al., 2008).

Consistent with a decline in protein levels of respiration complex subunits in mammals, rate of ATP production decreases with age in skeletal muscle of mice (Jang et al., 2009). A similar decline is described in rats. Compared to 6-month-old young adults, 24-month-old rats show 20-25% decay in ATP production rate in heart muscle (Preston et al., 2008).

Rate of respiration for ATP production in rats is stable from 3 months of age to adulthood, but it starts to decline at 16-20 months of age. Respiration rates in heart and skeletal muscle mitochondria of 28-month old rats is 17-19% lower than those of 12-month old rats (Chen, Warshaw, & Sanadi, 1972). An age-dependent decline in respiration rate is also documented in rabbit liver (Klein, Jenkins, Reviczky, & Fisher, 1981).

1.2.7.4 Mitochondrial biogenesis pathway in long-lived mice

Mice fed on a restricted diet, which live longer than mice with unrestricted access to food, exhibit indications of upregulated mitochondrial biogenesis. Calorie restricted (CR) mice show increased mitochondrial volume in skeletal muscle, and this increase requires PGC-1α

expression, which is also found to be upregulated in skeletal muscle of CR mice (Finley et al., 2012). Calorie restriction (both 3-month and 12-month) increases mtDNA content, ATP concentration, and expression of the key regulator of mitochondrial biogenesis *Pgc-1α* and mitochondrial transcription factor *Tfam* at least two-fold in white adipose tissue, and to a lesser extent but significantly in brain, liver, heart, and brown adipose tissue (Nisoli et al., 2005). Skeletal muscle of CR adult mice (12-month old) also shows upregulated nuclear protein levels of PGC-1α and elevated oxygen consumption (Hempenstall, Page, Wallen, & Selman, 2012). Increased respiration is also noted in calorie restricted *S. cerevisiae* (S. J. Lin et al., 2002) and *C. elegans* (Houthoofd et al., 2002).

Pgc-1α mRNA levels are elevated in epididymal fat and kidney from Ames (Menon et al., 2014) and GHR-KO mice (Gesing, Masternak, et al., 2011; Masternak et al., 2012). In GHR-KO mice, higher renal PGC-1α is documented also at protein level (Gesing, Bartke, et al., 2011). Skeletal muscle of GHR-KO mice shows higher average levels of *Pgc-1α* mRNA (Gesing, Masternak, et al., 2011). Of note, aforementioned studies on Pgc-1α expression in GHR-KO mice analyzed either male or female mice for each tissue and the mice were fasted over-night prior to dissection (Gesing, Bartke, et al., 2011; Gesing, Masternak, et al., 2011). Assessment of Pgc-1α expression in a broader set of tissues and metabolic conditions in GHR-KO mice, as well as in other long-lived mutant mice, is necessary to arrive a conclusion.

As noted in previous sections, both Ames and GHR-KO mice are deficient in IGF-1 signaling. Since IGF-1 activity is generally associated with organismal growth and anabolic metabolism,

the counterintuitive Pgc-1α upregulation in IGF-1-deficient mice seems to be an indirect effect. It would be of interest to see whether Snell mice, which are also deficient in GH/IGF-1 signaling, have elevated expression of Pgc-1α and other genes involved in mitochondrial biogenesis.

1.2.7.5 Mitochondrial stress response in aging and longevity

Lifespan extension in *C. elegans* can be induced by partial defects in mitochondrial protein homeostasis including those caused by mutations in ETC genes (Feng, Bussiere, & Hekimi, 2001), RNAi-mediated silencing of nuclear-encoded mitochondrial protein expression (Hamilton et al., 2005), and pharmacologic inhibition of mitochondrial translation (Tsang, Sayles, Grad, Pilgrim, & Lemire, 2001).

Electron transport chain complex IV subunit *cco-1* ("cytochrome c oxidase-1 subunit Vb"; *C. elegans* homolog of mammalian *Cox5b*) is one of the ETC genes whose inhibition results in prolonged lifespan in worms. It is found that, concurrent with lifespan extension, *C. elegans* deficient in *cco-1* expression exhibit upregulated expression of *hsp6* ("Heat shock protein 6"; mtUPR gene in *C. elegans*), suggesting involvement of mtUPR in nematode longevity (Durieux et al., 2011). Importantly, temporary knock-down of *cco-1* during the larva stage is sufficient for inducing lifespan extension and *hsp6* upregulation. Moreover, upregulated levels of *hsp6* expression persists throughout the worm lifespan even when the initial mitochondrial stress is discontinued. This observation indicated that short-term exposure to mitochondrial stress early in life can induce permanent reprogramming of the mtUPR pathway, and upregulation of mtUPR may be the factor that drives lifespan extension in worms. In line with this view, muscle-

specific overexpression of Hsp70F, a putative mtUPR protein in nematodes, result in more than 40% increase in worm lifespan (Yokoyama et al., 2002).

Partial deficiency in expression of mitochondrial genes can also extend mouse lifespan. *Mclk1* is the mouse orthologue of the *C. elegans* gene *clk-1*, a mitochondrial enzyme involved in ubiquinone biosynthesis. Mice homozygous for *Mclk1* deletion (*Mclk1*$^{-/-}$) are not viable (Levavasseur et al., 2001). However, deletion of only one copy of *Mclk1* increases both mean and the maximum lifespan, suggesting evolutionary conservation of mitochondrial-defect-mediated longevity pathway. Mitochondrial defects including reduced ATP synthesis are noted in Mclk1$^{+/-}$ mice (Lapointe & Hekimi, 2008), but it is not known whether they exhibit upregulated mtUPR.

A cross-species study found a correlation between maximum lifespan and HSP60 levels in liver, heart, and brain among species of mammals (Salway, Gallagher, Page, & Stuart, 2011). However, it is not yet known whether mtUPR is elevated in any of the long-lived mouse models.

1.3 Regulation of mRNA translation by N^6-adenosine methylation

Molecular pathways of the cell are highly regulated by chemical modifications targeting protein, DNA, and RNA molecules. Phosphorylation of certain key proteins, for example, can alter a wide range of cellular functions including protein synthesis, replication, and apoptosis. Eukaryotic messenger RNA molecules are also subject to post-synthesis modifications.

1.3.1 N^6-methyladenosine mRNA modification

Polyadenylation of mRNA in eukaryotes was discovered in 1971 (Darnell, Wall, & Tushinski, 1971; Edmonds, Vaughan, & Nakazato, 1971; S. Y. Lee, Mendecki, & Brawerman, 1971). This important finding led to rapid development of RNA isolation protocols based on mRNA polyadenylation which allowed preparation of sufficiently pure mRNA samples by reducing rRNA contamination (Brawerman, Mendecki, & Lee, 1972; Nakazato & Edmonds, 1972; Sheldon, Jurale, & Kates, 1972). In 1974, Perry and Kelley isolated polyadenylated mRNAs from mouse L cells labeled with ^3H methyl methionine and found that mRNA molecules were methylated in both ribose and base moieties (Perry & Kelley, 1974). The methylated residue was identified as N^6-methyladenosine (Desrosiers, Friderici, & Rottman, 1974; Perry, Kelley, Friderici, & Rottman, 1975).

Although the methylation of N^6-adenosine (N^6-methyladenosine; m^6A) in eukaryotic mRNA had been described by independent groups by 1975, it was not readily accepted as a biologically

relevant modification. The arguments about purity of analyzed mRNA samples persisted for the next couple of decades.

Nevertheless, in 2012, two independent reports reignited the interest in m^6A modifications. Application of transcriptome-wide m^6A-specific methylated mRNA immunoprecipitation followed by high-throughput sequencing referred as "m^6A-seq" (Dominissini et al., 2012) or "MeRIP-seq"(Meyer et al., 2012) led to the identification of ~13 thousand putative m^6A sites. The m^6A sites were found on coding sequences, 3'UTR, and with less abundance in the 5'UTR. The m^6A distribution data from these two transcriptome-wide studies established the first m^6A methylome. They also showed that the m^6A modification is dynamically regulated and preferentially associated with certain mRNA-binding proteins (Dominissini et al., 2012; Meyer et al., 2012).

Transcriptome-wide identification of m^6A sites at single nucleotide resolution

A transcriptome-wide m^6A screening study using "m^6A individual-nucleotide cross-linking and immunoprecipitation (miCLIP)" on human embryonic kidney cells, identified ~9000 putative m^6A sites (Linder et al., 2015). Another m^6A-seq analysis of changes in methylation patterns upon heat stress in mouse embryonic kidney cells suggested that increased m^6A marks in 5'UTR may play a role in translation of stress-induced mRNAs, and provided hints for an alternative translation mechanism not dependent on the 5'7-methylguanosine (m^7G) cap (J. Zhou et al., 2015). Independently, an *in vitro* toeprinting analysis using m^6A-containing synthetic mRNA, which allows dissection of individual components required for translation initiation, indicated

that translation-initiation complexes can form on m^6A-contatining mRNA even in the absence of cap(m^7G)-binding initiation factor eIF4E (Meyer et al., 2015).

In addition to setting the stage for investigation of m^6A-mediated cap-independent translation as a putative translation regulation mechanism, these studies provided insightful findings on the dynamic regulation of m^6A modifications, which will be discussed next.

1.3.1.1 Dynamic regulation of m^6A modifications

The m^6A modification status of mRNA transcripts is determined by the opposing actions of enzymes acting as m^6A "writers", which add methyl groups to adenine residues, and "erasers", which remove these methyl marks.

1.3.1.2 Addition of m^6A modifications

Early biochemical studies investigating the methylation of 20-nucleotide-long RNA polymers in a solution containing HeLa cell nuclear extracts found that m^6A modifications were preferentially located on specific mRNAs containing the consensus sequence GGACU with some variations (Harper, Miceli, Roberts, & Manley, 1990). Combined with other reports suggesting GAC, and with a lower frequency AAC, as targets of N^6-adenosine methylation, the nucleotide sequence G/A - $\underline{m^6A}$ - C emerged as the consensus sequence (Schibler, Kelley, & Perry, 1977). The proposed GAC / AAC consensus sequence has been confirmed by transcriptome-wide studies and broadened to DRACH (D=A/G/U; R=G(%70)/A(30%); H=A/C/U) motif, where A in the middle is the target of methylation (Linder et al., 2015). Of note, it is also established that *not*

all DRACH sequences are methylated; and most, but not all, m^6A modifications are found on DRACH sites (Linder et al., 2015).

The sequence specific nature of methylation implied that m^6A modifications did not occur randomly and presumably involved specific methyltransferases indicating the presence of a regulated methylation pathway with biological relevance.

1.3.1.2.1 METTL3 and METTL14

Methylation of N^6-adenosine mRNA residues is thought to be carried out by two methyltransferases designated methyltransferase-like 3 (METTL3) and 14 (METTL14).

METTL3 (also "N^6-adenosine-methyltransferase 70 kDa subunit") was purified from a protein complex referred as "mRNA N^6-adenosine methyltransferase" due to its ability to add methyl groups to N^6-adenosines *in vitro* (Bokar, Rath-Shambaugh, Ludwiczak, Narayan, & Rottman, 1994). Specificity of its methyltransferase activity on the previously described GAC and AAC sequences confirmed its role in N^6-adcenosine methylation (Narayan, Ludwiczak, Goodwin, & Rottman, 1994).

METTL3 has a *S*-Adenosyl methionine (SAM)-binding methyltransferase domain. Its homologues are found in the yeast *S. cerevisiae* (Clancy, Shambaugh, Timpte, & Bokar, 2002) and fruit fly *D. melanogaster* (Hongay & Orr-Weaver, 2011), both referred as "inducer of meiosis 4 (Ime4)".

METTL14 is the second of the two methyltransferases found in the N^6-adenosine-methyltransferase complex. It was recently identified by its interaction with METTL3 (Havugimana et al., 2012). Similar to METTL3, it methylates N^6-adenosines residing in GAC sequences *in vitro* (Ping et al., 2014), and forms protein complexes with METTL3 in cells (Liu et al., 2014; Y. Wang et al., 2014).

Both METTL3 and METTL14 can individually mediate the formation of m^6A mRNA modifications *in vitro*; however, when they are both present, their total methyltransferase activity is higher than the sum of their individual activities (Liu et al., 2014; Y. Wang et al., 2014), suggesting that their interaction may be required for increased enzymatic activity and either one of them is not sufficient alone. Supporting this idea, single knockdown of Mettl3 or Mettl14 in mouse embryonic stem cells results in partial reduction of m^6A modifications and disrupts stem cell maintenance (Y. Wang et al., 2014). It is not known whether the two enzymes target distinct populations of mRNAs.

1.3.1.2.2 WTAP

Wilms tumor 1-associated protein (WTAP) is also found in the N^6-adenosine methyltransferase complex (Liu et al., 2014). Although it does not show enzymatic activity, its interaction with N^6-adenosine methyltransferase subunits may be required for efficient mRNA methylation (Zhong et al., 2008).

1.3.1.3 Removal of m^6A modifications

The discovery of enzymes that could reverse m^6A modifications was particularly important. The opposing activity of m^6A methyltransferases and demethylases would provide a mechanism for dynamic m^6A regulation. Enzymatic control of N^6-adenosine methylation status in both directions was highly suggestive for a potential role of m^6A modifications in cellular function.

The reversion of N^6-adenosine modifications is achieved by demethylation. Two enzymes, fat mass and obesity-associated protein (FTO) and α-ketoglutarate-dependent dioxygenase alkB homologue 5 (ALKBH5), are thought to mediate demethylation of m^6A.

Although yeast has the machinery for m^6A addition (Schwartz et al., 2013), no enzymes for m^6A demethylation have been found so far. So, in some organisms negative regulation of m^6A mRNAs may be through passive mechanisms such as mRNA degradation.

1.3.1.3.1 FTO

The *Fto* gene was identified in 1999; its name (Peters, Ausmeier, & Ruther, 1999) reflects its deletion in fused-toes (ft) mice (van der Hoeven et al., 1994). In 2007, multiple studies found that human obesity showed a strong association with a single nucleotide polymorphism in the *FTO* gene which increases FTO expression. When the linkage between *FTO* and obesity had been established, its name was changed to “fat mass and obesity-associated protein,” abbreviated as “FTO,” avoiding inconsistency in the literature.

Fto-deficient mice are leaner, but show reduced growth starting 2 days after birth and exhibit 40% decrease in survival at 4 weeks of age (Fischer et al., 2009). In humans, FTO is required for development. A rare *FTO* mutation causing loss of function was detected in a family with severe phenotype. All eight children homozygous for the mutation had multiple health problems and died before the age of three. Thus, FTO function is indispensable for mammals.

FTO can demethylate m^{6}A. FTO is closely related to the bacterial alpha-ketoglutarate-dependent dioxygenase (AlkB) and its human homologues ABH2-3 (Gerken et al., 2007; Sanchez-Pulido & Andrade-Navarro, 2007). It catalyzes the oxidative demethylation of methylated thymidine and uracil (Gerken et al., 2007; G. Jia et al., 2008). Importantly, FTO can demethylate m^{6}A. Its overexpression in HeLa cells reduces m^{6}A levels in mRNA, while its knock-down increases them.

1.3.1.3.2 ALKBH5

Alkbh5-deficient mice are viable and exhibit good health at adulthood, except for a lower rate of successful breeding, presumably due to an increase in apoptotic cells in the testes and compromised spermatozoal motility detected in males (Zheng et al., 2013). Testis-specific deficiency in *Alkbh5*$^{-/-}$ is consistent with the pattern of *Alkbh5* expression in tissues of normal mice; the highest *Alkbh5* mRNA levels were found in testis, followed by lung, spleen, kidney and liver (Zheng et al., 2013).

ALKBH5 demethylates m^{6}A. *Alkbh5*$^{-/-}$ mice also show an increase in m^{6}A levels in lung and in testicular cells purified from seminiferous tubules. In HeLa cells, siRNA-mediated knock-down of ALKBH5 results in an increase in relative amount of m^{6}A compared to total cellular mRNA, whereas ALKBH5 overexpression decreases it (Zheng et al., 2013). The increase in m^{6}A in the tissues of *Alkbh5* knock-out mice where it is normally expressed the most, and in HeLa cells with suppressed ALKBH5 expression, suggest that ALKBH5 may have a role in m^{6}A demethylation. Indeed, biochemical analysis show that recombinant human ALKBH5 can completely demethylate m^{6}A in single stranded RNA *in vitro (Zheng et al., 2013)*, with an activity comparable to FTO (G. Jia et al., 2011). Moreover, proteomics analysis of mRNA-bound proteins in human embryonic kidney cells identified 800 mRNA-binding proteins including ALKHB5, which is confirmed to bind mRNA in an independent assay (Baltz et al., 2012).

Thus, the role of ALKHB5 and FTO in m^{6}A demethylation is well established, but the functional consequences of m^{6}A regulation have been uncovered only in last few years with the discovery of a new mRNA translation mechanism.

1.3.1.4 Recognition of m^{6}A modifications

Enzymatic control of m^{6}A addition by METTL3 and METTL14, and its removal by FTO and ALKHB5, suggested a functional role for m^{6}A modifications. Alteration of protein binding by chemical modification of nucleoside residues is a common regulatory mechanism in eukaryotes. Studies of RNA pulldown in mammalian cells followed by mass spectrometry analysis identified several proteins that preferentially bind to mRNAs bearing m^{6}A modifications (m^{6}A-mRNAs),

including YTH domain-containing family (YTHDF) proteins YTHDF1, YTHDF2, and YTHDF3 (Dominissini et al., 2012; X. Wang et al., 2014).

1.3.1.4.1 YTHDF1

Research on m^{6}A function highly benefited from development of new transcriptome-wide techniques for the assessment of protein-binding sites on mRNAs in living cells. Analysis of mRNA-protein interactions in HeLa cells by photoactivatable ribonucleoside crosslinking and immunoprecipitation (PAR-CLIP)(C. Zhang & Darnell, 2011) and RNA immunoprecipitation followed by high throughput sequencing (RIP-seq) showed that YTHDF1 binds to m^{6}A bearing mRNAs and facilitates their translation in HeLa cells (X. Wang et al., 2015).

Knock-down of YTHDF1 does not alter the m^{6}A/A ratio in HeLa cells, suggesting that YTHDF1 associates with but does not modify m^{6}A residues. However, overexpression of YTHDF1 in the same cell line increases the m^{6}A/A ratio in mRNA. This may represent an artificial increase in m^{6}A-mRNA stability as a result of elevated YTHD1 binding or may represent a stabilizing effect of active translation. Nevertheless, the current data is not sufficient for ruling out a possible effect of YTHDF1 on mRNA stability.

Experiments in HeLa cells with N_YTHDF1(N-terminal-domain)-tethered IRES reporters with varying dependency on eIFs suggested that YTHDF1-mediated translation requires eIFs and probably requires eIF4G-dependent loop formation (X. Wang et al., 2015).

1.3.1.4.2 YTHDF2

An analysis of the individual effects of YTHDF1 and YTHDF2 knock-downs in HeLa cells showed that 50% of the mRNA transcripts bound by one of them are also bound by the other. YTHDF1 knock-down decreases the translation of these "common target" mRNAs without altering their average lifetime; for YTHDF2, on the other hand, knock-down increases their average lifetime, with little effect on translation efficiency. These observations suggest that while YTHDF1 binding promotes translation, YTHDF2 binding promotes degradation (X. Wang et al., 2015).

Seemingly opposing actions of the two YTHDF proteins may be ideal for a hypothetical scenario where a short pulse of protein synthesis is required: YTHDF2 would promote degradation of m^6A-mRNAs, leaving a small time window for their translation, and YTHDF1 would enable rapid translation of those transiently-available mRNAs. In agreement with this idea, pulse-chase experiments suggest a sequential binding – most of the time, YTHDF1 binds to nascent mRNAs earlier than YTHDF2 (X. Wang et al., 2015).

1.3.1.4.3 Other proteins

Methylated RNA-binding 1 (Mrb1), the yeast homologue of YTHDF proteins, also has a YTH RNA binding domain, and binds to m^6A-mRNAs in yeast (Schwartz et al., 2013). Pulldown studies on yeast extracts also found additional proteins associated with m^6A-mRNAs. However, since pulldown results do not discriminate between proteins directly interacting with m^6A

modifications and those interacting with other parts of the ribonucleoprotein complex, assessment of the role of these proteins on m^6A-mRNA recognition requires further research.

1.3.2 m^6A-mediated cap-independent translation

Protein synthesis in eukaryotic cells is mainly achieved by a mechanism referred as "cap-dependent translation", which requires recognition of the 5' N^7methylguanosine(m7G) cap for translation initiation. Briefly, the eukaryotic translation initiation complex eIF4F, which consists of initiation factors eIF4E, eIF4G, and eIF4A, binds to the 5'cap and recruits 40S ribosomal subunit and other initiation factors to initiate mRNA translation. However, some mRNAs can be translated by a cap-independent process, which can proceed even under conditions where eIF4F-mediated cap-dependent translation initiation is compromised. One such mechanism relies on 5'UTR internal ribosome entry site (IRES) motifs which are found in viral mRNAs but rarely observed in eukaryotic mRNAs. Maintenance of eukaryotic protein synthesis under conditions where cap-dependent translation initiation machinery is not functional indicates existence of an alternative translation pathway.

The proposal of m^6A-mediated cap-independent translation as an alternative translation mechanism is very recent. The first hints of a possible role of 5'UTR m^6A modifications in facilitating mRNA translation independent of the cap-dependent translation initiation mechanism were provided by studies combining high-throughput approaches including transcriptome-wide immunoprecipitation of m^6A-containing mRNAs, parallel sequencing, and

use of genomic database resources for sequence alignment (Meyer et al., 2015; J. Zhou et al., 2015). Follow up studies (Coots et al., 2017) established that certain mRNA transcripts bearing 5'UTR m^6A modifications can be translated in a cap-independent manner. This mechanism is referred as m^6A-mediated cap-independent translation (hereafter "m^6A-CIT").

1.3.2.1 Current model of m^6A-mediated cap-independent translation regulation

According to a current model (Fig. 1.1), METTL3 and METTL14 preferentially methylate adenosine residues found in DRACH (D=A/G/U; R=G/A; H=A/C/U) motifs to form N^6-methyladenosine. The N^6-methyladenosine modifications can be reversed by two demethylases FTO and ALBH5. YTHDF proteins recognize and bind to m^6A-bearing mRNAs and facilitate their translation either by recruiting translation initiation factors or by increasing their stability. ABCF1 has been suggested as another m^6A "reader" in a recent report (Coots et al., 2017), but further studies are needed to confirm its role in m^6A-CIT.

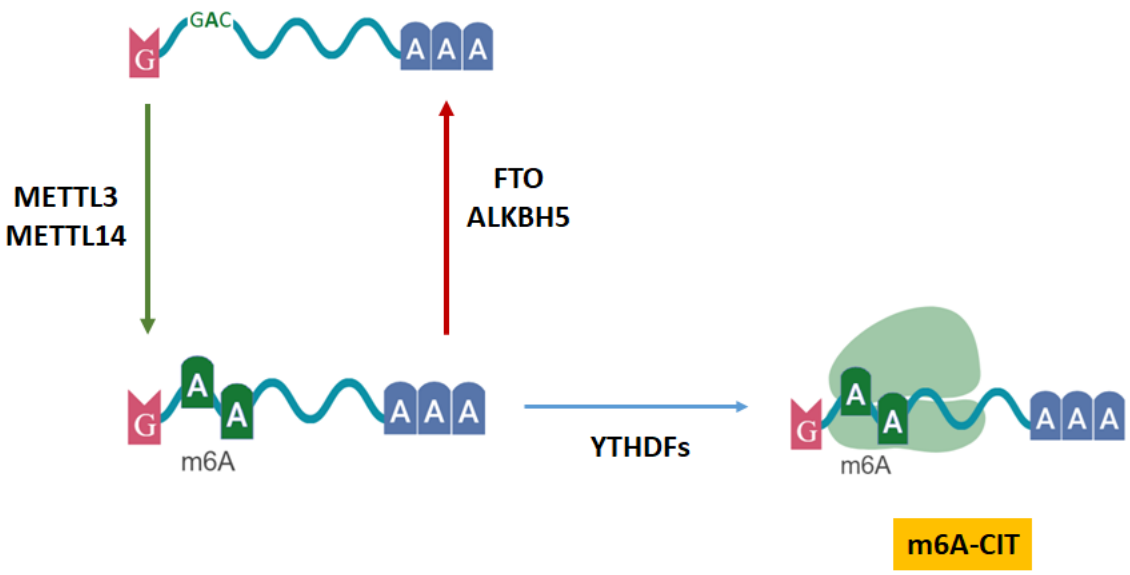

Figure 1.2 Regulation of m^{6}A-CIT by "writer", "eraser" and "reader" proteins.

METTL3 and METTL14 add m^{6}A modification to mRNA transcripts in 5'UTR. FTO and ALKBH5 remove m^{6}A marks. YTHDF1 and YTHDF2 recognize m^{6}A marks and promote translation of m^{6}A-bearing transcripts through m^{6}A-CIT.

Chapter 2 - Mitochondrial stress response in fibroblasts from long-lived Snell mice

2.1 Introduction

Primary fibroblasts isolated from Snell mice are more resistant to cell death induced by UV radiation, hydrogen peroxide, cadmium, and paraquat (Murakami et al., 2003). Among those, paraquat is known to induce mtUPR in *C. elegans* (Yoneda et al., 2004). Hence, higher paraquat resistance of Snell fibroblasts may be partly due to an improved mitochondrial stress response. It is not known whether Snell fibroblasts exhibit elevated mtUPR.

A recent study showed that, primary cells derived from long-lived *Surf1 -/-* mice (Dell'agnello et al., 2007) exhibit higher survival rate and mtUPR protein levels after treatment with certain doses of paraquat (Pharaoh, Pulliam, Hill, Sataranatarajan, & Van Remmen, 2016). Basal mtUPR, as measured by the abundance of mtUPR proteins HSP60 and LONP1, is also higher in primary fibroblasts from *Surf1 -/-* mice. Mitochondrial function was not assessed in this study, so it is not known to what extent *Surf1 -/-* fibroblasts, which show elevated mtUPR, can maintain ATP production or oxidative respiration after paraquat treatment.

The mitochondrial stress response pathway can be analyzed in two different parameters. The first parameter is “basal mtUPR”, which is measured by abundance of mtUPR proteins in the absence of any imposed mitochondrial stressor. The second parameter is “mtUPR induction”,

which is the percentage increase in the mtUPR protein levels after exposure to a specific form and dose of stress. Since the cell culture conditions may intrinsically induce mitochondrial stress, the "basal mtUPR" measurements in cell culture studies may not be sufficient for assessment of mtUPR. We measure both parameters to understand how Snell cells differ from normal cells in (i) basal expression levels of mtUPR proteins, and (ii) their capacity to respond to mitochondrial stress.

Prior data on primary fibroblasts isolated from Snell dwarf mice indicate comparable mitochondrial abundance (Page et al., 2009). However, similar levels of mitochondrial content does not imply comparable mitochondrial function, as exemplified by brown fat mitochondria in *Pgc-1α*$^{-/-}$ mice, where mitochondrial function is compromised despite normal levels of mitochondrial abundance (Leone et al., 2005). In addition to mtUPR, we assess mitochondrial function after mitochondrial stress exposure by measuring cellular ATP content and real-time oxidative respiration rates in normal and Snell cells.

2.2 mtUPR in Snell cells in response to mitochondrial stress

HSP60 is required for folding of mitochondrial peptides into functional proteins, and its expression increases as a part of the mtUPR (Martinus et al., 1996). Doxycycline, an antibiotic of the tetracycline class, binds to the larger subunit of bacterial and mitochondrial ribosomes in their mRNA-bound state. Doxycycline binding halts mitochondrial translation, results in loss of ribosome-bound mRNA molecules through degradation, disrupts electron transport chain protein stoichiometry, and induces mtUPR.

We compared levels of HSP60 in Snell and control fibroblasts with or without exposure to doxycycline. HSP60 levels in Snell cells were significantly elevated compared to normal cells without exposure to doxycycline (Fig. 2.1A, B). Doxycycline treatment increased HSP60 levels in both normal and Snell cells, as expected ($p=0.001$ for drug effect), and Snell cells had higher levels of HSP60 than normal cells. We did not detect a difference in the response of Snell versus normal cells by two-way ANOVA interaction analysis ($p=0.19$). Another indicator of mtUPR, mitochondrial protease LONP1, was also elevated in Snell cells with or without doxycycline exposure (Fig. 2.1A, C). The degree of LONP1 upregulation in response to doxycycline did not differ between normal and Snell cell types.

Thiamphenicol, another inducer of mtUPR, blocks mitochondrial translation by interacting with the smaller subunit of the mitochondrial ribosome, a mode of action distinct from that of doxycycline. Compared to normal cells, we noted significantly higher levels of HSP60 in Snell cells (Fig. 2.2A, B), regardless of thiamphenicol treatment. In response to thiamphenicol

treatment, HSP60 induction was higher in Snell cells (p=0.0005 for the interaction term). Snell cells had higher LONP1 levels with or without thiamphenicol exposure, but unlike doxycycline, thiamphenicol had no significant effect on LONP1 levels (Fig. 2.2A, C).

We considered the hypothesis that elevated levels of HSP60 and LONP1 might reflect higher levels of mitochondria in Snell fibroblasts, despite flow cytometric data to the contrary (Page et al., 2009). We therefore measured levels of ATP5A and UQCRC2, mitochondrial ETC proteins encoded in the nucleus, and saw no difference between Snell and control cells (Fig. 3A-B). Differences in mitochondrial content in two cell populations can also be detected by comparing mtDNA/nDNA ratios. We measured mtDNA/nDNA ratio in Snell and normal cells by performing qPCR for nucleotide sequences residing in the *Atp6* gene in mtDNA and in the *Hsp60* gene in nDNA. We found no differences in ratio of mitochondrial DNA to nuclear DNA (Fig. 2.4A). We confirmed our findings with another pair of mtDNA/nDNA sequences residing in mitochondrial *CoxI* and nuclear *CoxIVi* genes, both of which encode subunits of ETC complex IV (Fig. 2.4B).

Taken together, our results indicate that the mitochondrial chaperone HSP60 and mitochondrial protease LONP1, two components of the mitochondrial stress response, are elevated in Snell cells, and remain so after exposure to either of two inducers of mitochondrial stress.

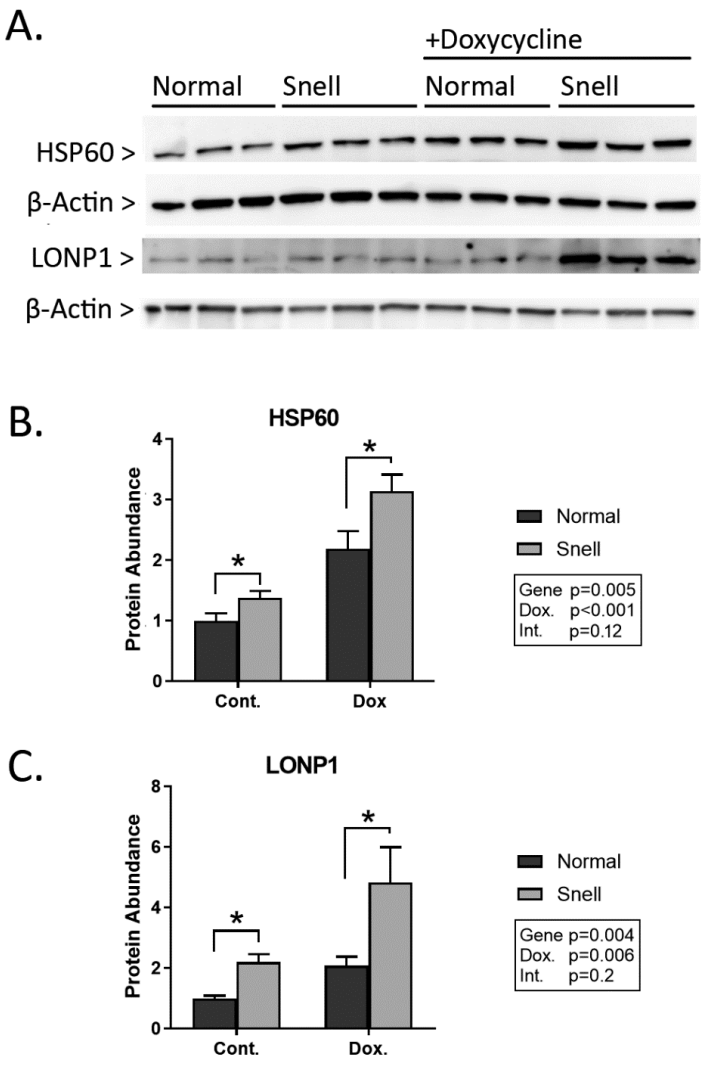

Figure 2.1 HSP60 and LONP1 protein levels after doxycycline treatment.

(A) Immunoblot for HSP60 and LONP1 in normal and Snell cells after 48 hr. exposure to control media or media with 30 ng/ul doxycycline. β-actin is shown as a loading control. (B) Mean and SEM for N=6 mice for HSP60 and (C) LONP1. (*) indicates $p < 0.05$ by Student's t-test for comparison between normal and Snell cells. Results of two-factor ANOVA are shown in the boxed inset, with p-values for the interaction ("Int.") effects.

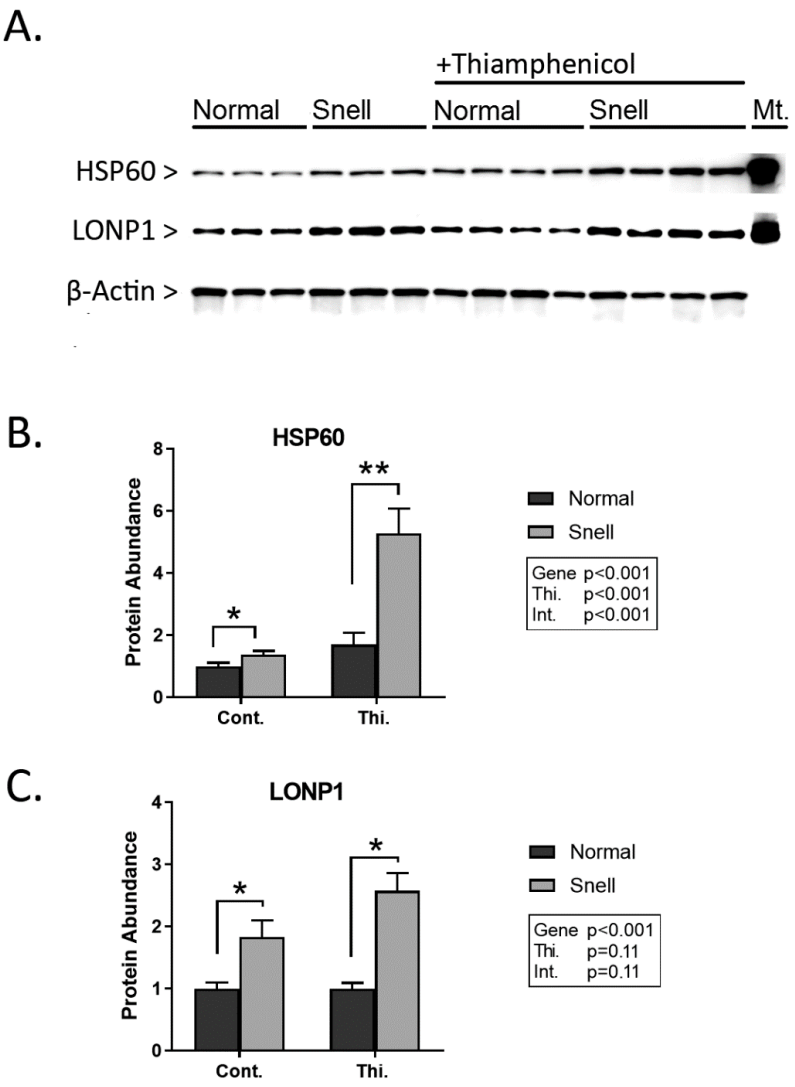

Figure 2.2 HSP60 and LONP1 protein levels after thiamphenicol treatment.

(A) Immunoblot for HSP60 and LONP1 in normal and Snell cells after 48 hr. exposure to control media or media with 50 ng/ul thiamphenicol. Lane 'Mt.' is mitochondria sample isolated from rat heart as positive control. (B) Results for HSP60 and (C) LONP1. (*) indicates $p < 0.05$; (**) indicates $p < 0.01$ by Student's t-test for comparison between normal and Snell cells (N=3-4). Results of two-factor ANOVA are shown in the boxed inset, with p-values for the Interaction ("Int.") effects.

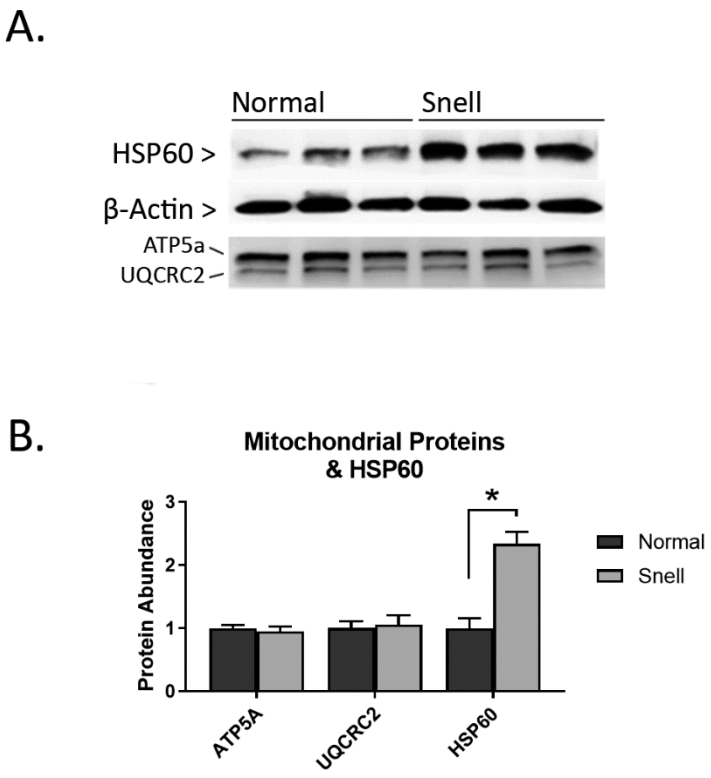

Figure 2.3 Levels of mitochondrial proteins in normal and Snell cells.

(A) Immunoblot for HSP60 and mitochondrial proteins ATP5A and UQCRC2 in normal and Snell fibroblasts; with β-actin shown as a control. Three mice of each genotype are shown. (B) Statistical results for N=3 mice of each genotype. (*) indicates $p < 0.05$ by Student's t-test for comparison between normal and Snell cells.

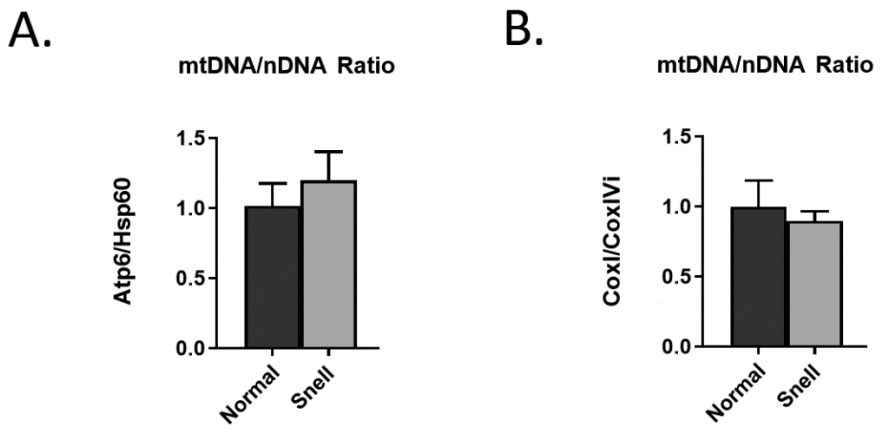

Figure 2.4 Mitochondrial DNA to nuclear DNA ratios in normal and Snell cells.

Ratio of mitochondrial DNA levels to nuclear DNA levels measured by (A) *Atp6*/*Hsp60*, and (B) as *CoxI*/*CoxIV* in primary fibroblasts from normal and Snell mice (N=6). No significant difference between normal and Snell fibroblasts is detected by Student's t-test.

2.3 Electron transport chain protein stoichiometry after stress exposure

The electron transport chain (ETC), a multi-component system needed for oxidative respiration, is formed by a combination of peptides, some of which are encoded in nuclear DNA and others in mitochondrial DNA. In order to examine the relative levels of mitochondrial versus nuclear transcripts after mitochondrial stress, we measured the change in the expression of mtDNA-encoded cytochrome c oxidase subunit 1 (*CoxI),* and nDNA-encoded cytochrome c oxidase subunit 4 (*CoxIVi)*, each of which is a subunit of ETC complex IV.

Nuclear DNA-encoded gene expression (*CoxIVi)* was not inhibited by doxycycline in either Snell or control cells, confirming specific inhibition of mitochondrial translation and reduction in mitochondrial mRNA levels (Fig. 2.5A). Of note, a change in the opposite direction was noted, where nDNA-encoded *CoxIVi* transcript levels were higher after doxycycline treatment.

We observed a decrease of more than 50% in the expression of mtDNA-encoded *CoxI* in normal cells exposed to doxycycline, but doxycycline had no effect in Snell cells, suggesting resistance of Snell cells to doxycycline-mediated reduction of mitochondrial transcript levels (Fig. 2.5B).

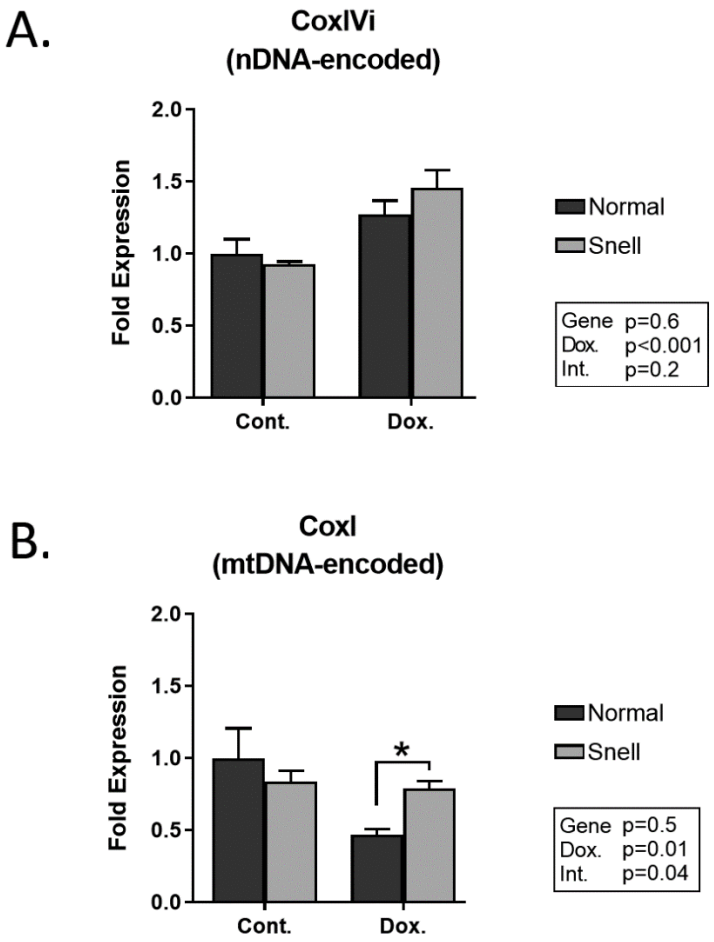

Figure 2.5 Snell cells maintain mtDNA-encoded *CoxI* transcript levels after doxycycline exposure.

(A) Average values of Nuclear-DNA-encoded (*CoxIVi*) and (B) mitochondrial-DNA-encoded (*CoxI*) transcript levels in normal and Snell fibroblasts. Error bars represent SEM. (*) indicates $p < 0.05$ by Student's t-test for comparison between normal and Snell cells (N=6). Results of two-factor ANOVA are shown in the boxed inset, with p-values for the Interaction ("Int.") effects.

2.4 Induction of the mitochondrial biogenesis pathway in response to mitochondrial stress

We considered two possible explanations for maintained mtDNA-encoded gene expression in Snell cells. The efficacy of doxycycline might be low on Snell cells; the failure of the drug to halt mitochondrial translation and induce degradation of ribosome-bound mRNAs might be due, for example, to rapid degradation of the drug by Snell fibroblasts. Alternatively, doxycycline might inhibit mitochondrial translation effectively, but Snell cells may have a mechanism to compensate for this effect.

To address the first idea, we noted that in both cell types doxycycline treatment resulted in a similar upregulation of *Hsp60* and *Hsp10* gene expression, which confirms that this drug is indeed effective on Snell fibroblasts, and activates the mtUPR as expected (Fig. 2.6). Accordingly, we next focused on pathways which might protect Snell cells from doxycycline effects by increasing mitochondrial transcription and biogenesis. We found that, in response to doxycycline treatment, the level of increase in mRNA for *Tfam* (Mitochondrial Transcription Factor A), a regulator of mitochondrial transcription, was 2-fold higher in Snell cells (Fig. 2.7A). In addition, mRNA for *Pgc-1α*, the main regulator of mitochondrial biogenesis, was upregulated only in Snell cells (Fig. 2.7B). Intrigued by Snell cell-specific upregulation *Pgc-1α* transcript levels by doxycycline, we measured PGC-1α protein levels before and after exposure to thiamphenicol, which also induces mitochondrial stress. Thiamphenicol exposure led to higher PCG-1α protein levels in Snell cells compared to control cells (Fig. 2.8A, B).

We also noted that, prior to stress exposure, Snell fibroblasts showed higher PGC-1α protein expression (Fig. 2-8A, B) despite comparable mRNA levels of (Fig 2.7A, B). This phenotype is investigated separately and presented in Chapter 4.

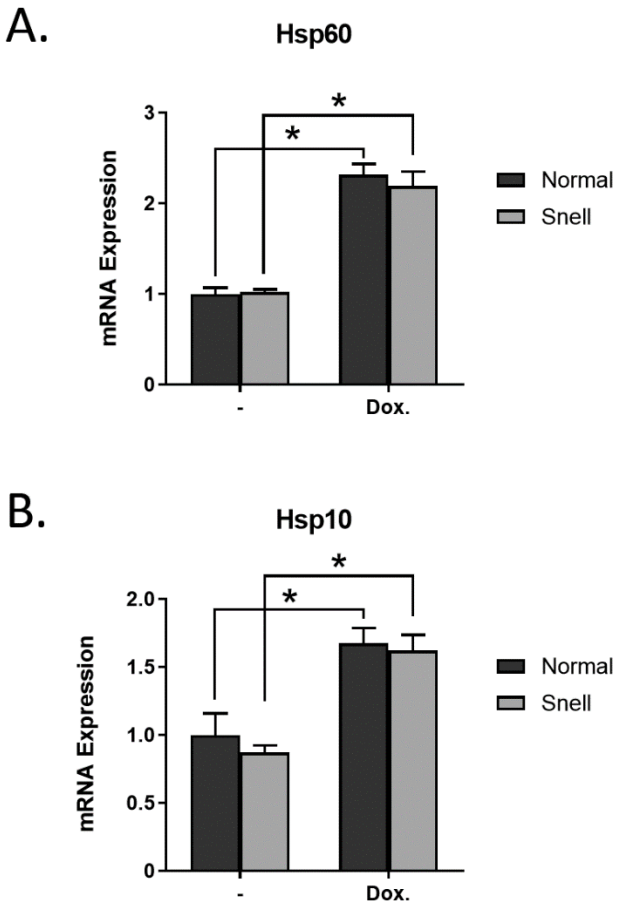

Figure 2.6 Normal and Snell cells show similar levels of *Hsp60* and *Hsp10* mRNA upregulation.

(A) Mean *Hsp60* and (B) *Hsp10* transcript levels in normal and Snell cells before and after doxycycline treatment. Error bars represent SEM. (*) indicates $p < 0.05$ by Student's t-test for comparison between mock and doxycycline treated cells (N=6).

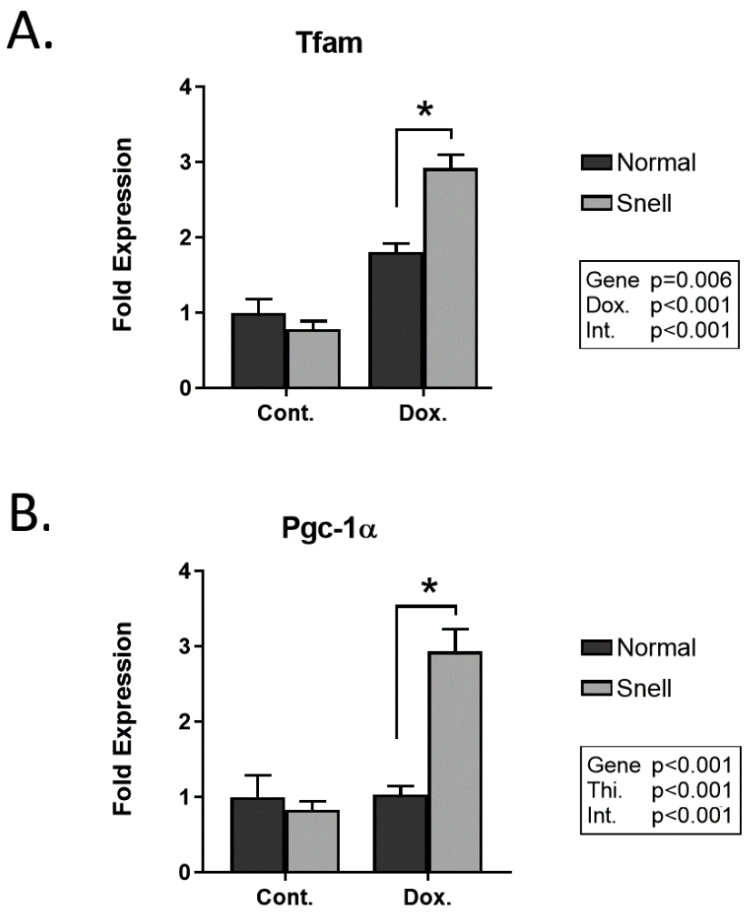

Figure 2.7 *Tfam* and *Pgc-1α* are upregulated in Snell cells in response to mitochondrial stress.

(A) *Tfam* and (B) *Pgc-1α* mRNA levels after doxycycline treatment in normal and Snell primary fibroblasts for N=6 mice. Error bars represent SEM. (*) indicates $p < 0.05$ by Student's t-test for comparison between normal and Snell cells. Results of two-factor ANOVA are shown in the boxed inset, with p-values for the Interaction ("Int.") effects.

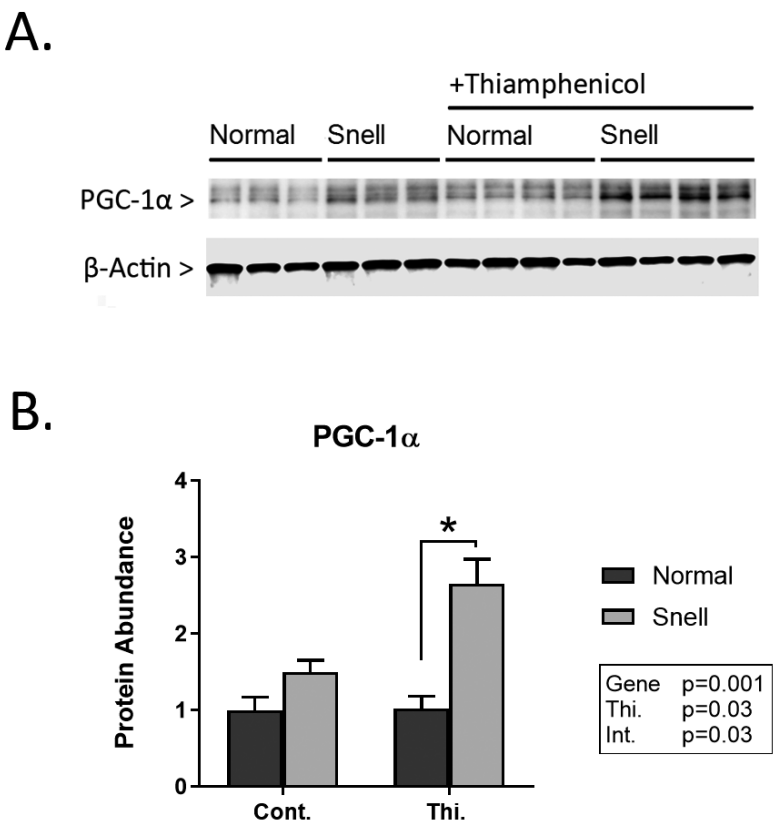

Figure 2.8 Higher levels of PGC-1α protein expression in Snell cells after mitochondrial stress.

(A) Western blot image and (B) average values for PGC-1α protein expression after thiamphenicol treatment in normal and Snell fibroblasts for N=3-4 mice. Error bars represent SEM. (*) indicates $p < 0.05$ by Student's t-test for comparison between normal and Snell cells. Results of two-factor ANOVA are shown in the boxed inset, with p-values for the Interaction ("Int.") effects.

2.5 Snell cells are resistant to mitochondrial stress

Snell fibroblasts were previously found to exhibit higher survival rates (as measured by the WST-1 cell viability assay) compared to those of normal cells after exposure to UV radiation, hydrogen peroxide, paraquat, and cadmium (Murakami et al., 2003). Our results demonstrating elevated levels of basal and induced mtUPR in Snell cells (Figures 2.1 and 2.2) suggested that Snell cells might be better protected from mitochondrial stressors, such as doxycycline.

Treatment of fibroblasts with 30 ng/µl doxycycline does not induce cell death in 48 hours, but upregulates mtUPR in primary mouse fibroblasts. To investigate whether Snell fibroblasts resist lethal and metabolic effects of mitochondrial stress, we measured cell viability using a WST-1 assay after exposing cells to 30 ng/µl and higher doses of doxycycline for 72 hours. Both normal and Snell fibroblasts showed a dose-dependent response (Fig. 2.9A). The Lethal Dose 50 (LD50), the dose of doxycycline that kills 50% of the initial population, was 2 fold higher in Snell cells (Fig. 2.9B), indicating elevated resistance to doxycycline-mediated cell death.

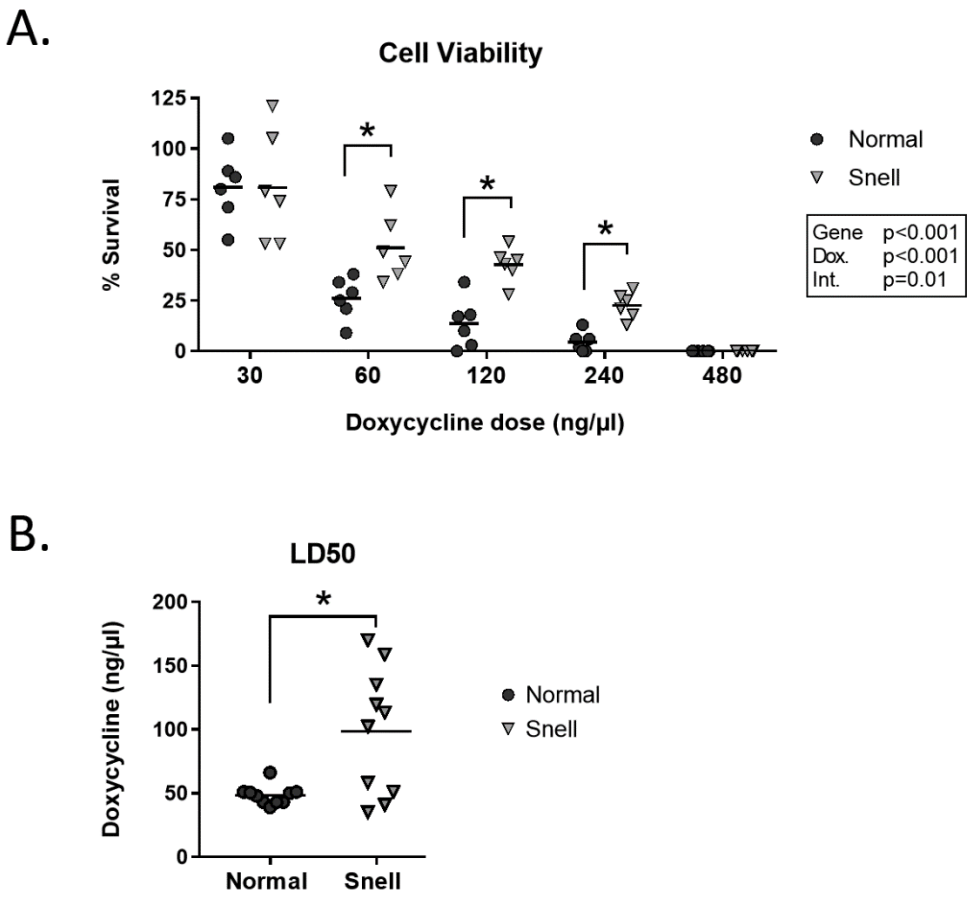

Figure 2.9 Snell cells survive higher doses of doxycycline-induced mitochondrial stress.

(A) Cell viability (WST-1 assay) after 72-hour incubation in media with varying doses of doxycycline. Each symbol represents cells from an individual mouse; the same mice were used to generate data at each dose of doxycycline. (B) LD50 for normal and Snell cells. Normal cells are represented by dark circles; Snell cells are represented by light triangles for N=6 mice for each group. Horizontal bars represent the mean for each group. (*) indicates $p < 0.05$ by Student's t-test for comparison between normal and Snell cells. Results of two-factor ANOVA are shown in the boxed inset, with p-values for the Interaction ("Int.") effects.

2.6 Mitochondrial function after stress exposure: Cellular ATP content

To gain a better understanding of the effect of mitochondrial stress exposure on mitochondrial function in Snell and normal cells, we measured cellular ATP content after incubating cells in medium containing increasing doses of doxycycline. Normal cells lost 60% of their cellular ATP content after 72 hours of 30 ng/µl doxycycline treatment, whereas Snell cells maintained ATP content under the same conditions. When the doxycycline dose was increased to 60 ng/µl, normal cells lost almost all their ATP, while Snell cells retained 25% of initial ATP content (Fig. 2.10A).

In order to rule out the possibility that preservation of ATP content in Snell cells was because of lower ATP consumption rate instead of maintenance of ATP generation, we treated cells with rotenone, a chemical inhibitor of ETC complex I. Rotenone suppresses ATP production but does not directly disturb mitochondrial proteostasis or induce mtUPR; If Snell cells maintained ATP levels because they consumed less ATP, cellular ATP content would also be maintained when ATP synthesis was blocked by rotenone. However, rotenone treatment caused similar loss of ATP levels in normal and Snell cells, and there was no detectable difference in cellular ATP content (Fig. 2.10B), implying that normal and Snell cells have similar ATP consumption rates under these conditions. Taken together, our results indicate that Snell cells are able to maintain cellular ATP content at a higher level than normal cells after doxycycline-induced mitochondrial stress.

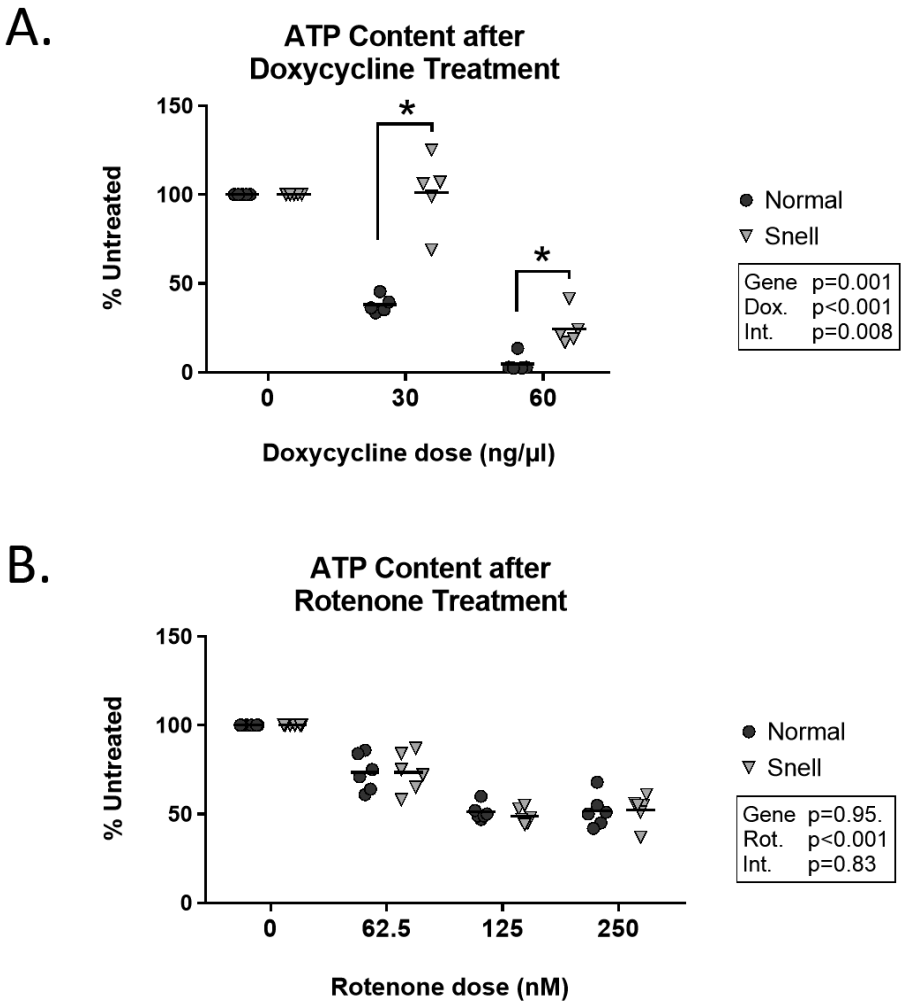

Figure 2.10 Snell cells maintain cellular ATP content after mitochondrial stress exposure.

(A) Cellular ATP content after 72 hr. exposure to doxycycline, and (B) rotenone, which does not induce mtUPR. Normal cells are represented by dark circles; Snell cells are represented by light triangles for N=5-6 mice for each group. Horizontal bars represent the mean for each group. (*) indicates $p < 0.05$ by Student's t-test for comparison between normal and Snell cells. Results of two-factor ANOVA are shown in the boxed inset, with p-values for the Interaction ("Int.") effects.

2.7 Mitochondrial function after stress exposure: Oxidative respiration

A more direct indicator of mitochondrial function is the rate of oxidative respiration. In order to assess whether mitochondrial respiration is maintained after pre-exposure to mitochondrial stress, we exposed primary fibroblasts from normal and Snell mice to doxycycline (0, 30, and 60 ng/µl for 24 hrs.) pre-treatment followed by an hour of rest-period in fresh medium in the absence of doxycycline, and then measured oxidative phosphorylation rates using the Seahorse system (Fig. 2.11). Of note, neither 30 ng/µl nor 60 ng/µl doxycycline treatment induces cell death at this timepoint, but does trigger mtUPR in primary mouse fibroblasts and hepatocytes (Houtkooper et al., 2013).

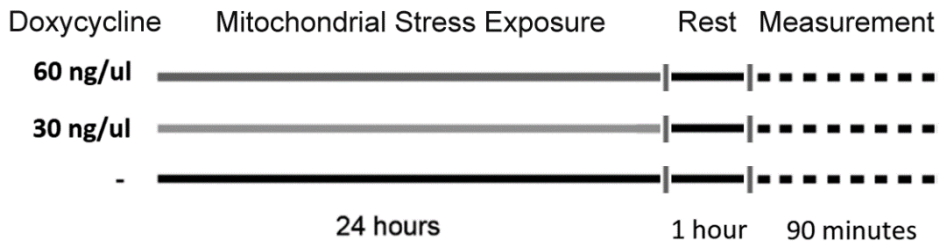

Figure 2.11 Experimental design for measurement of real-time oxidative respiration after doxycycline pre-treatment.

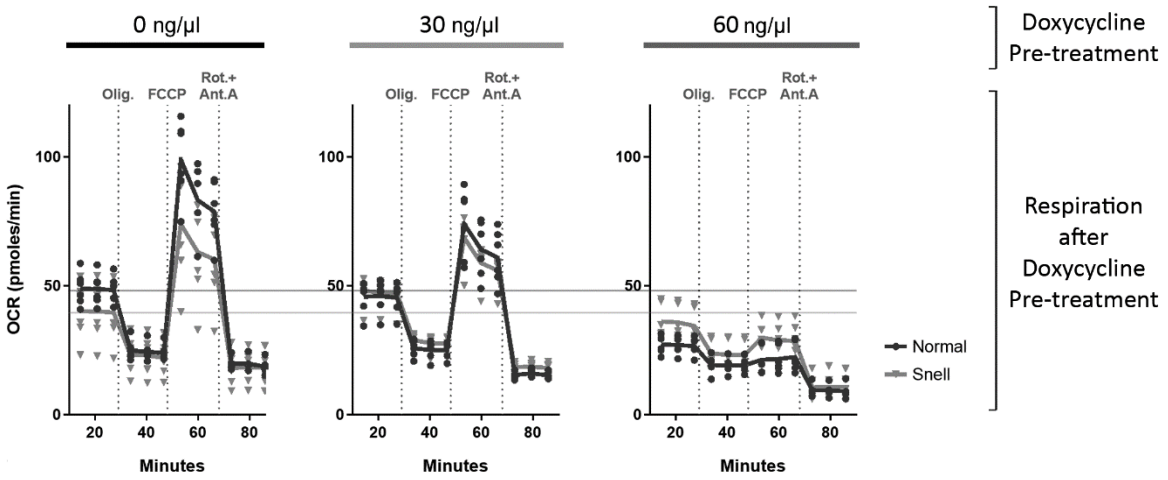

Figure 2.12 Respiration rate curves for normal and Snell cells.

(A) Respiration rate curves obtained with or without pre-treatment by doxycycline (0, 30, and 60 ng/µl for 24 hours). Oxygen consumption rates in four different phases separated by injections of oligomycin, FCCP, and rotenone with antimycin A were measured for analysis of individual respiration parameters. Each line represents the average oxygen consumption rate for each group of N=6 mice; values for individual mice are shown by dark circles (normal) and light triangles (Snell). Horizontal lines (dark for normal, light for Snell cells) are shown across three graphs to serve as reference points for basal respiration levels in the absence of prior stress treatment.

We calculated the rates of total cellular respiration, respiration for ATP production, proton leak, and non-mitochondrial respiration by measuring oxygen consumption in four phases separated by injections of oligomycin, FCCP (carbonyl cyanide-4-trifluoromethoxy phenylhydrazone), and rotenone with antimycin A, which inhibit different components of ETC complex (Fig. 2.12; see methods for detailed information).

At the basal level, where neither Snell nor normal cells had been pre-treated with doxycycline, the level of total respiration was similar, with Snell cells showing a slightly lower level that did not differ significantly ($p=0.053$) from normal controls (Fig. 2.13A). Further analysis comparing respiration rates before and after complex V (ATP synthase) inhibition by oligomycin revealed that oxygen consumption utilized for ATP production was 29% lower in Snell cells in the absence of prior doxycycline treatment (Fig. 2.13B). Doxycycline pre-treatment, however, lowered both total and ATP-synthesis-linked respiration normal cells, an effect to which Snell cells were resistant. After exposure to 60 ng/μl doxycycline, Snell cells exceeded normal cells in both total (Fig 2.13A) and oligomycin-inhibited O_2 consumption (Fig 2.13B). ATP-synthesis-coupled respiration in normal cells pre-treated with 60 ng/μl doxycycline decreased approximately 70%, while the loss in respiration rate in Snell cells was only 30%. Thus, when the both normal and Snell cells had been pre-exposed to mitochondrial stress, respiration rate in Snell cells was resistant to the stress effect, and thus surpassed that in normal cells (Fig. 2.13A-B, Fig. 2.12).

Spare respiration capacity was higher in normal fibroblasts when cells are not pre-exposed to doxycycline. Pre-exposure to 60 ng/ul doxycycline diminished spare respiration capacity in both normal and Snell fibroblasts. As noted previously, efficacy of doxycycline in inducing mitochondrial stress is similar in normal and Snell cells (Chap. 2.4; Fig 2.6). Nevertheless, in order to confirm that the maintenance of respiration rate in Snell cells was not due to inefficient mitochondrial stress induction, we calculated the level of mitochondrial stress-induced proton leak. The level of initial damage induced by doxycycline, measured by proton leak-linked oxygen consumption, was ~12 x 10^{-12} moles/min in doxycycline-treated Snell cells and ~10 x 10^{-12} moles/min in normal cells, demonstrating that the efficacy of stress exposure on Snell cells was at least as high as on normal cells, if not higher (Fig. 2.13D).

We saw no significant difference in non-mitochondrial respiration rates (Fig. 2.13E), confirming that the higher respiration rate in Snell cells was not due differences in non-mitochondrial factors such as cell size or cytosolic redox reactions.

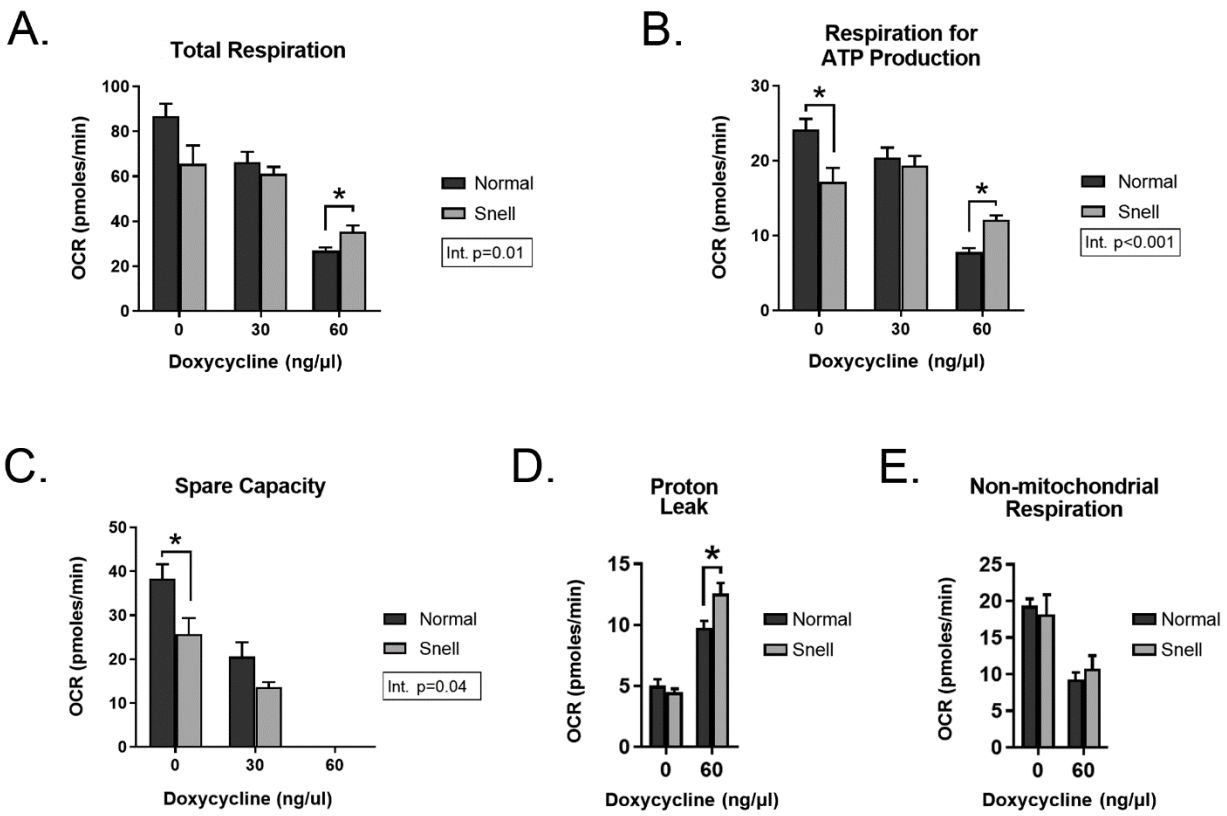

Figure 2.13 Snell cells maintain mitochondrial function after stress.

Real-time oxygen consumption rates were measured after pre-incubating cells in control media or media with 30 or 60 ng/µl doxycycline for 24 hours and individual respiration parameters were calculated. (A) Total respiration, (B) oxygen consumption linked to ATP production, (C) spare capacity, (D) proton leak, and (E) non-mitochondrial oxygen consumption. Mean values for fibroblasts from N=6 mice are shown for each group. Error bars represent SEM. (*) indicates $p < 0.05$ by Student's t-test for comparison between normal and Snell cells.

2.8 Conclusions

Primary fibroblasts from Snell dwarf mice are resistant to several forms of stress including paraquat, hydrogen peroxide, and cadmium exposure (Murakami et al., 2003). Here we show that Snell cells are also resistant to mitochondrial stress, specifically the effects of doxycycline on cell viability (Fig. 2.9), cellular ATP content (Fig. 2.10A), total oxidative respiration (Fig. 2.13A), and rate of oxygen respiration linked to ATP synthesis (Fig. 2.13B).

Increased mitochondrial stress resistance observed at the cellular level in Snell fibroblasts was consistent with higher mtUPR (HSP60 and LONP1) levels detected (Fig. 2.1, 2.2). Confirming previous findings (Page et al., 2009), analysis of mitochondrial protein levels (Fig. 2.3) and mtDNA content indicated that mitochondrial abundance was comparable in normal and Snell cells (Fig 2.4), suggesting that elevated expression levels of HSP60 and LONP1 in Snell fibroblasts cannot be explained by alterations in mitochondrial content, but indicate upregulation of mtUPR in fibroblasts isolated from long-lived Snell mice.

In contrast to normal fibroblasts, Snell fibroblasts were able to maintain *CoxI* (mtDNA-encoded) transcript levels after inhibition of mitochondrial translation by doxycycline (Fig 2.5). Investigating this phenotype, we found that, in response to mitochondrial stress, upregulation of mitochondrial transcriptional factor *Tfam* was higher in Snell cells compared to normal cells, suggesting induction of mitochondrial transcription, which might have a role in maintenance of mtDNA-encoded *CoxI* transcript levels in Snell cells. In addition, *Pgc-1α*, the main regulator of mitochondrial biogenesis, was upregulated exclusively in Snell cells (Fig 2.7B). Snell-cell-specific

induction of PGC-1α was also detected at the protein level and was not specific to the agent used to induce mitochondrial stress (Fig 2.8). Taken together, our findings suggest that, in addition to mtUPR induction, Snell fibroblasts can also upregulate regulators of mitochondrial transcription and biogenesis, which may facilitate mitochondrial damage repair in cases where mtUPR upregulation is not sufficient (see discussion).

2.9 Materials and methods

2.9.1 Mice

Snell dwarf and littermate control mice were produced by crossing (DW/J x C3H/HeJ) Pit1$^{dw/+}$ heterozygous parents. Snell mice with dw/dw genotype were identified by their small size at the age of 3 weeks. Heterozygotes and +/+ mice, which are not distinguishable phenotypically, were used as normal littermate controls. The mice were housed in microisolator cages with 1/8" Bed-O-Cob bedding (The Andersons, Maumee, OH). The mice had free access to tap water and Purina 5001 Rodent Chow (St. Louis, MO). Snell mice were caged with normal sized females to prevent premature death from hypothermia. All experiments were performed in accordance with guidelines and regulations provided by the University of Michigan University Committee on Use and Care of Animals.

2.9.2 Primary fibroblast cell culture

Tail snips (~5 mm) were taken from 6-month-old Snell mice and normal siblings, washed with ethanol twice, and rinsed in PBS. Growth media (GM) was prepared by supplementing DMEM (Gibco, 11965-092) with 10% FBS and 1% penicillin/streptomycin (Gibco, 15140-122), resulting in a final concentration of 100 units/ml penicillin and 100 µg/ml streptomycin. Fibroblast isolation media (FIM) was prepared by dissolving Collagenase Type II (Gibco, 17101-015) in GM (400 U/ml), and sterilized by passing through a 0.2 µm filter. Individual tail snips were

transferred into 60 mm petri dishes containing a few drops of FIM, and minced using sterile scalpels to produce pieces smaller than 1 mm on each side. 4 ml of FIM was added to each dish, and minced tails were incubated 24 hours at 37 °C, 10% CO_2. After incubation, the media with minced tail pieces was pipetted up and down several times, passed through sterile nylon netting (100 μm) to remove larger pieces, and centrifuged at 1000 g for 3 minutes. Supernatant was removed. The cells were re-suspended in 10 ml GM, seeded on 10 cm cell culture dishes and incubated at 37 °C, 10% CO_2. When confluent, the cells were transferred to 15 cm dishes. After no more than 3 weeks of growth, primary fibroblasts were used for experiments.

2.9.3 Mitochondrial stress treatments for protein and mRNA analysis

The cells were counted and seeded on cell culture dishes (10^6 cells in 10 ml media per 10 cm dish) in GM. After 6 hours, GM was removed and replaced with cell media (CM; serum-free DMEM with no antibiotic). The next day, CM was removed and replaced with fresh CM containing either 30 μg/ml doxycycline (Santa Cruz, sc204734), 50 μg/ml thiamphenicol (Millipore Sigma, T0261), or an equal volume of diluent as control. The cells were incubated at 37 °C, 10% CO_2 for time intervals indicated for each experiment. For treatments longer than 24 hours, the medium was replaced every day with fresh CM containing the compound of interest. At the end of treatment, the medium was removed. Cells were carefully washed with PBS, scraped, collected in 1 ml cold PBS, transferred to microcentrifuge tubes, and centrifuged for 3 minutes at 1000 x g at 4 °C to remove PBS. Cell pellets were used for protein or RNA extraction.

2.9.4 Measurement of cell viability and lethal dose 50 (LD50)

For cell viability assays, cells were seeded on 96-well cell culture plates (30 x 10^3 cells in 100 µl medium per well) in GM. After a 6-hour incubation, GM was replaced by CM. The next day, the medium was removed and CM containing doxycycline at the indicated concentrations was added. After 72 hours, WST-1 Cell Proliferation Reagent (Millipore Sigma, 05015944001) was added (10 µl/well), and the plate was incubated for 4 hours. Absorbance at λ = 440 nm was measured using a microplate spectrophotometer. The lethal dose 50 (LD50), i.e. the doxycycline dose corresponding to 50% decrease in formazan dye signal (produced by metabolically active cells) compared to untreated controls, was calculated.

2.9.5 Measurement of cellular ATP content

For ATP content measurements, primary fibroblasts were seeded (30 x 10^3 cells in 100 µl media per well) in a 96-well plate. Opaque-walled cell culture plates were used to prevent luminescence cross-talk between wells. After 6-hour incubation in GM, the medium was removed and replaced with CM. Cells were incubated overnight in CM. The next day, the medium was removed and CM containing doxycycline or rotenone (Millipore Sigma, R8875) at the indicated concentrations was added. After 72-hour incubation, ATP content was measured using a CellTiter-Glo® Assay Kit (Promega, G7571) as described in the product protocol. Luminescence signal was measured on a SynergyTM HT Multi-Mode Microplate Reader (BioTek® Instruments, Inc). All incubations were performed at 37 °C, 10% CO_2.

2.9.6 Measurement of real-time oxidative consumption

Real time measurement of oxygen consumption rates was performed using the XF Cell Mito Stress Test Kit (Agilent Technologies, 103015-100), XF FluxPak mini cartridge pack (Agilent Technologies, 102601-100), and XF Base medium (Agilent Technologies, 102353-100). Cells were seeded (10^4 cells in 200 µl GM per well) on a 96 well XF cell culture plate. After 6 hours, GM was replaced with CM and the cells were incubated overnight. The next day CM was removed and CM containing 0, 30, or 60 µg/ml doxycycline was added to induce mitochondrial stress. The cells were incubated for 24 hours at 37 °C, 10% CO_2. In parallel, the sensor cartridge was placed in a utility plate (Agilent Technologies, 102601-100) containing 200 µl/well XF Calibrant (Agilent Technologies, 102601-100) and incubated overnight at 37 °C in non-CO_2 incubator for hydration. The next day, assay medium (AM) containing 1 mM pyruvate, 2 mM glutamine, and 10 mM glucose in XF Base medium was freshly prepared. AM was warmed to 37 °C, adjusted to pH of 7.4 with 0.1 N NaOH, and sterilized by filtering. Cells were washed with AM by discarding 175 µl of 200 µl media and adding 175 µl AM three times, to prevent cell disruption. After the wash, 175 µl media was removed and 150 µl AM was added, leaving 175 µl AM in each well. Cell were examined under a microscope to make sure they were not detached during washes. The cells were incubated at 37 °C in a non-CO_2 incubator for 45 minutes. In parallel, oligomycin (8 µM), FCCP (9 µM), and rotenone/antimycin A (5 µM) solutions were prepared in AM and loaded to cartridge ports A, B, and C respectively (25 µl per port). The cartridge with the utility plate was placed in a Seahorse XFe96 Extracellular Flux Analyzer (Agilent Technologies), and calibration was started. At the end of 45-minute incubation, the

utility plate in the XFe96 Extracellular Flux Analyzer was replaced with the cell plate and the measurement protocol was started. The operating software Wave (Agilent Technologies) was programmed in advance to perform measurements every ~6 minutes, injecting 25 µl oligomycin solution (final 1 µM) at t=28 min, 25 µl FCCP solution (final 1 µM) at t=47 min, and 25 µl Rotenone/Antimycin A solution (final 0.5 µM) at t=66 minutes. Oxygen consumption rate at each time point was calculated by Wave software according to readings collected from the XFe96 Extracellular Flux Analyzer. Each data point is the average of 5 technical replicates.

2.9.7 Calculation of respiration parameters

Respiration parameters were calculated by analyzing real-time oxygen consumption rate (OCR) measurements in four phases separated by injections of oligomycin, FCCP, and rotenone/antimycin A, which inhibit or activate specific pathways allowing the dissection of individual components of respiration. Total respiration is the oxygen consumption rate measured before the addition of oligomycin.

$$\text{Total Respiration} = OCR_{t=27'}$$

Respiration for ATP production was calculated by subtracting the oxygen consumption rate after inhibition of ATP synthase (ETC complex V) by oligomycin, the oxygen consumption that is not linked to ATP production, from total respiration rate

$$\text{Respiration for ATP production} = OCR_{t=27'} - OCR_{t=46'}$$

Non-mitochondrial respiration is the reading after the mitochondrial ETC is totally blocked by addition of complex I/III inhibitors rotenone and antimycin A.

$$\text{Non-mitochondrial Respiration} = OCR_{t=85'}$$

Total mitochondrial respiration is calculated by subtracting non-mitochondrial respiration from total cellular respiration.

$$\text{Total mitochondrial respiration} = OCR_{t=27'} - OCR_{t=85'}$$

Proton leak was calculated by subtracting respiration for ATP production from total mitochondrial respiration:

$$\text{Proton Leak} = [OCR_{t=27'} - OCR_{t=85'}] - [OCR_{t=27'} - OCR_{t=46'}] = OCR_{t=46'} - OCR_{t=85'}$$

2.9.8 Western blot and antibodies

Cell pellets were lysed in 200 µl RIPA buffer with protease inhibitor cocktail (ThermoFisher, 78430) by incubating on ice for 20 minutes, vortexing every five minutes for 5 seconds each time. The lysates were centrifuged for 20 minutes at 8000 x g at 4 °C. The supernatants were collected in new tubes. Protein concentration was estimated using BCA Protein Assay (ThermoFisher, 23225) and adjusted accordingly. Laemmli protein sample buffer (BioRad, 161-0747) containing β-mercaptoethanol (1.42 M) was added. Samples were incubated for 5 minutes at 100 °C, cooled to room temperature, run on polyacrylamide gel, and transferred to PVDF membranes. The membranes were blocked with 2% bovine serum albumin (BSA) in TBST

solution (20 mM Tris, 500 mM sodium chloride, 0.9 mM polyoxyethylene-20-sorbitan monolaurate in deionized water), probed with primary antibodies β-Actin[C4]-HRP (Santa Cruz, sc47778HRP), PGC-1α (Millipore, ST1202), HSP60 (Santa Cruz, sc1052), or LONP1 (Abcam, ab103809) at 1:1000 dilution and incubated for 18 hours at 4 °C with shaking. Mitochondrial ETC proteins ATP5A, and UQCRC2 were detected using MitoProfile® Total OXPHOS Rodent WB Antibody Cocktail (Abcam, ab110413). Mouse IgG-HRP (Santa Cruz, sc2031), goat IgG-HRP (Santa Cruz, sc2350), and rabbit IgG-HRP (Cell Signaling, 7074S) were used as secondary antibodies at 1:2000 dilution. The membranes were incubated with secondary antibodies on a shaker for 90 minutes at room temperature. After primary and secondary incubations, the membranes were washed three times in TBST for 10 minutes each time to minimize non-specific binding. Protein bands were detected using enhanced chemiluminescent substrate (ThermoFisher, 34075) and a chemiluminescence imager. Signal strength was quantified using ImageJ software.

2.9.9 mRNA extraction and q-rtPCR

Frozen cell pellets were lysed in 1 ml TRIzol reagent (ThermoFisher) by sonication on ice for 30 seconds with 1 second on/off cycles. The lysates were transferred to pre-cooled Phase Lock Gel-Heavy tubes. Chloroform (0.2 ml for 1 ml TRIzol) was added. After 3 minutes of incubation at room temperature, the tubes were centrifuged for 15 minutes at 7500 x g at 4 °C. Aqueous phase (~0.5 ml) was transferred to new tubes. Isopropanol (0.5 ml) was added. After 10 minutes of incubation at room temperature, the RNA was precipitated by centrifugation at

7500 x g at 4 °C. The supernatant was discarded. The precipitated RNA was washed with 75% ethanol (1 ml), and then centrifuged for 5 minutes at 7500 x g at 4 °C. The supernatant was carefully discarded. Precipitated RNA was air-dried and resuspended in 50 µl RNase-free water. RNA concentration was measured by nanodrop. cDNA was produced by iScript cDNA Synthesis Kit (BioRad, 1708890) according to the protocol provided by the manufacturer. qPCR was performed using Fast SYBR™ Green Master Mix (ThermoFisher, 4385612) according to product protocol. The primers are listed below in the format described on the first row:

[Gene], [PubMed Gene ID], [Forward primer sequence], [Reverse primer sequence].

Hsp60, 15528, tgtttggagaagaggggttg, cgctcgttcagcttttcttt.

Hsp10, 15528, gggtcaggagggaaaggaaa, cagcttcacgtgacaccatt.

Lonp1, 74142, tggttgagctcctgagaagg, aacttgtctccgaggtcctg.

Vdac1, 22333, agaggtacagcagaaacccc, aggtgtgtacatgcttccga.

Pgc-1α (*Ppargc1a*), 19017, atgtgtcgccttcttgctct, atctactgcctggggacctt.

Tfam, 21780, agccaggtccagctcactaa, aaacccaagaaagcatgtgg.

CoxI (*mt-Co1*), 17708, tcatcccttgacatcgtgct, gtctgagtagcgtcgtggta.

Cox4i (*Cox4i1*), 12857, ccatgtcacgatgctgtctg, ctcccaaatcagaacgagcg.

2.9.10 Statistical analysis

Prism (GraphPad Software, Inc) was used for statistical analysis and graphical representation of the data. Error bars represent SEM. Comparisons between groups were performed using Student's t-test. For experiments involving more than one variable, two-way ANOVA was used to analyze individual effects of and interaction between the two factors. Differences with p values smaller than 0.05 were considered significant.

Chapter 3 - Mitochondrial stress response and ETC proteostasis in Snell mice

3.1 Introduction

Mouse lifespan can be extended both by genetic alterations and by post-natal treatments (Flurkey et al., 2010; Miller et al., 2005; L. Sun, Sadighi Akha, Miller, & Harper, 2009). Snell mice, one of the most studied long-lived mouse models, have a single point mutation in *Pit1*, and show more than 40% increase in mean and maximal lifespan (Flurkey et al., 2001) (see section 1.1.3.1). Negative effects of the *Pit1* mutation on growth hormone (Wilson & Wyatt, 1986b)(Sinha, Salocks, & Vanderlaan, 1975), prolactin (Wilson & Wyatt, 1986b), thyroid-stimulating hormone (Wilson & Wyatt, 1986a), and IGF-1 signaling (van Buul-Offers et al., 1994) are well established in Snell mice. However, how these alterations result in prolonged lifespan and delayed onset of aging-associated pathologies remains elusive.

Upregulation of the mitochondrial stress response (mtUPR) has been proposed as a common longevity mechanism linking mitochondrial disruption to longevity (Houtkooper et al., 2013). Mitochondrial stress applied early in life by temporary silencing of cytochrome c oxidase-1 subunit Vb/COX4 (*cco-1*), which results in lifespan extension in *C. elegans*, also causes mtUPR (*hsp6*) upregulation that persists throughout the lifespan long after withdrawal of the initial stress (Durieux et al., 2011). Maintenance of *hsp6* upregulation after transient exposure to

mitochondrial stress indicates that nematode mtUPR pathway can be rewired permanently during larva stages. Transgenic worms with muscle-specific overexpression of nematode mtUPR protein Hsp70F live more than 40% longer, implying that mtUPR upregulation may be sufficient for lifespan extension in worms (Yokoyama et al., 2002). Overall, accumulating data from studies in *C. elegans* suggest a prolongevity role for mtUPR upregulation.

Mclk1 is the mouse orthologue of the *C. elegans* gene *clk-1*, which encodes a mitochondrial enzyme involved in ubiquinone biosynthesis. Although the homozygous deletion of *Mclk1* in mice is lethal (Levavasseur et al., 2001), mice heterozygous for *Mclk1* show prolonged average and maximum lifespan, suggesting evolutionary conservation of this longevity pathway. No data are available on the levels of mtUPR in $Mclk1^{+/-}$ mice. It is likely that decreased expression of *Mclk-1* induces mtUPR, since $Mclk1^{+/-}$ mice show reduced mitochondrial electron transport and ATP synthesis, indicating mitochondrial defects (Lapointe & Hekimi, 2008). Mice with deleted *Surf1*, a putative ETC complex IV gene, also live longer (Dell'agnello et al., 2007), suggesting that sublethal defects in mitochondrial proteome may induce lifespan extension not only in worms but also in mammals.

In the previous chapter, we presented data demonstrating that primary fibroblasts isolated from long-lived Snell mice exhibit elevated levels of basal and induced mtUPR. In addition, cellular ATP content, and oxidative respiration rate is maintained in Snell cells after mitochondrial stress exposure, suggesting improved resistance to mitochondrial stress.

Fibroblasts from long-lived *Surf1*$^{-/-}$ mice also show elevated mtUPR (Pharaoh et al., 2016). However, it is not known whether mtUPR is elevated *in vivo* in any long-lived mouse model.

In this work, in order to examine whether the mtUPR is elevated in Snell mice, we assess hepatic mtUPR and mito-nuclear protein stoichiometry in normal and Snell mice after 2-week of *in vivo* doxycycline treatment. Since our work suggested a rewiring in the mitochondrial biogenesis pathway in Snell mice, we also evaluated *Tfam* and *Pgc-1α* expression.

3.2 Mitochondrial biogenesis pathway is constitutively upregulated in Snell liver

Our finding that Snell fibroblasts have elevated expression of *Tfam* and *Pgc-1α* suggested that components of the mitochondrial biogenesis pathway may have altered regulatory mechanisms in Snell mice. To assess *in vivo* gene expression, we measured *Tfam* and *Pgc-1α* mRNA levels in liver tissue samples from normal and Snell mice. First, we monitored mRNA levels of three independently regulated genes encoding mitochondrial proteins to test if Snell liver shows a general alteration in transcript levels of genes associated with mitochondrial function. *Vdac1* (*Porin*) encodes a mitochondrial transport channel protein which is widely used as a mitochondrial loading control. *Cox4i* encodes a nuclear-DNA-encoded ETC protein, and *CoxI* encodes a mitochondrial-DNA-encoded ETC protein. We did not find any difference in the mRNA levels of nDNA encoded *Vdac1* or *Cox4i,* or in mtDNA encoded *CoxI* (Fig. 3.1A).

In contrast to comparable mRNA levels of *Vdac1*, *CoxIVi*, and *CoxI*, we observed a small but significant elevation in *Tfam* expression (~1.5-fold, $p=0.03$) in Snell liver. Intriguingly, compared to normal mice, we detected a dramatic upregulation of *Pgc-1α* expression (5±2-fold, $p<0.001$) in the liver of Snell mice (Fig. 3.1B). We further confirmed this result by performing an independent experiment with an additional set of mice comprising both sexes and noted that the phenotype was not gender specific; *Pgc-1α* expression was also elevated in female Snell mice (Fig. 3.1C). In addition, we found elevated levels of TFAM and PGC-1α protein in Snell liver (Chap. 4.4; Fig. 4.2A, B). Previously, PGC-1α protein has been reported to be elevated in the liver of long-lived GHR-KO mice (Al-Regaiey, Masternak, Bonkowski, Sun, & Bartke, 2005).

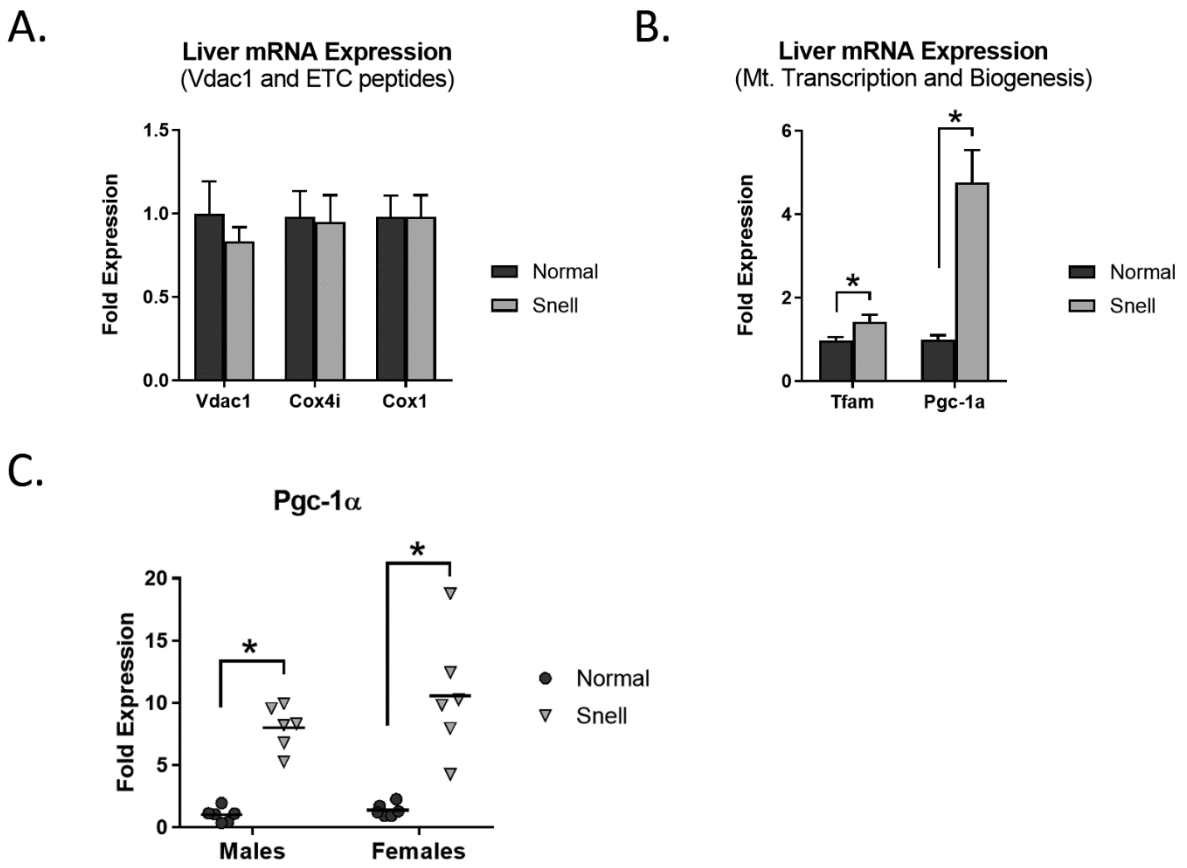

Figure 3.1 *Tfam* and *Pgc-1α* expression are constitutively upregulated in Snell liver.

(A) mRNA levels of *Vdac1*, *Cox4i*, *Cox1*, and (B) *Tfam* and *Pgc-1α* in the liver tissue of normal and Snell mice (N=6, males). Mean values are shown. Error bars represent SEM. (C) *Pgc-1α* transcript levels in the liver tissue of an independent set of normal and Snell mice of both genders (N=6). Normal mice are represented by dark circles; Snell mice are represented by light triangles. Horizontal bars represent the mean for each group. (*) indicates $p < 0.05$ by Student's t-test for comparison between normal and Snell mice.

3.3 Acute mitochondrial stress does not cause weight loss

Acute doxycycline treatment of mice has been shown to disturb mitochondrial protein stoichiometry in liver by decreasing the ratio of mtDNA-encoded respiratory chain proteins to those encoded in the nuclear DNA (Moullan et al., 2015). We exposed normal and Snell mice to *in vivo* mitochondrial stress by feeding them a doxycycline diet for two weeks. Following the treatment, we assessed the level of mtUPR induction and maintenance of mito-nuclear protein balance as indicators of mitochondrial stress response and protection against mitochondrial stress at the organismal level (Fig. 3.2). We did not detect any effect on food consumption or change in body weight in normal or Snell mice (Fig. 3.3).

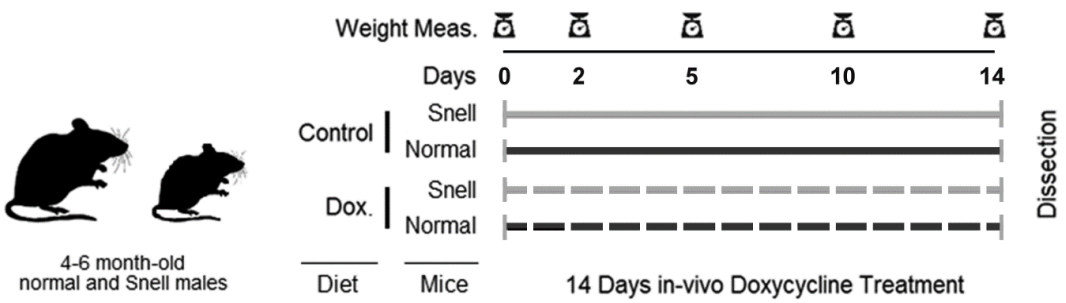

Figure 3.2 *In vivo* doxycycline treatment.

Normal and Snell young adult (6-month-old) mice were exposed to acute mitochondrial stress by in-vivo doxycycline treatment for two-weeks (N=6 mice per group). Weight measurements were taken on days indicated in the figure. Dissections were performed on day 15. Mice were not fasted prior to dissection.

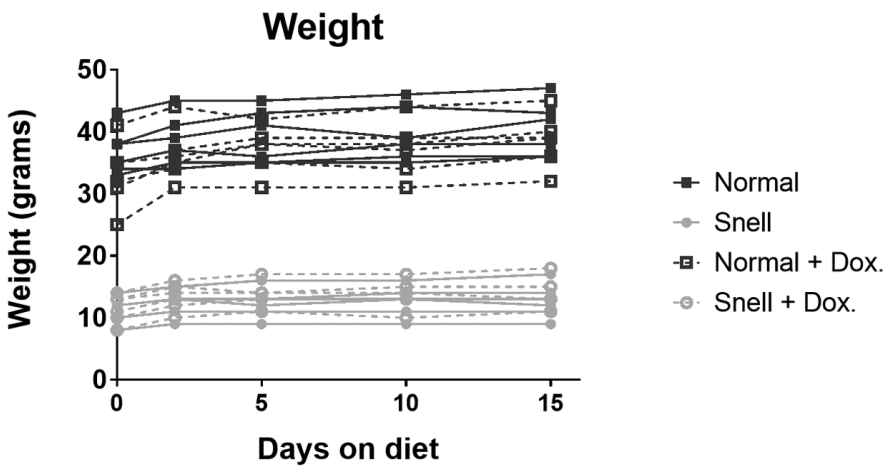

Figure 3.3 Doxycycline diet does not affect body weight of normal or Snell mice.

Body weight of each mouse on indicated days of the treatment period. Normal mice are represented by dark lines; Snell mice are represented light lines. Mice fed on doxycycline diet are represented by dashed lines.

3.4 Hepatic mtUPR induction is higher in Snell liver

In our cell culture studies, we noted elevated levels of HSP60 and LONP1 in primary fibroblasts from Snell mice, independent of mitochondrial stress exposure (Chap. 2.2; Fig. 2.1, 2.2). As opposed to our findings in Snell fibroblasts, HSP60 and LONP1 protein levels (basal mtUPR) in liver were comparable in normal and Snell mice on the control diet (Fig. 3.4A-C, control diet).

However, when the mice were exposed to acute mitochondrial stress by *in vivo* doxycycline treatment, both HSP60 (Fig. 3.4B) and LONP1 (Fig. 3.4C) protein levels were higher in Snell liver samples. Average HSP60 induction in response to doxycycline-mediated mitochondrial stress was 2.9% in normal mice and 54.3% in Snell mice ($p=0.01$); average LONP1 induction was 12.6% in normal mice and 57.2% in Snell mice ($p=0.02$) (Fig. 3.4D).

Overall, our results demonstrate that the basal mtUPR levels in Snell liver tissues are comparable to those in normal liver, while the average mtUPR induction in response to the doxycycline treatment is much higher in Snell livers.

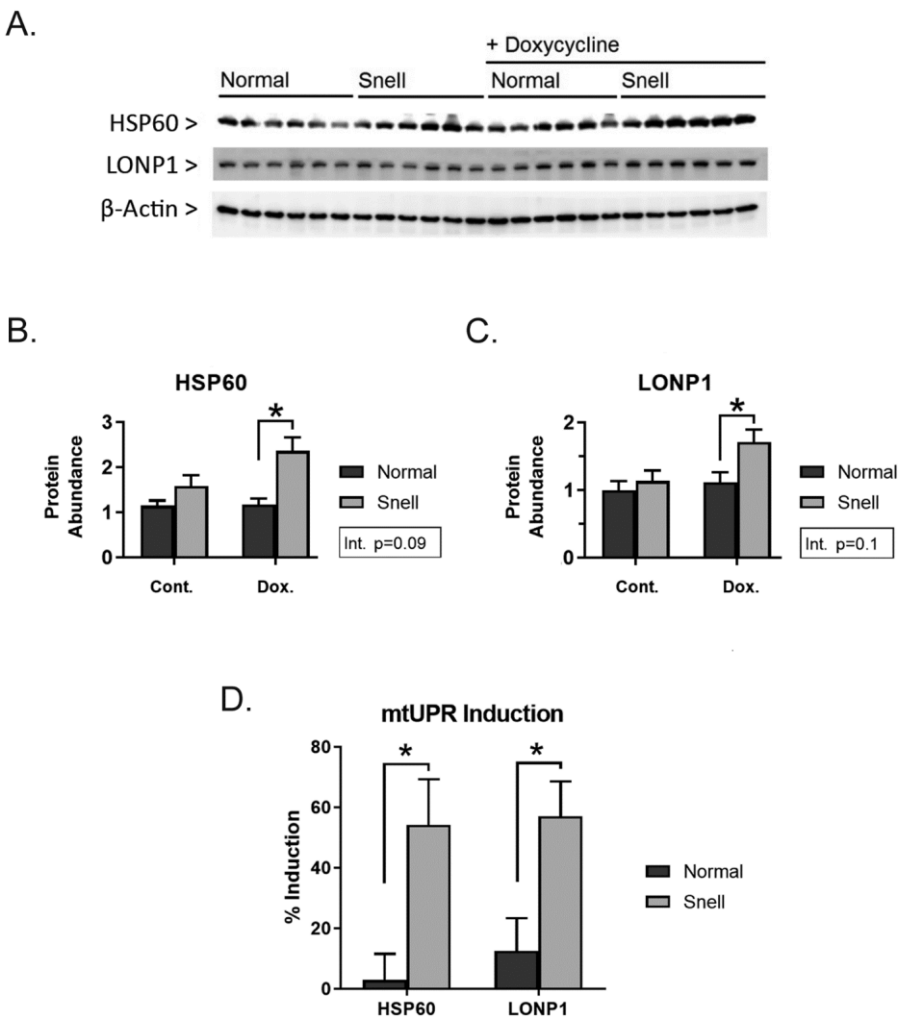

Figure 3.4 Higher mtUPR induction in Snell liver

(A) HSP60 and LONP1 protein blots for liver tissue samples from normal and Snell mice. (B) Basal and induced levels of HSP60 and (C) LONP1 protein expression. (D) Level of HSP60 and LONP1 induction (mtUPR induction) in response to mitochondrial stress exposure. Mean values for each group are shown (N=6). Error bars represent SEM. (*) indicates $p < 0.05$ by Student's t-test for comparison between normal and Snell mice. Results of two-factor ANOVA are shown in the boxed inset, with p-values for the Interaction ("Int.") effects.

3.5 Effect of *in vivo* mitochondrial stress on mitochondrial ETC protein stoichiometry

To determine whether Snell mice were resistant to disruption of mitochondrial electron transport chain (ETC) protein stoichiometry, we measured protein levels of COXI, a mitochondrial-DNA-encoded subunit of ETC complex IV, and ATP5A, nuclear-DNA-encoded subunit of ETC complex V, in liver tissues of normal and Snell mice (Fig. 3.5A). Because doxycycline inhibits mitochondrial translation without affecting cytosolic translation, we expected to observe a decrease in COXI levels, with no effect on ATP5A levels. Inhibition of COXI expression would result in a decrease in COXI/ATP5A ratio, resulting in an imbalance between mtDNA- and nDNA- encoded ETC proteins in the mitochondria.

In the absence of doxycycline treatment, COXI/ATP5A ratios were comparable in normal and Snell mice, with no indication of an alteration in ETC stoichiometry in Snell mice (Fig. 3.5B-C, mice on control diet). As predicted, doxycycline treatment inhibited COXI expression in the liver (Houtkooper et al., 2013), but disturbance of ETC protein stoichiometry was weaker in Snell mice. Average COXI/ATP5A ratio was 0.62 in normal and 0.80 in Snell livers.

ATP5A is a subunit of ATP synthase (complex V) which differs from the other four complexes (see *chap. 1.2.3 Respiratory Chain*). As electron transport can be uncoupled from ADP phosphorylation, expression of ATP synthase subunits can be regulated independent of complexes I-IV. Mouse brown fat, for example, shows low ATP synthase levels, despite high abundance of mitochondrial mass and presence of a proton gradient generated by electron transport chain complexes I-IV (Lindberg et al., 1967). To rule out an ATP synthase-specific

effect of doxycycline treatment, we also assessed protein levels of UQCRC2, a subunit of ETC complex III, and calculated the COXI/UQCRC2 ratio as an additional measure of mito-nuclear protein balance.

As in the case of COXI/ATP5A, we did not detect a difference in COXI/UQCRC2 protein ratios between normal and Snell livers in mice fed on control diet. However, in doxycycline treated mice, COXI/UQCRC2 ratio was 0.61 in normal and 0.95 in Snell livers. Of note, the weaker disruption observed in Snell mice was not due to lower efficacy of mitochondrial stress treatment since the induced mtUPR was higher in Snell liver both at protein (Fig. 3.4) and mRNA levels (Fig. 3.6). Our findings suggest that, after two-week mitochondrial stress exposure, ETC protein stoichiometry is preserved better in Snell liver than in normal liver.

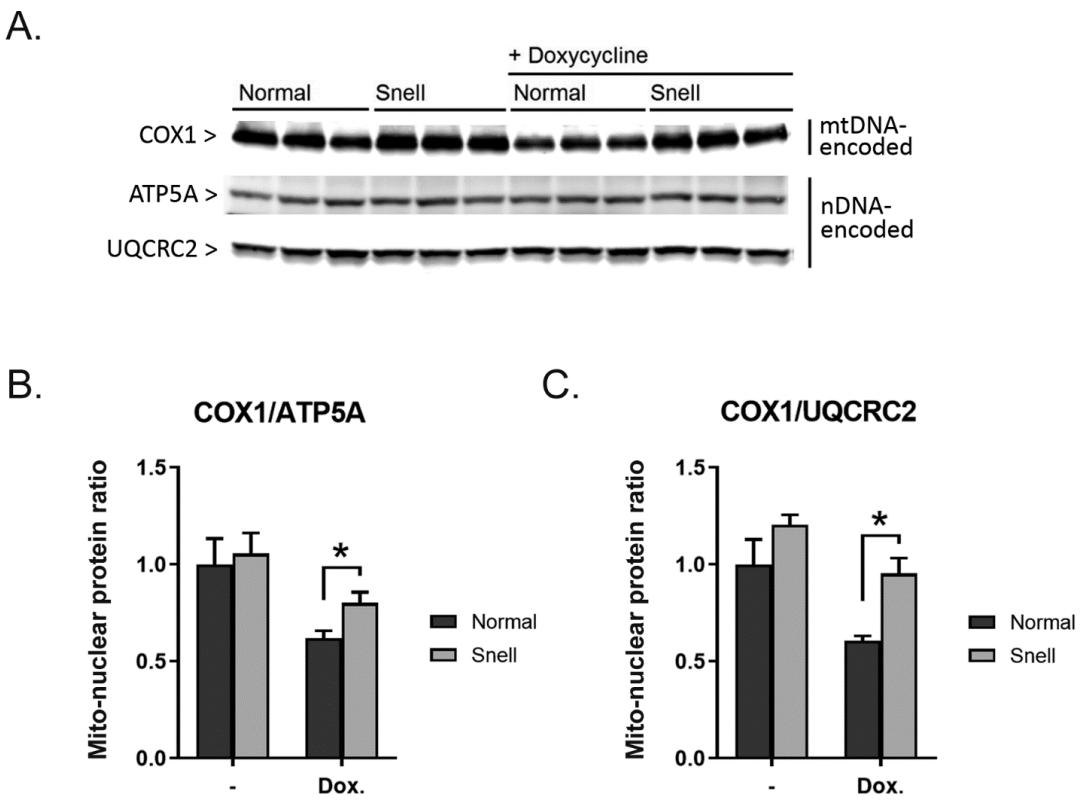

Figure 3.5 Mito-nuclear protein stoichiometery in Snell liver

Liver tissues of normal and Snell mice were analyzed to assess mito-nuclear protein stoichiometry after two-week *in vivo* doxycycline treatment. (A) Mitochondrial-DNA-encoded COX1, and nuclear-DNA-encoded ATP5A and UQCRC2 protein blots, and (B) mito-nuclear protein balance measured by COX1/ATP5A and (C) COX1/UQCRC2 ratios for normal and Snell liver samples from mock and doxycycline-treated mice. Mean values for each group are shown (N=6). Error bars represent SEM. (*) indicates $p < 0.05$ by Student's t-test for comparison between normal and Snell cells.

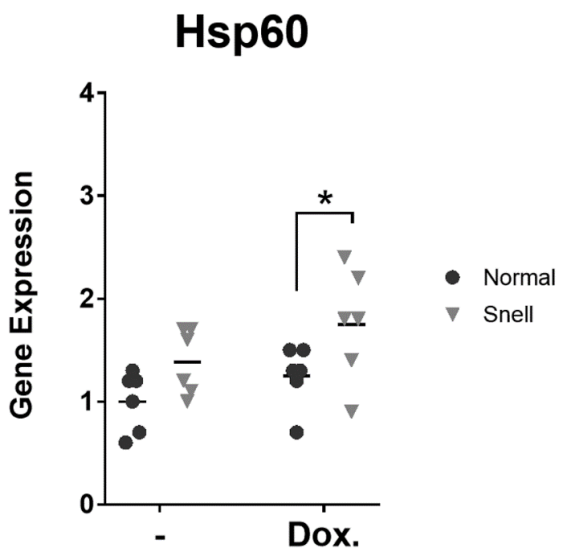

Figure 3.6 Higher levels of induced *Hsp60* mRNA expsression in Snell liver.

Liver tissues of normal and Snell mice were analyzed by qPCR to assess Hsp60 gene expression after two-week *in vivo* doxycycline treatment. Normal mice are represented by dark circles; Snell mice are represented by light triangles. Horizontal bars represent the mean for each group (N=6). (*) indicates $p < 0.05$ by Student's t-test for comparison between normal and Snell mice.

3.6 Conclusions

In cell culture, only Snell fibroblasts show *Pgc-1α* upregulation in response to mitochondrial stress (Fig. 2.7B). In order to test whether *Pgc-1α* expression was altered *in vivo*, we analyzed liver tissues from Snell and normal mice without mitochondrial stress exposure, and found that *Pgc-1α* mRNA levels are constitutively upregulated in the livers of Snell mice. *Pgc-1α* transcript levels in Snell liver samples were 5-10 fold higher than those in normal controls (Fig. 3.1B), independent of sex (Fig. 3.1C). Expression of *Tfam,* another indicator of mitochondrial biogenesis, was also upregulated in Snell liver. Although upregulation of *Tfam* and *Pgc-1α* may imply increased mitochondrial biogenesis in Snell mice, further experiments are required to test this suggestion.

As noted in the previous chapter, compared to those in normal fibroblasts, levels of the mtUPR proteins HSP60 and LONP1 were higher in Snell fibroblasts even in the absence of mitochondrial stress exposure, indicating elevated levels of basal mtUPR in Snell fibroblasts in cell culture (Fig. 2.1, 2.2). To assess mtUPR *in-vivo*, we exposed normal and Snell mice to mitochondrial stress by doxycycline treatment.

In contrast to our findings in fibroblasts, basal mtUPR levels in liver were comparable in normal and Snell mice fed on the control diet. However, in response to doxycycline treatment, Snell mice showed stronger mtUPR induction. Upon mitochondrial stress exposure, the increase in protein levels of HSP60 and LONP1 was 50-60% in Snell liver, and only 2-15% in normal mice (Fig. 3.4D). Importantly, disruption of respiratory chain protein stoichiometry as measured by

the alteration in the ratio of mtDNA-encoded COXI to nDNA-encoded ATP5A and UQCRC2 was 5-20% in Snell mice and 40% in normal mice (Fig 3.5). Stronger mtUPR induction in Snell liver accompanied by indications of improved maintenance of mito-nuclear protein balance in Snell liver suggests that Snell mice may have an improved capacity to respond to mitochondrial stress and, in turn, experience lower mitochondrial damage.

3.7 Materials and methods

3.7.1 Mice

Snell dwarf and littermate control mice were produced and housed as explained in Chap 2. The mice were either euthanized for tissue collection or used in doxycycline treatment experiments at the age of 6 months. All experiments were performed in accordance with guidelines and regulations provided by the University of Michigan University Committee on Use and Care of Animals.

3.7.2 *In vivo* doxycycline treatment

6-month-old male Snell mice (N=6) and normal siblings (N=6) were fed control (BioServ, S4207) or doxycycline chow (BioServ, S3888), corresponding to 50 mg per kg body weight per day doxycycline intake. Weight measurements were taken on days 0, 2, 5, 10, and 14 of doxycycline treatment. The mice were dissected on day 15, without a period of fasting prior to euthanasia. Liver tissue samples were collected and frozen in liquid nitrogen. Frozen tissue samples were reduced to powder using a mortar and pestle, and stored at -80 °C.

° ° °

Western blot analysis, mRNA extraction, and q-rtPCR were performed as explained in Chap 2; instead of cell pellets, powdered tissue samples were used to prepare samples. Methods for mice generation and husbandry and statistical analysis were presented in Chap 2.

Chapter 4 - N^6-methyladenosine-mediated cap-independent translation in long-lived Snell dwarf mice

4.1 Introduction

Several long-lived mouse models including rapamycin treated mice, GHR-KO mice (Dominick et al., 2015), Ames mice (Sharp & Bartke, 2005), and Snell mice (Dominick et al., 2015) show reduced mTORC1 signaling, which results in a decrease in 4E-BP1 phosphorylation, leading to suppression of canonical cap-dependent translation (see section 1.1.5.2 for details). Despite a general decline in protein synthesis, cells with diminished mTORC1 activity still exhibit upregulated levels of certain proteins functioning in pathways critical for survival such as maintenance of DNA integrity (Dominick, Bowman, Li, Miller, & Garcia, 2017), proteostasis (Pickering et al., 2015), and autophagy (M. Wang & Miller, 2012a).

Dr. Garcia from our group recently reported that two proteins involved in DNA damage repair, NDRG1 and MGMT, exhibit elevated protein levels in Snell liver without a detectable increase in corresponding mRNA levels (Dominick et al., 2017). During our investigation of mtUPR in Snell mice, we observed a similar phenomenon where elevated levels of mtUPR protein LONP1 and mitochondrial biogenesis proteins TFAM and PGC-1α in Snell cells and tissues were often not accompanied by comparable increases in corresponding mRNA levels. While upregulation of

protein expression without an alteration in mRNA levels implies regulation of protein expression at translational level, it is not clear how translation of certain transcripts are promoted in Snell mice despite an overall decline in cap-dependent translation.

Recently, a new mechanism for cap-independent translation initiation has been described, where mRNA transcripts bearing a 5'UTR motif with N^6-methyladenosine modification are selectively translated (N^6-methyladenosine-mediated cap-independent translation; m^6A-CIT) (Linder et al., 2015; Meyer et al., 2015; X. Wang et al., 2015; J. Zhou et al., 2015). In essence, two methyltransferases, METTL3 and METTL14, preferentially methylate adenosine residues found in DRACH (D=A/G/U; R=G/A; H=A/C/U) motifs located in 5'UTR mRNA regions to form N^6-methyladenosine. The demethylases FTO and ALBH5 can remove the N^6-methyladenosine modifications. YTHDF proteins promote translation of m^6A-bearing mRNAs (see section 1.3 for details).

We hypothesized that the aforementioned proteins found to be upregulated in long-lived Snell mice are synthesized through m^6A-CIT, and that m^6A-CIT is elevated in Snell mice. To test our hypothesis, we investigated whether (i) protein expression of NDRG1, MGMT, TFAM, PGC-1α, and LONP1 are regulated by m^6A-CIT, and (ii) m^6A-CIT translation pathway is elevated in Snell mice, i.e. the expression of m^6A-CIT promoting proteins, m^6A "writers" METTL3/14 and m^6A "readers" YTHDF1/2, are upregulated relative to m^6A-CIT impeding proteins, m^6A "erasers" ALKBH5 and FTO.

4.2 NDRG1, MGMT, TFAM, PGC-1α, and LONP1 are upregulated in Snell fibroblasts without comparable increases in corresponding transcript levels

In a collaborative effort with Dr. Garcia, we performed a detailed analysis of protein and mRNA expression levels of Ndrg1, Mgmt, Tfam, Pgc-1α, and Lonp1. We found higher protein levels of NDRG1 in Snell fibroblasts despite lower mRNA levels. MGMT protein levels in Snell cells were ~5 fold higher than those in normal cells, while *Mgmt* transcript levels were 1.3-fold higher in Snell cells. Mitochondrial protease LONP1 protein levels higher in Snell cells, despite comparable mRNA expression in normal and Snell cells. TFAM and PGC-1α were upregulated in Snell cells only at protein level. Average transcript levels of *Tfam* and *Pgc-1α* were lower in Snell cells, but the differences were not significant ($p=0.07$ and $p=0.2$, respectively).

Overall, four out of five genes analyzed showed elevated protein levels in Snell cells without a parallel increase in corresponding transcript levels. Although we detected higher mRNA levels (1.3-fold) of *Mgmt* in Snell cells, difference in corresponding protein levels (5-fold) were much higher.

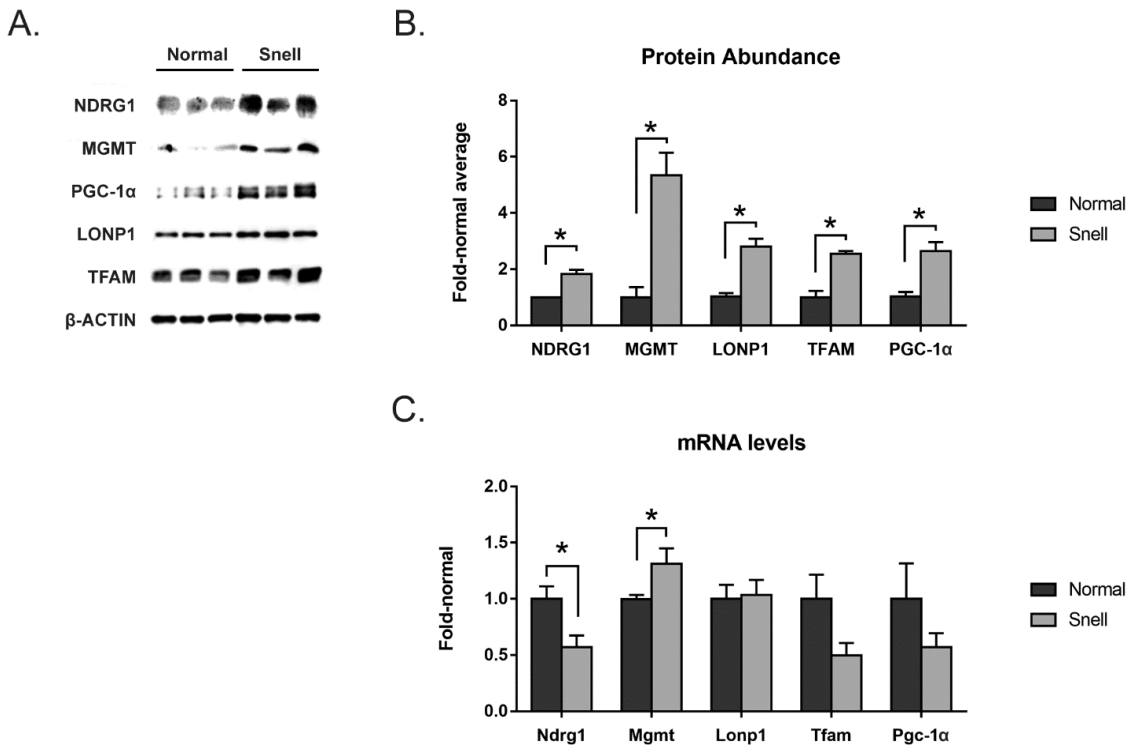

Figure 4.1 NDRG1, MGMT, LONP1, TFAM, and PGC-1α protein and mRNA expression levels in primary fibroblasts isolated from normal and Snell mice.

Primary fibroblasts from normal and Snell mice were analyzed for protein and mRNA levels. (A) Protein blots of NDRG1, MGMT, LONP1, TFAM, PGC-1α, and β-ACTIN for control are shown. (B) Protein, and (C) mRNA levels normalized to corresponding expression levels found in normal fibroblasts for each gene. Mean values are shown for each group (N=6). Error bars represent SEM. (*) indicates $p < 0.05$ by Student's t-test for comparison between normal and Snell fibroblasts.

4.3 NDRG1, MGMT, TFAM and LONP1, but not PGC-1α, are upregulated in Snell liver without comparable increases in corresponding transcript levels

Previously we found that NDRG1 and MGMT protein levels are elevated in Snell liver, but no significant alteration was detected in corresponding mRNA levels (Dominick et al., 2017). In this prior study, mice were fasted 18 hours before dissection. We asked whether LONP1, TFAM, and PGC-1α also exhibit a similar pattern in Snell liver under these conditions (Fig. 4.2A).

We found that expression of the mitochondrial protease LONP1 was 3-4-fold higher in Snell liver, while elevation in *Lonp1* mRNA levels was slightly less than 2-fold but the difference did not reach significance (p=0.1). TFAM protein levels were ~2 fold higher in Snell liver, while corresponding transcript levels were elevated 1.4 fold. In contrast, the difference in PGC-1α protein levels between Snell and normal samples was 1.5 fold, while the difference in mRNA levels was 3.4 fold, which differs from the pattern found in Snell fibroblasts and does not suggest translational regulation.

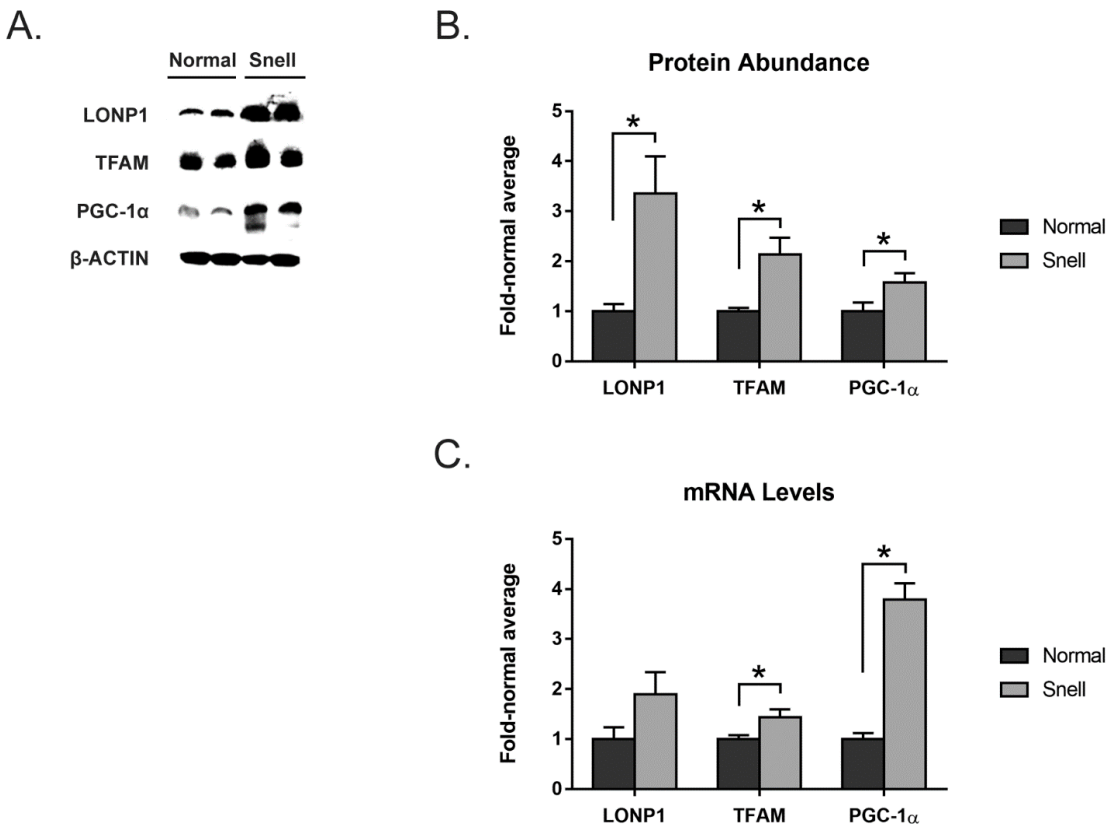

Figure 4.2 LONP1, TFAM, and PGC-1α protein and mRNA expression levels in liver of normal and Snell mice.

Liver tissue samples from normal and Snell mice are analyzed for protein and mRNA levels. (A) Protein blots of LONP1, TFAM, PGC-1α, and β-ACTIN as control are shown. (B) Protein, and (C) mRNA levels normalized to corresponding expression levels found in normal fibroblasts for each gene. Mice were fasted 18-hours prior to dissection. Mean values are shown for each group (N=6). Error bars represent SEM. (*) indicates $p < 0.05$ by Student's t-test for comparison between normal and Snell mice.

4.4 m^{6}A-CIT regulates protein levels of NDRG1, MGMT, TFAM, and PGC-1α, but not of LONP1

For all five genes investigated, we noted a marked discrepancy between mRNA and protein expression levels in fibroblasts or liver from Snell mice, suggesting an upregulation at the translational level. Analysis of 5'UTR mRNA sequences revealed that *Ndrg1*, *Mgmt*, *Lonp1*, *Tfam*, and *Pgc-1α* transcripts carried the consensus motif for m^{6}A modification, making them putative targets of m^{6}A-CIT (Linder et al., 2015; J. Zhou et al., 2015).

METTL3 is one of the m^{6}A "writer" proteins which adds N^6-methyladenosine modifications on mRNA transcripts. Deletion of METTL3 leads to loss of m^{6}A marks on target transcripts, and reduces their translation through m^{6}A-CIT (Meyer et al., 2015; X. Wang et al., 2015). In order to assess whether NDRG1, MGMT, LONP1, TFAM, and PGC-1α protein levels are regulated by m^{6}A-CIT, we knocked-down METTL3 expression in HEK-293T cells, and performed western blot analysis.

Cells transfected with *shMETTL3* showed ~70% inhibition in METTL3 expression compared to cells transfected with control *shRNA* (Fig. 4.3A). Downregulation of m^{6}A-CIT by METTL3 knock-down resulted in a decrease in protein levels of NDRG1, MGMT, TFAM, and PGC-1α, confirming that these proteins were partly synthesized through m^{6}A-CIT. Effect of METTL3 knock-down on PGC-1α expression (20% decrease) was weaker than its effect on NDRG1, MGMT, and TFAM expression (50-60% decrease). On the other hand, we did not detect an effect on β-ACTIN or

LONP1 protein levels. Accordingly, we ruled out LONP1, and confirmed NDRG1, MGMT, TFAM, and PGC-1α as targets of m^6A-mediated cap-independent translation.

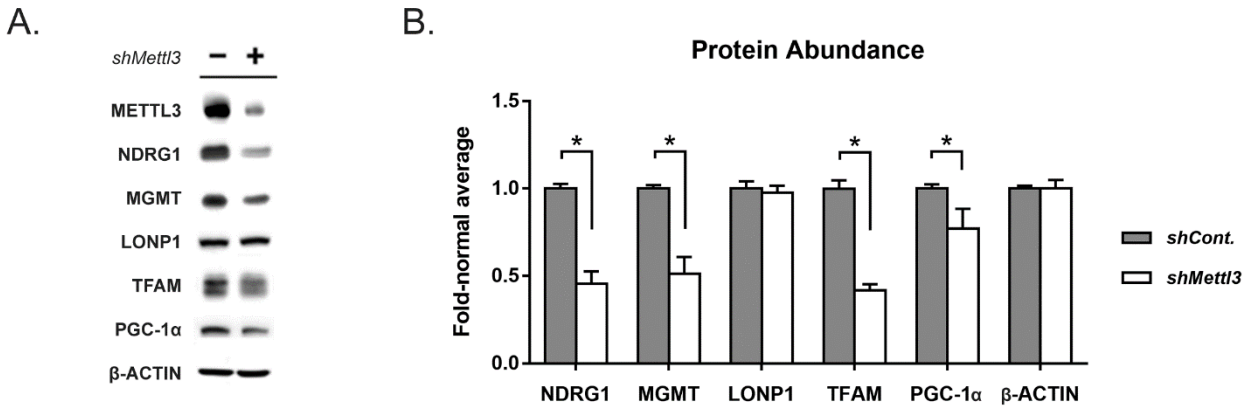

Figure 4.3 Protein levels of NDRG1, MGMT, TFAM and PGC-1α, but not LONP1 decrease upon METTL3 knock-down.

HEK 293 cells were transfected with control *shRNA* or *shMETTL3* and analyzed for protein expression. (A) Representative protein blot. (B) Protein levels normalized to controls. Mean values for N=6 different transfections are shown. Error bars represent SEM. (*) indicates $p < 0.05$ by Student's t-test for comparison between control and METTL3 knock-out cells.

4.5 m^6A-CIT pathway is upregulated in multiple tissues of Snell mice

In the previous sections we presented data demonstrating elevated protein levels of NDRG1, MGMT, LONP1, TFAM, and PGC-1α in Snell fibroblasts without a comparable elevation in corresponding transcript levels (Fig. 4.1). A similar pattern was observed in Snell liver for NDRG1, MGMT (Dominick et al., 2017), LONP1, and TFAM (Fig. 4.2). We were able to confirm that protein levels of NDRG1, MGMT, TFAM, and PGC-1α, but not of LONP1 are regulated by m^6A-CIT (Fig. 4.3). These findings suggested that m^6A-CIT might play a role in upregulation of NDRG1, MGMT, TFAM, and to a lesser extent, of PGC-1α in Snell mice. Accordingly, we sought to assess whether proteins regulating the m^6A-CIT pathway were differentially expressed in Snell mice (Fig. 4.4A).

METTL3 and METTL14 methylate N^6-adenosine residues residing in the 5'UTR of mRNA transcripts. We found that protein levels of m^6A "writers", METTL3 and METTL14, were ~80% elevated in liver of Snell mice, compared to those in normal controls (Fig. 4.4B). The transcripts bearing the 5'UTR m^6A modifications are recognized by YTHDF1 and YTHDF2, which promote their translation via m^6A-CIT. Both YTHDF1 and YTHDF2 protein levels were 3-4-fold higher in Snell liver (Fig. 4.4C). In contrast, protein levels of negative regulators of m^6A-CIT, ALKBH5 and FTO, which remove m^6A modifications from target transcripts, were either only ~20% higher (ALKBH5) in Snell liver or similar (FTO) in liver of Snell and normal mice (Fig. 4.4D).

To further investigate this phenotype, we assessed protein expression levels of m^6A-CIT regulators in kidney and skeletal muscle of Snell and normal mice. Protein levels of the m^6A

"writer" METTL3 were 3-fold higher in Snell kidney samples (Fig. 4.5A). METTL14 expression was comparable in Snell and normal samples. The m^6A "readers", YTHDF1 and YTHDF2, were elevated 7-fold and 3-fold in Snell kidneys, respectively. Protein levels of the negative regulators of m^6A-CIT, however, were either comparable (FTO) in kidneys of Snell and normal mice, or even lower (ALKBH5) in Snell mice. In skeletal muscle, we observed a very similar pattern, except one difference: both m^6A "writer" proteins, METTL3 and METTL14, were elevated in Snell mice (Fig. 4.5B).

Overall, in all three tissues tested, we observed elevated levels of m^6A "writer" and "reader" proteins, which promote m^6A-CIT, but either downregulated or unaltered levels of "eraser" proteins, which negatively regulate m^6A-CIT. This protein expression pattern indicates that m^6A-CIT pathway is upregulated in long-lived Snell dwarf mice.

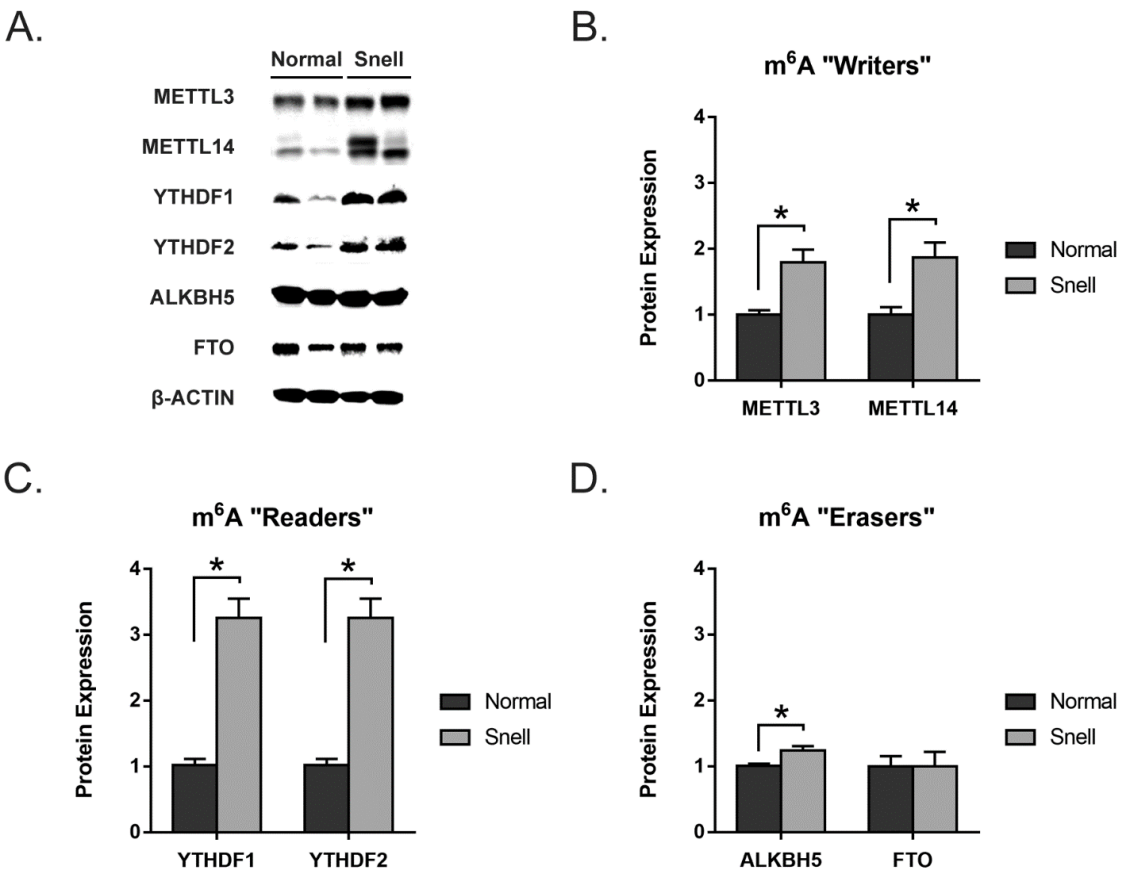

Figure 4.4 Elevated levels m^{6}A writer and reader proteins in Snell liver.

Liver protein expression in normal and Snell mice. (A) Protein blots for N=2 mice are shown. (B) Protein levels of m^{6}A writers, (C) readers, and (D) erasers normalized to normal controls. Mice were fasted 18-hours prior to dissection. Mean values are shown for each group (N=6). Error bars represent SEM. (*) indicates $p < 0.05$ by Student's t-test for comparison between normal and Snell mice.

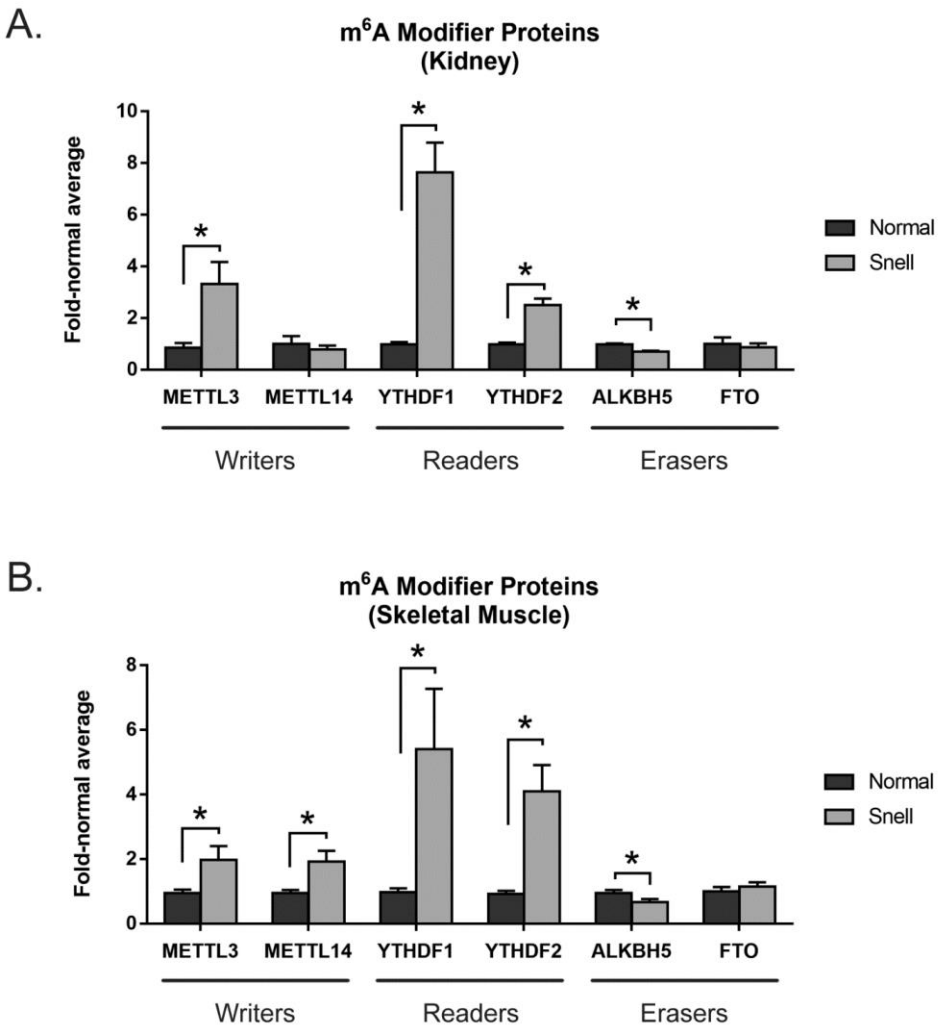

Figure 4.5 Protein levels of m^{6}A regulators in Snell kidney and skeletal muscle.

Kidney and skeletal muscle tissue samples from normal and Snell mice were analyzed for protein expression. (A) Protein levels in kidney and (B) skeletal muscle tissue samples are shown normalized to normal littermate controls. Mice were fasted 18 hours prior to dissection. Mean values are shown for each group (N=6). Error bars represent SEM. (*) indicates $p < 0.05$ by Student's t-test for comparison between normal and Snell mice.

4.6 Conclusions

In Snell fibroblasts, we noted elevated protein levels of NDRG1, MGMT, LONP1, TFAM, and PGC-1α (Fig. 4.1A, B). In contrast, corresponding mRNA levels were either lower than or comparable to those in normal controls (Fig. 4.1C). *In vivo*, similar to the expression pattern reported for the DNA repair proteins NDRG1 and MGMT (Dominick et al., 2017), we detected elevated protein levels of LONP1 and TFAM in Snell liver (Fig. 4.2A, B), without comparable increases in corresponding mRNA levels (4.2C). These observations suggested that protein expression of NDRG1, MGMT, LONP1, TFAM, and PGC-1α might be upregulated by a selective translation mechanism.

Transcripts bearing 5'UTR N^6-methyladenosine modifications can be translated by m^6A-mediated cap-independent translation (m^6A-CIT). We found that that m^6A "writers" METTL3 and METTL14, which mark target mRNAs for m^6A-CIT, and m^6A "readers" YTHDF1 and YTHDF2, which recognize m^6A marks and promote translation of m^6A-tagged mRNAs, are upregulated in liver, kidney, and skeletal muscle of Snell mice. In contrast, m^6A "erasers" ALKBH5 and FTO, which negatively regulate m^6A-CIT by removing m^6A marks, were either downregulated or not altered, indicating that elements that promote the m^6A-CIT pathway are upregulated in tissues of Snell mice (Fig. 4.4, 4.5).

The consensus motif which identifies putative targets of m^6A-CIT is found in 5'UTRs of *Ndrg1*, *Mgmt*, *Tfam*, *Lonp1*, and *Pgc-1α* mRNAs. We tested whether the levels of corresponding proteins are regulated by m^6A-CIT by knocking-down METTL3 in HEK 293 cells, and found that

protein levels of NDRG1, MGMT, and TFAM, but not of LONP1, are regulated by m^6A-CIT (Fig. 4.3).

Our findings indicate that m^6A-CIT is upregulated in long-lived Snell mice. In principle, upregulated m^6A-CIT might partly account for the elevated levels of NDRG1, MGMT, TFAM, and PGC-1α in Snell mice, however, further experiments are required to verify this suggestion.

4.7 Materials and methods

4.7.1 Mice

Snell dwarf and littermate control mice were produced and housed as explained in Chap 2. The mice were fasted for 18 hours prior to dissection. All experiments were performed in accordance with guidelines and regulations provided by the University of Michigan University Committee on Use and Care of Animals.

4.7.2 *METLL3* knock-down

HEK 293T cells were transfected with *shMETLL3* or control *shRNA* (Sigma, SHCLNG-NM_019852) using Lipofectamine 3000 transfection reagent (ThermoFisher, L3000) as described in the protocol provided by the manufacturer. Cell were collected for protein analysis 96 hours after transfection. Knock-down was confirmed by western blot analysis of METTL3 expression which showed 70% decrease in METTL3 protein levels.

4.7.3 Western blot and antibodies

Western blot analysis was performed as explained in Chap2; instead of cell pellets, powdered tissue samples were used to prepare the samples. In addition to those listed in Chap 2, the membranes were probed with primary antibodies NDRG1 (Cell Signaling, 9408), MGMT (MyBioSource, 9409314), LONP1 (Cell Signaling, 28020), TFAM (Origene, AP26439), METTL3

(Abcam, ab195352), METTL14 (Millipore, ABE1338), YTHDF1 (Origene, TA347608), YTHDF2 (Origene, TA331921), ALKBH5 (Millipore, ABE1013), and FTO (ThermoFisher, PA1-46310) at 1:1000 dilution and incubated for 18 hours at 4 °C with shaking.

4.7.4 RNA extraction and q-rtPCR

RNA extraction and q-rtPCR were performed as explained in Chap 2. For tissue analysis, powdered tissue samples, instead of cell pellets, were used to prepare the samples. The additional primers are listed below in the format described in the first row:

[Gene], [PubMed Gene ID], [Forward primer sequence], [Reverse primer sequence].

Ndrg1, 17988, cgagagctacatgacgtgga, aagaggggttgtagcaggt.

Mgmt, 17314, aaacactgaccccacagagg, aacacagggtgatggagagc.

° ° °

Methods for the isolation of primary fibroblasts, fibroblast cell culture, and statistical analysis were presented in Chap 2.

Chapter 5 - Discussion

5.1 Improved mitochondrial stress response in long-lived Snell dwarf mice

Compared to tests in lower organisms, life-span experiments on mice are more expensive and time consuming. Accordingly, only a small percentage of null mutations of interest are tested for their pro-longevity effects in mice. As a complementary approach, comparison of long-lived mice to matched controls focusing on specific molecular pathways can provide useful insights into the molecular mechanisms involved in increased mouse longevity. In this work, we used Snell dwarf mice to assess whether improved mtUPR is a feature of one of the longest-lived single-gene mutant mouse models.

5.1.1 Primary fibroblasts from Snell mice are resistant to mitochondrial stress

Higher resistance of primary fibroblasts isolated from Snell and Ames dwarf mice to cellular stressors such as UV light, heat, paraquat, hydrogen peroxide, and cadmium has been noted previously (Murakami et al., 2003; Salmon et al., 2005). Paraquat induces mtUPR in *C. elegans* (Yoneda et al., 2004). Hence, it is likely that increased resistance to paraquat may, in principle, stem partially from elevated mtUPR. Nevertheless, it has not been known whether fibroblasts from long-lived mutant mice exhibit improved resistance to mitochondrial stress.

We show that primary fibroblasts isolated from Snell mice are resistant to mitochondrial stress, specifically the effects of doxycycline on cell viability (Fig. 2.9A-B), cellular ATP content (Fig. 2.10A), and oxidative respiration (Fig. 2.12, 2.13A-B). Consistent with increased resistance to mitochondrial stress resistance, we detected elevated levels of mtUPR proteins HSP60 and LONP1 in Snell fibroblasts (Fig. 2.1, 2.2), despite comparable mitochondrial abundance in normal and Snell fibroblasts (Fig. 2.3, 2.4).

5.1.2 Snell cells exhibit elevated mtUPR independent of mitochondrial stress exposure

In comparison to normal fibroblasts, Snell fibroblasts exhibited elevated levels of mtUPR proteins even when the cells are not exposed to mitochondrial stress (Fig. 2.1-2, untreated cells; Fig 2.3). We considered the possibility that the process of fibroblast isolation or cell culture conditions might induce mitochondrial stress, and the difference in mtUPR levels might reflect a stronger stress response in Snell cells.

Cells respond to acute mitochondrial stress by transcriptional induction of *Hsp60* and *Hsp10*, which leads to increased protein synthesis (Martinus et al., 1996; Zhao et al., 2002). Without stress exposure, both *Hsp60* and *Hsp10* mRNA levels were almost the same in Snell and normal cells (Fig. 2.6A-B, untreated cells), suggesting that even if the cell culture conditions caused mtUPR induction, the effect did not differ between two groups. Interestingly, doxycycline exposure increased *Hsp60* and *Hsp10* mRNA levels ~2.2-fold and ~1.7 fold respectively, in *both* Snell and normal cells, indicating that mtUPR response at the transcriptional level was

comparable in the two groups (Fig. 2.6A-B). As transcriptional upregulation also caused an increase in the protein levels, HSP60 protein levels in Snell cells remained higher than those in normal cells (Fig. 2.1B). Taken together, these observations suggest that elevated HSP60 protein expression stems from either upregulated translation of *Hsp60* transcripts or an increase in the stability of HSP60, suggesting a permanent change in mtUPR protein regulation in Snell cells.

5.1.3 The mechanism underlying elevated mtUPR in Snell fibroblasts remains elusive

Our analyses in HEK 293 cells deficient in METTL3 expression suggest that, although *Lonp1* mRNA bears a 5'UTR consensus motif for m^6A modification, LONP1 protein synthesis is not regulated by m^6A-CIT in these cells (Fig. 4.3). It is possible that LONP1 synthesis in Snell mouse fibroblasts might be altered by their upregulated expression of METTL3 and METTL14, but our data do not address this directly. Our attempts to silence *Mettl3* expression in Snell fibroblasts by transfection were not successful. The possible role of m^6A-CIT in regulation of LONP1 protein levels in Snell fibroblasts can be assessed in future studies by knocking-down METTL3 expression using lentiviral transduction. For now, how Snell fibroblasts maintain elevated levels of HSP60 and LONP1 without an increase in corresponding mRNA levels remains elusive.

5.1.4 Tfam and Pgc-1α, indicators of mitochondrial biogenesis, are upregulated in response to mitochondrial stress in Snell fibroblasts

We found that, in response to mitochondrial stress exposure by doxycycline treatment, mRNA levels of *Pgc-1α*, the main regulator of mitochondrial biogenesis, were upregulated exclusively in Snell cells (Fig. 2.7 B). Snell-cell-specific induction of Pgc-1α was also detected at the protein level and was not specific to the agent used to induce mitochondrial stress (Fig 2.8A-B). Upregulation of genes involved in mitochondrial biogenesis in response to mitochondrial stress has not been reported previously. Indeed, in normal fibroblasts, we did not detect an increase in mRNA or protein levels of Pgc-1α upon mitochondrial stress exposure. Only in Snell cells did we see Pgc-1α upregulation after doxycycline and thiamphenicol treatments.

Our analysis, however, does not answer whether upregulation of *Pgc-1α* and *Tfam* expression is an important factor for increased mitochondrial stress resistance in Snell fibroblasts. Assessment of individual roles of HSP60, LONP1, TFAM and PGC-1α in mitochondrial stress resistance by knock-down protocols would be challenging, since these proteins are indispensable for cell function. It is plausible that the improved mitochondrial stress resistance observed in Snell cells may reflect the combined effects of mtUPR and mitochondrial biogenesis. The elevated mtUPR in Snell cells may decrease the response time to mitochondrial stress and minimize irreversible protein aggregation, while in parallel the mitochondrial pool may be replenished through concurrent upregulation of the mitochondrial biogenesis pathway.

5.1.5 Is mitophagy elevated in Snell cells?

Alternatively, Snell cells may have elevated mitochondrial turnover. In support of this idea, the ratio of mitochondrial protein synthesis rate to DNA synthesis rate is higher in Snell heart and muscle (Drake et al., 2015). Since we observe indications of elevated levels of mitochondrial biogenesis in doxycycline-treated Snell fibroblasts (Fig. 2.7) without a detectable increase in mitochondrial mass, the rate of mitochondrial clearance may be upregulated as well. It is likely that mitophagy plays an active role in restoring mitochondrial homeostasis after mitochondrial stress exposure in Snell cells.

Mitophagy is a term coined to describe selective degradation of mitochondria by autophagy (I. Kim, Rodriguez-Enriquez, & Lemasters, 2007). As opposed to mitochondrial biogenesis, mitophagy functions in the degradation of mitochondria to adjust mitochondrial abundance and in elimination of damaged mitochondria (Suen, Narendra, Tanaka, Manfredi, & Youle, 2010). Mitophagy and mitochondrial biogenesis are required to maintain steady-state mitochondrial turnover and mitochondrial function (Palacino et al., 2004; Stichel et al., 2007). Thus, the combined effects of elevated mitophagy and upregulated mitochondrial biogenesis may provide a possible mechanism for maintained mitochondrial function in Snell cells.

Mitophagy is preceded and promoted by mitochondrial fission, which divides long mitochondrial bodies into smaller pieces to be engulfed by autophagosomes, and also leads to isolation of damaged sections of individual mitochondria (Twig et al., 2008). This mechanism provides a measure to estimate the level of mitophagy. Cells and tissue samples can be fixed,

stained with mitochondria-specific markers, and examined under microscope to assess mitochondrial size and number. The presence of small globular mitochondria high in abundance in one group of cells, as opposed lower number of large, elongated mitochondria in another group of cells, would suggest that the cells in the first group are more likely to have activated mitophagy. Although mitochondrial morphology provides some clues on mitophagy, it is far from being conclusive, and requires additional measures for confirmation.

PARKIN is an E3 ubiquitin ligase (Shimura et al., 2000), the mutant form of which can cause early onset hereditary forms of Parkinson's disease (Kitada et al., 1998). Upon loss of mitochondrial inner membrane potential, PARKIN is recruited to the outer mitochondrial membrane (D. Narendra, Tanaka, Suen, & Youle, 2008), where it ubiquitinates mitochondrial substrates (Geisler et al., 2010). PARKIN-mediated ubiquitination is thought to serve as a marker for mitophagy-mediated recycling of mitochondria, since it is followed by degradation of target mitochondria (Geisler et al., 2010; Derek Narendra, Kane, Hauser, Fearnley, & Youle, 2010). Accordingly, PARKIN localization to mitochondria can be used as a marker of mitophagy initiation, and can be utilized as an additional indication of mitophagy in future studies to test whether mitophagy activity is elevated in tissues of Snell mice in comparison to those of normal mice.

One problem with this approach is that PARKIN localization may imply mitophagy initiation but does not guarantee complete execution of mitophagy-mediated mitochondrial degradation (Geisler et al., 2010). Therefore, microscopic analyses of mitochondrial morphology and PARKIN

localization should be utilized as pre-screening tools, and positive results should be followed up by the assessment of mitochondrial turnover, which can be measured by protein labeling and pulse-chase experiments as discussed in section 5.2.2.

5.1.6 Effects of GH/IGF-1 and TH signaling on PGC-1α expression

In keeping with data from Snell fibroblasts, we observed that *Pgc-1α* mRNA levels in Snell liver were 5-10-fold higher than those in normal controls (Fig. 3.1B). To a lesser extent, PGC-1α protein levels were also elevated in Snell liver (Fig 4.2A-B). Previously, elevated Pgc-1α expression was reported in liver and kidney of GHR-KO mice (Al-Regaiey et al., 2005; Gesing, Bartke, et al., 2011), which also have defective growth hormone signaling and show lifespan extension, suggesting that the mitochondrial biogenesis pathway may be regulated by GH/IGF-1 signaling. Supporting this idea, mice over-expressing GH show decreased Pgc-1α expression (Al-Regaiey et al., 2005).

GH/IGF-1 signaling promotes mTORC1 activity through the IGF-1R/PI3K/AKT pathway. Accordingly, Snell mice, which are deficient in GH/IGF-1, exhibit downregulated mTORC1 signaling. It is believed that mTORC1 activity promotes mitochondrial biogenesis by upregulating *Pgc-1α* (Cunningham et al., 2007; Laplante & Sabatini, 2013). Intriguingly, despite GH/IGF-1 deficiency and consequent downregulation of mTORC1 activity, Snell mice and GHR-KO mice still exhibit elevated *Pgc-1α* expression. Calorie restriction, which induces robust lifespan extension in wild-type mice, also upregulates PGC-1α protein levels in liver (Al-Regaiey

et al., 2005) despite a suppressive effect on mTORC1 activity. Thyroid hormone (TH) signaling, specifically 3,5,4'-triido-L-thyronine (T_3), upregulates both *Pgc-1α* (Weitzel, Radtke, & Seitz, 2001) and *Tfam* expression (Garstka, Facke, Escribano, & Wiesner, 1994). Although Snell mice are deficient in thyroid hormone secretion, they still have upregulated levels of *Pgc-1α*. Overall, these observations in long-lived mice suggest that neither TH nor mTORC1 activity is required for *Pgc-1α* or *Tfam* upregulation. It seems likely that Snell mice activate an alternative pathway independent of GH/IGF-1 and TH signaling to upregulate mitochondrial biogenesis, which might be essential for lifespan extension.

5.1.7 Snell mice show improved mtUPR induction in response to *in vivo* doxycycline treatment

The role of mitochondria on health and lifespan gained attention when unbiased RNAi screens in *C. elegans* showed that at least one third of the longevity-associated genes encoded proteins required for mitochondrial function (Hamilton et al., 2005; S. S. Lee et al., 2003). Upregulation of mtUPR emerged as a mechanism linking changes in the mitochondrial protein stoichiometry to nematode lifespan extension (Durieux et al., 2011). This view was further supported by the observation that over-expression of a single mtUPR gene was sufficient to extend life span in *C. elegans* (Yokoyama et al., 2002).

Mutations in gene encoding clock abnormal protein 1 (clk-1), a mitochondrial protein involved in ubiquinone biosynthesis, extends lifespan in *C. elegans*. *Mclk1+/-* mice deficient in *Mclk1*,

mouse ortholog of *clk-1*, also show lifespan extension. RNAi mediated inhibition of genes encoding subunits of the mitochondrial respiratory chain extends *C. elegans* lifespan (Hamilton et al., 2005; S. S. Lee et al., 2003). In mice, deletion of *Surf1*, a putative mitochondrial respiratory chain gene, also extends lifespan. Similar longevity effects of defective mitochondrial protein expression in *C. elegans* and mice suggest that lifespan extension in *Mclk1+/-* and *Surf1-/-* mice may be mediated by mtUPR. However, *in vivo* mtUPR levels are not investigated in either model. We observed that, while both basal and stress-induced mtUPR levels were elevated in primary fibroblasts isolated from Snell mice, *in vivo* mtUPR levels in Snell liver were higher than those in normal controls *only* after doxycycline-induced mitochondrial stress exposure (Fig 3.4). Assessment of mtUPR in *Mclk1+/-* and *Surf1-/-* mice, as well as in other long-lived mouse models – not only at the basal level, but also after acute mitochondrial stress exposure – may provide invaluable insights into the involvement of mtUPR in mammalian aging.

5.1.8 Snell mice might maintain respiration rates after stress exposure

In primary fibroblasts, we analyzed both mtUPR and mitochondrial function after exposure to mitochondrial stress. Elevated levels of mtUPR in Snell cells suggested that Snell cells might be resistant to mitochondrial stress. As expected, after doxycycline exposure, Snell cells preserved mitochondrial function as indicated by maintained ATP content and respiration rates compared to normal cells. Our *in vivo* analysis, which demonstrated 4-5-fold higher levels of mtUPR induction upon doxycycline treatment, suggests that Snell mice might also be protected from

mitochondrial stress at the organismal level. Although we have not addressed this suggestion in the current study, it warrants consideration for the future studies.

5.1.9 While mitochondrial damage increases, mtUPR weakens with age; improved mtUPR might help prevent the former

The first indications of age-related decline in mitochondrial health came from histological studies of human and rat tissue samples fifty years ago (Tauchi & Sato, 1968). Mitochondrial function declines in liver (Yen, Chen, King, Yeh, & Wei, 1989), heart, skeletal muscle (Short et al., 2005), kidney , and brain (Ojaimi, Masters, Opeskin, McKelvie, & Byrne, 1999) during aging, while mitochondrial stress increases through accumulation of defects such as mtDNA mutations (Corral-Debrinski et al., 1992; Yen, Su, King, & Wei, 1991), damaged mitochondrial proteins (Bakala et al., 2003), and loss of mitochondrial proteostasis (Benzi et al., 1992).

Despite an increase in the mitochondrial stress load during aging, a corresponding increase in the mtUPR has not been reported. On the contrary, LONP1 activity in rat liver is 49% lower in old animals (Bakala et al., 2003). In mouse skeletal muscle, *Lonp1* expression decreases with age (Bota, Van Remmen, & Davies, 2002), and this age-related decline can be totally prevented by caloric restriction at a level that extends rodent lifespan (C. K. Lee, Klopp, Weindruch, & Prolla, 1999). Recent evidence suggests that reversal of the age-related decline in mtUPR may prove beneficial for mammalian health: muscle stem cells from old mice show decreased expression of mtUPR genes *Hsp60* and *Hsp10*, and nicotinamide riboside treatment starting at

old age (22-24 month old), which reverses this decline in the mtUPR pathway, induces neurogenesis and increases mean lifespan of old mice (H. Zhang et al., 2016). Snell mice exhibit improved capacity to induce both HSP60 and LONP1 levels in response to acute mitochondrial stress (Fig 3.4D). Importantly, increased mtUPR induction, by doxycycline, is detected in young adult mice with the Snell mutation. As it precedes the onset of age-associated mitochondrial deteriorations, improved mtUPR might provide enhanced protection against mitochondrial stress and may have a role in healthspan extension in Snell mice.

Our results indicate improved mtUPR in the liver of Snell mice in response to doxycycline-induced mitochondrial stress and provide a rationale for future mouse lifespan experiments involving compounds, like doxycycline, that induce mtUPR. Preliminary data from ongoing experiments in our lab suggest that acute exposure of normal adult mice to mild mitochondrial stress by doxycycline-supplemented diet may induce an upregulation of genes found to be elevated in Snell mice, such as *Pgc-1α* (Data not shown). Further experiments are required to understand the effects of transient mitochondrial stress exposure in mammals.

5.1.10 Minocycline-treated mice

Minocycline, like doxycycline, is an antibiotic of the tetracycline family. Minocycline ($C_{23}H_{27}N_3O_7$) and doxycycline ($C_{22}H_{24}N_2O_8$) have similar molecular structures with four carbon rings (Fig. 5.1), and they both inhibit mitochondrial (and bacterial) translation by binding to the smaller subunit of the mitochondrial ribosome. Although it has not been demonstrated yet,

given its inhibitory effect on mitochondrial translation, it is highly likely that minocycline treatment induces mtUPR. Importantly, minocycline extends lifespan in *C. elegans* and *Drosophila*. The effect of minocycline on mouse lifespan is currently being tested as a part of Interventions Testing Program (ITP). This study may provide valuable insights into the role of the mtUPR in mammalian lifespan.

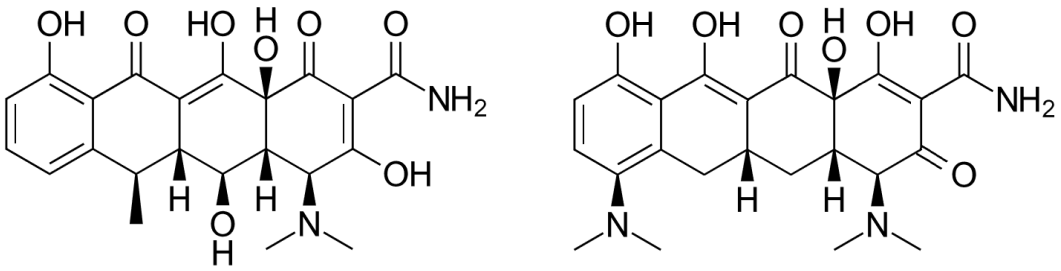

Figure 5.1 Molecular structures of doxycycline and minocycline

One of the possible outcomes, *i.e.* detection of prolonged lifespan in minocycline-treated mice in comparison to the control group, would support the hypothesis that inhibition of mitochondrial translation might extend mammalian lifespan. In this positive scenario, it would be of interest to investigate several endpoints to examine whether the longevity effect may be due to mtUPR upregulation, as in the case of *C. elegans*. Since tissue samples from minocycline treated mice will be available for follow up studies, the analysis of frozen tissue samples to measure basal mtUPR levels in minocycline-treated mice will be possible. However, one should be cautious against premature interpretation of such analyses depending solely on basal mtUPR levels. Our results from Snell mice demonstrate that long-lived mice may exhibit unaltered

levels of basal mtUPR and still have an improved capacity to induce mtUPR upon mitochondrial stress exposure. Accordingly, minocycline-treated mice should also be examined for their capacity to induce mtUPR, which would require preparation of an additional mouse colony of minocycline-treated and control mice for *in vivo* treatments. A possible experimental approach could be feeding 6-month old mice on minocycline/control diet for 6-12 months, followed by acute mitochondrial stress treatment (for example by 2-week doxycycline treatment) and measurement of mtUPR protein levels in tissue samples.

The other possible outcome, *i.e.* detection of no effect or a negative effect of minocycline treatment on mouse lifespan, would be equally informative. In this negative scenario, analysis of mito-nuclear protein stoichiometry and mtUPR levels in minocycline-treated mice would be critical for the interpretation of the results. If no alteration in basal or induced mtUPR levels is detected in the experimental group, then no conclusion can be made for the effect of mtUPR in mouse lifespan. It would merely indicate that minocycline treatment at the selected dose does not induce mtUPR in mice. On the other hand, if mtUPR is upregulated with no longevity effect, the interpretation would be complex and further analysis would be necessary to reach a conclusion. While it may well be the case that mtUPR upregulation does not prolong mouse lifespan, it is also possible that the minocycline dose might be too high so that consequent mitochondrial damage might not be reversed by mtUPR. Such an effect could be confirmed by a sharp decrease in mtDNA-encoded respiratory chain protein levels in minocycline-treated mice. Alternatively, chronic inhibition of mitochondrial translation - even if it is tolerated by the mitochondria - might gradually induce detrimental effects in tissues with high energy demand

such as brain and muscle. In these scenarios, where either the drug dose or the treatment length is not ideal, a modified lifespan study with a lower dose of minocycline, a shorter treatment period, or a treatment regimen with alternating periods of minocycline/mock treatments may be required to observe a prolongevity effect.

5.2 m^{6}A-mediated cap-independent translation in long-lived Snell mice

In this work, we presented evidence indicating that the m^{6}A-CIT pathway is upregulated in long-lived Snell dwarf mice. Previously, NDRG1 and MGMT, which are involved in DNA damage repair, were found to be upregulated in Snell liver (Dominick et al., 2017). We demonstrated that protein levels of NDRG1 and MGMT are regulated by m^{6}A-CIT in cultured HEK 293 cells, suggesting that m^{6}A-CIT may have a role in their upregulation in mouse tissues as well. In addition, our work on mitochondrial stress response in Snell mice revealed that elevation in protein levels of mitochondrial protease LONP1 are not accompanied by a comparable increase in *Lonp1* mRNA levels, suggesting that LONP1 protein levels might be upregulated by increased translation. Although *Lonp1* mRNA has a consensus motif for m^{6}A modification and is listed among putative m^{6}A-CIT targets, we were not able to detect an effect of *Mettl3* inhibition on LONP1 protein levels in HEK-293K cells, indicating that LONP1 is likely *not* regulated by m^{6}A-CIT at least in HEK cells. On the other hand, we confirmed that TFAM and PGC-1α are partly synthesized through m^{6}A-CIT. Hence m^{6}A-CIT may also have a role in upregulated levels of TFAM and PGC-1 in Snell liver.

5.2.1 Implications of the upregulated m^{6}A-CIT pathway in Snell mice

Discovery of m^{6}A-CIT is very recent. Although the presence of N^6-methyladenosine residues in eukaryotic mRNA has been known since seventies (Desrosiers et al., 1974; Perry & Kelley, 1974; Perry et al., 1975), their function remained elusive for the next forty years. The use of

transcriptome-wide high-throughput sequencing techniques developed in the new millennium revealed ubiquitous distribution of m^6A modifications along mRNA transcripts. m^6A marks are found in 5'UTR, exon, intron, and 3'UTR fragments of ~7K mature mRNA sequences in HeLa cells and mouse tissues (Dominissini et al., 2012; Meyer et al., 2012). However, the role for N^6-methyladenosine residues located in 5'UTRs of mRNAs in a hitherto unknown mechanism of cap-independent translation was discovered only three years ago, and led to the identification of N^6-methyladenosine-mediated cap-independent translation (Meyer et al., 2015; J. Zhou et al., 2015).

Implications of our findings indicating elevated m^6A-CIT in Snell mice are broader than its possible role in NDGR1, MGMT, TFAM, and PGC-1α expression. In principle, elevated m^6A-CIT activity may result in upregulation of thousands of additional putative targets of m^6A-CIT functioning a variety of pathways including heat shock response (J. Zhou et al., 2015). So far, aside from our data confirming NDRG1, MGMT, TFAM, and PGC-1α as m^6A-CIT targets, only HSP70 (J. Zhou et al., 2015) has been demonstrated to be synthesized through m^6A-CIT. As the list of confirmed m^6A-CIT targets grows in the future, so will the list of candidate proteins whose protein levels may be upregulated in long-lived Snell mice.

5.2.2 Increased protein stability as an alternative mechanism

Four out of five proteins for which we noted elevated protein levels in Snell mice without comparable levels of upregulation in mRNA levels (NDRG1, MGM1, TFAM, and LONP1) include

DRACH consensus motif in the 5'UTRs of the corresponding mRNA transcripts, suggesting that they are putative targets of m^6A-CIT (Linder et al., 2015; J. Zhou et al., 2015). Tempted by this fact, we focused on translational regulation as a candidate mechanism for the discrepancy noted between the protein and mRNA levels. However, our findings do not rule out alternative mechanisms, which deserve further attention.

One such mechanism involves a decrease in the rate of protein turnover. Select proteins in Snell mice may have longer half-lives, resulting in increased protein stability and higher protein/mRNA ratios, independent of translation. This hypothesis can be tested by protein labeling or chemical inhibition of translation. Radioactive isotopes are widely used for protein labeling. In this approach, the cells are incubated in a medium supplemented with amino acids containing radioactive isotopes, for example ^{35}S methionine. This step, where 35S methionine is incorporated into newly synthesized proteins, is followed by incubation of cells in fresh medium with non-labeled amino acids. The relative proportion of radioactively labeled proteins in cells collected at later time points depends on the protein stability. Proteins of interest can be immunoprecipitated and the ratio of radiolabeled proteins can be assessed by measurement of radioactivity, which positively correlates with protein stability, and negatively correlates with the rate of protein degradation. Analysis of normal and Snell cells by this method would allow comparison of relative stability of individual proteins in two cell populations.

Alternatively, chemical inhibition of translation, for example by cycloheximide treatment, followed by analysis of protein abundance at a later timepoint could reveal how fast a protein is

degraded. However, inhibition of translation might induce cellular stress, and result in transcriptional upregulation of stress genes such as *Lonp1*. Unless translation mechanism is blocked completely, transcriptional upregulation can increase protein abundance, making it harder to interpret the results. Simultaneous inhibition of both transcription and translation can be suggested, however, this might be toxic for cells, and induce unintended effects.

5.2.3 m^{6}A-CIT upregulation may be a shared feature of long-lived mutant mice

Following up on our work, Dr. Garcia investigated levels of proteins regulating m^{6}A-CIT pathway in two more long-lived mouse models. In summary, compared to control mice, both GHR-KO and PAPPA-KO mice exhibited elevated levels of m^{6}A writers (METTL3, METTL14) and readers (YTHDF1, YTHDF2), but either downregulated or unaltered levels of m^{6}A eraser proteins (ALKBH5, FTO) in liver, kidney, and skeletal muscle tissues, suggesting that m^{6}A-CIT upregulation is not limited to Snell mice (Ozkurede *et al*. *manuscript under review*).

5.2.4 Upregulation of m^{6}A-CIT might be induced by inhibition of cap-dependent translation

Inhibition of cap-dependent translation by the synthetic molecule 4EGI-1, which suppresses recruitment of the translation initiation complex to 5'-cap, induces upregulation of NDRG1, MGMT, TFAM, and PGC-1α both in primary fibroblasts and in liver of normal mice (Ozkurede *et al*. *manuscript under review*). Moreover, mRNA levels of the m^{6}A writer *Mettl3* are also upregulated after 4EGI-1 treatment, suggesting that m^{6}A-CIT pathway may be induced when

cap-independent translation is inhibited. Analysis of protein levels of m^6A-CIT regulators is required to test this idea, and is currently in progress.

5.3 Final remarks

I find it helpful to compare mitochondria to nuclear power plants. They both increase energy production enormously. However, they have to be maintained with extreme care. As defective mitochondria can lead to loss of a cell, a damaged nuclear power plant can devastate a whole city. Also, once a city develops relying on nuclear power as its main energy source, it cannot sustain itself without such an energy resource. The same is true for mitochondria. Mitochondria and nuclear power plants can harm the ecosystem they inhabit both when they misfunction and when they do not function at all. Accordingly, it is not surprising that cells have a specific mechanism to respond to mitochondrial stress, and that this mechanism is found to be enhanced in a long-lived mouse model.

While current findings suggest a positive correlation between mtUPR and mouse lifespan, there is a lot to be discovered before one can speculate on ways to enhance mtUPR to increase lifespan and improve health in mammals. How is mtUPR regulated? Is overexpression of a single component of mtUPR, such as, HSP60 is sufficient to increase mammalian lifespan? Can we fine-tune the expression levels of individual mtUPR proteins? Does elevated mtUPR have negative health effects? Is it more advantageous if mtUPR is upregulated temporarily or only in specific tissues?

Given the progress on mtUPR research during the first two decades following its discovery, there is enough reason to be optimistic that we will be able to answer many of these questions in the near future.

References

Aguiar-Oliveira, M. H., Oliveira, F. T., Pereira, R. M., Oliveira, C. R., Blackford, A., Valenca, E. H., . . . Salvatori, R. (2010). Longevity in untreated congenital growth hormone deficiency due to a homozygous mutation in the GHRH receptor gene. *J Clin Endocrinol Metab, 95*(2), 714-721. doi:10.1210/jc.2009-1879

Al-Regaiey, K. A., Masternak, M. M., Bonkowski, M., Sun, L., & Bartke, A. (2005). Long-lived growth hormone receptor knockout mice: interaction of reduced insulin-like growth factor i/insulin signaling and caloric restriction. *Endocrinology, 146*(2), 851-860. doi:10.1210/en.2004-1120

Altmann, R. (1890). *Die elementarorganismen und ihre beziehungen zu den zellen*. Leipzig,: Veit & comp.

Ames, B. N., Shigenaga, M. K., & Hagen, T. M. (1993). Oxidants, antioxidants, and the degenerative diseases of aging. *Proc Natl Acad Sci U S A, 90*(17), 7915-7922.

Andersen, B., Pearse, R. V., 2nd, Jenne, K., Sornson, M., Lin, S. C., Bartke, A., & Rosenfeld, M. G. (1995). The Ames dwarf gene is required for Pit-1 gene activation. *Dev Biol, 172*(2), 495-503.

Anderson, S., Bankier, A. T., Barrell, B. G., de Bruijn, M. H., Coulson, A. R., Drouin, J., . . . Young, I. G. (1981). Sequence and organization of the human mitochondrial genome. *Nature, 290*(5806), 457-465.

Anfinsen, C. B. (1973). Principles that govern the folding of protein chains. *Science, 181*(4096), 223-230.

Aquila, H., Misra, D., Eulitz, M., & Klingenberg, M. (1982). Complete amino acid sequence of the ADP/ATP carrier from beef heart mitochondria. *Hoppe Seylers Z Physiol Chem, 363*(3), 345-349.

Arany, Z., He, H., Lin, J., Hoyer, K., Handschin, C., Toka, O., . . . Spiegelman, B. M. (2005). Transcriptional coactivator PGC-1 alpha controls the energy state and contractile function of cardiac muscle. *Cell Metab, 1*(4), 259-271. doi:10.1016/j.cmet.2005.03.002

Bakala, H., Delaval, E., Hamelin, M., Bismuth, J., Borot-Laloi, C., Corman, B., & Friguet, B. (2003). Changes in rat liver mitochondria with aging. Lon protease-like reactivity and N(epsilon)-carboxymethyllysine accumulation in the matrix. *Eur J Biochem, 270*(10), 2295-2302.

Baltz, A. G., Munschauer, M., Schwanhausser, B., Vasile, A., Murakawa, Y., Schueler, M., . . . Landthaler, M. (2012). The mRNA-bound proteome and its global occupancy profile on protein-coding transcripts. *Mol Cell, 46*(5), 674-690. doi:10.1016/j.molcel.2012.05.021

Barsyte, D., Lovejoy, D. A., & Lithgow, G. J. (2001). Longevity and heavy metal resistance in daf-2 and age-1 long-lived mutants of Caenorhabditis elegans. *FASEB J, 15*(3), 627-634. doi:10.1096/fj.99-0966com

Bartke, A., & Brown-Borg, H. M. (2004). Life Extension in the Dwarf Mouse. In G. P. Schatten (Ed.), *Current Topics in Developmental Biology* (Vol. 63): Elsecier Inc.

Bashore, T. M., Magorien, D. J., Letterio, J., Shaffer, P., & Unverferth, D. V. (1987). Histologic and biochemical correlates of left ventricular chamber dynamics in man. *J Am Coll Cardiol, 9*(4), 734-742.

Benzi, G., Pastoris, O., Marzatico, F., Villa, R. F., Dagani, F., & Curti, D. (1992). The mitochondrial electron transfer alteration as a factor involved in the brain aging. *Neurobiol Aging, 13*(3), 361-368.

Bibb, M. J., Van Etten, R. A., Wright, C. T., Walberg, M. W., & Clayton, D. A. (1981). Sequence and gene organization of mouse mitochondrial DNA. *Cell, 26*(2 Pt 2), 167-180.

Bjedov, I., Toivonen, J. M., Kerr, F., Slack, C., Jacobson, J., Foley, A., & Partridge, L. (2010). Mechanisms of life span extension by rapamycin in the fruit fly Drosophila melanogaster. *Cell Metab, 11*(1), 35-46. doi:10.1016/j.cmet.2009.11.010

Boffoli, D., Scacco, S. C., Vergari, R., Solarino, G., Santacroce, G., & Papa, S. (1994). Decline with age of the respiratory chain activity in human skeletal muscle. *Biochim Biophys Acta, 1226*(1), 73-82.

Bokar, J. A., Rath-Shambaugh, M. E., Ludwiczak, R., Narayan, P., & Rottman, F. (1994). Characterization and partial purification of mRNA N6-adenosine methyltransferase from HeLa cell nuclei. Internal mRNA methylation requires a multisubunit complex. *J Biol Chem, 269*(26), 17697-17704.

Bokov, A. F., Garg, N., Ikeno, Y., Thakur, S., Musi, N., DeFronzo, R. A., . . . Richardson, A. (2011). Does reduced IGF-1R signaling in Igf1r+/- mice alter aging? *PLoS One, 6*(11), e26891. doi:10.1371/journal.pone.0026891

Borg, K. E., Brown-Borg, H. M., & Bartke, A. (1995). Assessment of the primary adrenal cortical and pancreatic hormone basal levels in relation to plasma glucose and age in the unstressed Ames dwarf mouse. *Proc Soc Exp Biol Med, 210*(2), 126-133.

Bota, D. A., Van Remmen, H., & Davies, K. J. (2002). Modulation of Lon protease activity and aconitase turnover during aging and oxidative stress. *FEBS Lett, 532*(1-2), 103-106.

Bowling, A. C., Mutisya, E. M., Walker, L. C., Price, D. L., Cork, L. C., & Beal, M. F. (1993). Age-dependent impairment of mitochondrial function in primate brain. *J Neurochem, 60*(5), 1964-1967.

Brand, M. D. (1990). The proton leak across the mitochondrial inner membrane. *Biochim Biophys Acta, 1018*(2-3), 128-133.

Brawerman, G., Mendecki, J., & Lee, S. Y. (1972). A procedure for the isolation of mammalian messenger ribonucleic acid. *Biochemistry, 11*(4), 637-641.

Brown-Borg, H. M., Borg, K. E., Meliska, C. J., & Bartke, A. (1996). Dwarf mice and the ageing process. *Nature, 384*(6604), 33. doi:10.1038/384033a0

Bulpitt, K. J., & Piko, L. (1984). Variation in the frequency of complex forms of mitochondrial DNA in different brain regions of senescent mice. *Brain Res, 300*(1), 41-48.

Carsner, R. L., & Rennels, E. G. (1960). Primary site of gene action in anterior pituitary dwarf mice. *Science, 131*(3403), 829.

Chandrashekar, V., & Bartke, A. (1993). Induction of endogenous insulin-like growth factor-I secretion alters the hypothalamic-pituitary-testicular function in growth hormone-deficient adult dwarf mice. *Biol Reprod, 48*(3), 544-551.

Chandrashekar, V., Dawson, C. R., Martin, E. R., Rocha, J. S., Bartke, A., & Kopchick, J. J. (2007). Age-related alterations in pituitary and testicular functions in long-lived growth hormone receptor gene-disrupted mice. *Endocrinology, 148*(12), 6019-6025. doi:10.1210/en.2007-0837

Chen, J. C., Warshaw, J. B., & Sanadi, D. R. (1972). Regulation of mitochondrial respiration in senescence. *J Cell Physiol, 80*(1), 141-148. doi:10.1002/jcp.1040800115

Clancy, M. J., Shambaugh, M. E., Timpte, C. S., & Bokar, J. A. (2002). Induction of sporulation in Saccharomyces cerevisiae leads to the formation of N6-methyladenosine in mRNA: a potential mechanism for the activity of the IME4 gene. *Nucleic Acids Res, 30*(20), 4509-4518.

Conover, C. A., & Bale, L. K. (2007). Loss of pregnancy-associated plasma protein A extends lifespan in mice. *Aging Cell, 6*(5), 727-729. doi:10.1111/j.1474-9726.2007.00328.x

Conover, C. A., Bale, L. K., Mader, J. R., Mason, M. A., Keenan, K. P., & Marler, R. J. (2010). Longevity and age-related pathology of mice deficient in pregnancy-associated plasma protein-A. *J Gerontol A Biol Sci Med Sci, 65*(6), 590-599. doi:10.1093/gerona/glq032

Coots, R. A., Liu, X. M., Mao, Y., Dong, L., Zhou, J., Wan, J., . . . Qian, S. B. (2017). m6A Facilitates eIF4F-Independent mRNA Translation. *Mol Cell*. doi:10.1016/j.molcel.2017.10.002

Corral-Debrinski, M., Horton, T., Lott, M. T., Shoffner, J. M., Beal, M. F., & Wallace, D. C. (1992). Mitochondrial DNA deletions in human brain: regional variability and increase with advanced age. *Nat Genet, 2*(4), 324-329. doi:10.1038/ng1292-324

Cortopassi, G. A., & Arnheim, N. (1990). Detection of a specific mitochondrial DNA deletion in tissues of older humans. *Nucleic Acids Res, 18*(23), 6927-6933.

Coschigano, K. T., Clemmons, D., Bellush, L. L., & Kopchick, J. J. (2000). Assessment of growth parameters and life span of GHR/BP gene-disrupted mice. *Endocrinology, 141*(7), 2608-2613. doi:10.1210/endo.141.7.7586

Coschigano, K. T., Holland, A. N., Riders, M. E., List, E. O., Flyvbjerg, A., & Kopchick, J. J. (2003). Deletion, but not antagonism, of the mouse growth hormone receptor results in severely decreased body weights, insulin, and insulin-like growth factor I levels and increased life span. *Endocrinology, 144*(9), 3799-3810. doi:10.1210/en.2003-0374

Cunningham, J. T., Rodgers, J. T., Arlow, D. H., Vazquez, F., Mootha, V. K., & Puigserver, P. (2007). mTOR controls mitochondrial oxidative function through a YY1-PGC-1alpha transcriptional complex. *Nature, 450*(7170), 736-740. doi:10.1038/nature06322

Darnell, J. E., Wall, R., & Tushinski, R. J. (1971). An adenylic acid-rich sequence in messenger RNA of HeLa cells and its possible relationship to reiterated sites in DNA. *Proc Natl Acad Sci U S A, 68*(6), 1321-1325.

Dell'agnello, C., Leo, S., Agostino, A., Szabadkai, G., Tiveron, C., Zulian, A., . . . Zeviani, M. (2007). Increased longevity and refractoriness to Ca(2+)-dependent neurodegeneration in Surf1 knockout mice. *Hum Mol Genet, 16*(4), 431-444. doi:10.1093/hmg/ddl477

Desrosiers, R., Friderici, K., & Rottman, F. (1974). Identification of methylated nucleosides in messenger RNA from Novikoff hepatoma cells. *Proc Natl Acad Sci U S A, 71*(10), 3971-3975.

Dominick, G., Berryman, D. E., List, E. O., Kopchick, J. J., Li, X., Miller, R. A., & Garcia, G. G. (2015). Regulation of mTOR activity in Snell dwarf and GH receptor gene-disrupted mice. *Endocrinology, 156*(2), 565-575. doi:10.1210/en.2014-1690

Dominick, G., Bowman, J., Li, X., Miller, R. A., & Garcia, G. G. (2017). mTOR regulates the expression of DNA damage response enzymes in long-lived Snell dwarf, GHRKO, and PAPPA-KO mice. *Aging Cell, 16*(1), 52-60. doi:10.1111/acel.12525

Dominissini, D., Moshitch-Moshkovitz, S., Schwartz, S., Salmon-Divon, M., Ungar, L., Osenberg, S., . . . Rechavi, G. (2012). Topology of the human and mouse m6A RNA methylomes revealed by m6A-seq. *Nature, 485*(7397), 201-206. doi:10.1038/nature11112

Drake, J. C., Miller, R. A., Miller, B. F., & Hamilton, K. L. (2015). Long-lived Snell dwarf mice display increased proteostatic mechanisms that are not dependent on decreased mTORC1 activity. *Aging Cell*. doi:10.1111/acel.12329

Duquesnoy, R. J. (1972). Immunodeficiency of the thymus-dependent system of the Ames dwarf mouse. *J Immunol, 108*(6), 1578-1590.

Durieux, J., Wolff, S., & Dillin, A. (2011). The cell-non-autonomous nature of electron transport chain-mediated longevity. *Cell, 144*(1), 79-91. doi:10.1016/j.cell.2010.12.016

Edmonds, M., Vaughan, M. H., Jr., & Nakazato, H. (1971). Polyadenylic acid sequences in the heterogeneous nuclear RNA and rapidly-labeled polyribosomal RNA of HeLa cells: possible evidence for a precursor relationship. *Proc Natl Acad Sci U S A, 68*(6), 1336-1340.

Eicher, E. M., & Beamer, W. G. (1976). Inherited ateliotic dwarfism in mice. Characteristics of the mutation, little, on chromosome 6. *J Hered, 67*(2), 87-91.

Ellis, J. (1987). Proteins as molecular chaperones. *Nature, 328*(6129), 378-379. doi:10.1038/328378a0

Ellis, R. J., & Minton, A. P. (2006). Protein aggregation in crowded environments. *Biol Chem, 387*(5), 485-497. doi:10.1515/bc.2006.064

Ernster, L., & Schatz, G. (1981). Mitochondria: a historical review. *J Cell Biol, 91*(3 Pt 2), 227s-255s.

Fabrizio, P., Pozza, F., Pletcher, S. D., Gendron, C. M., & Longo, V. D. (2001). Regulation of longevity and stress resistance by Sch9 in yeast. *Science, 292*(5515), 288-290. doi:10.1126/science.1059497

Feng, J., Bussiere, F., & Hekimi, S. (2001). Mitochondrial electron transport is a key determinant of life span in Caenorhabditis elegans. *Dev Cell, 1*(5), 633-644.

Finley, L. W., Lee, J., Souza, A., Desquiret-Dumas, V., Bullock, K., Rowe, G. C., . . . Haigis, M. C. (2012). Skeletal muscle transcriptional coactivator PGC-1alpha mediates mitochondrial, but not metabolic, changes during calorie restriction. *Proc Natl Acad Sci U S A, 109*(8), 2931-2936. doi:10.1073/pnas.1115813109

Fischer, J., Koch, L., Emmerling, C., Vierkotten, J., Peters, T., Bruning, J. C., & Ruther, U. (2009). Inactivation of the Fto gene protects from obesity. *Nature, 458*(7240), 894-898. doi:10.1038/nature07848

Fisher, R. P., & Clayton, D. A. (1988). Purification and characterization of human mitochondrial transcription factor 1. *Mol Cell Biol, 8*(8), 3496-3509.

Fisher, R. P., Topper, J. N., & Clayton, D. A. (1987). Promoter selection in human mitochondria involves binding of a transcription factor to orientation-independent upstream regulatory elements. *Cell, 50*(2), 247-258.

Fleury, C., Neverova, M., Collins, S., Raimbault, S., Champigny, O., Levi-Meyrueis, C., . . . Warden, C. H. (1997). Uncoupling protein-2: a novel gene linked to obesity and hyperinsulinemia. *Nat Genet, 15*(3), 269-272. doi:10.1038/ng0397-269

Flurkey, K., Astle, C. M., & Harrison, D. E. (2010). Life extension by diet restriction and N-acetyl-L-cysteine in genetically heterogeneous mice. *J Gerontol A Biol Sci Med Sci, 65*(12), 1275-1284. doi:10.1093/gerona/glq155

Flurkey, K., Papaconstantinou, J., Miller, R. A., & Harrison, D. E. (2001). Lifespan extension and delayed immune and collagen aging in mutant mice with defects in growth hormone production. *Proc Natl Acad Sci U S A, 98*(12), 6736-6741. doi:10.1073/pnas.111158898

Garami, A., Zwartkruis, F. J., Nobukuni, T., Joaquin, M., Roccio, M., Stocker, H., . . . Thomas, G. (2003). Insulin activation of Rheb, a mediator of mTOR/S6K/4E-BP signaling, is inhibited by TSC1 and 2. *Mol Cell, 11*(6), 1457-1466.

Garstka, H. L., Facke, M., Escribano, J. R., & Wiesner, R. J. (1994). Stoichiometry of mitochondrial transcripts and regulation of gene expression by mitochondrial transcription factor A. *Biochem Biophys Res Commun, 200*(1), 619-626. doi:10.1006/bbrc.1994.1493

Geisler, S., Holmstrom, K. M., Skujat, D., Fiesel, F. C., Rothfuss, O. C., Kahle, P. J., & Springer, W. (2010). PINK1/Parkin-mediated mitophagy is dependent on VDAC1 and p62/SQSTM1. *Nat Cell Biol, 12*(2), 119-131. doi:10.1038/ncb2012

Gerken, T., Girard, C. A., Tung, Y. C., Webby, C. J., Saudek, V., Hewitson, K. S., . . . Schofield, C. J. (2007). The obesity-associated FTO gene encodes a 2-oxoglutarate-dependent nucleic acid demethylase. *Science, 318*(5855), 1469-1472. doi:10.1126/science.1151710

Gesing, A., Bartke, A., Wang, F., Karbownik-Lewinska, M., & Masternak, M. M. (2011). Key regulators of mitochondrial biogenesis are increased in kidneys of growth hormone receptor knockout (GHRKO) mice. *Cell Biochem Funct, 29*(6), 459-467. doi:10.1002/cbf.1773

Gesing, A., Masternak, M. M., Wang, F., Joseph, A. M., Leeuwenburgh, C., Westbrook, R., . . . Bartke, A. (2011). Expression of key regulators of mitochondrial biogenesis in growth hormone receptor knockout (GHRKO) mice is enhanced but is not further improved by other potential life-extending interventions. *J Gerontol A Biol Sci Med Sci, 66*(10), 1062-1076. doi:10.1093/gerona/glr080

Gimeno, R. E., Dembski, M., Weng, X., Deng, N., Shyjan, A. W., Gimeno, C. J., . . . Tartaglia, L. A. (1997). Cloning and characterization of an uncoupling protein homolog: a potential molecular mediator of human thermogenesis. *Diabetes, 46*(5), 900-906.

Godfrey, P., Rahal, J. O., Beamer, W. G., Copeland, N. G., Jenkins, N. A., & Mayo, K. E. (1993). GHRH receptor of little mice contains a missense mutation in the extracellular domain that disrupts receptor function. *Nat Genet, 4*(3), 227-232. doi:10.1038/ng0793-227

Guevara-Aguirre, J., Balasubramanian, P., Guevara-Aguirre, M., Wei, M., Madia, F., Cheng, C. W., . . . Longo, V. D. (2011). Growth hormone receptor deficiency is associated with a major reduction in pro-aging signaling, cancer, and diabetes in humans. *Sci Transl Med, 3*(70), 70ra13. doi:10.1126/scitranslmed.3001845

Gustafsson, C. M., Falkenberg, M., & Larsson, N. G. (2016). Maintenance and Expression of Mammalian Mitochondrial DNA. *Annu Rev Biochem, 85*, 133-160. doi:10.1146/annurev-biochem-060815-014402

Gwinn, D. M., Shackelford, D. B., Egan, D. F., Mihaylova, M. M., Mery, A., Vasquez, D. S., . . . Shaw, R. J. (2008). AMPK phosphorylation of raptor mediates a metabolic checkpoint. *Mol Cell, 30*(2), 214-226. doi:10.1016/j.molcel.2008.03.003

Haines, D. C., Chattopadhyay, S., & Ward, J. M. (2001). Pathology of aging B6;129 mice. *Toxicol Pathol, 29*(6), 653-661. doi:10.1080/019262301753385988

Hamilton, B., Dong, Y., Shindo, M., Liu, W., Odell, I., Ruvkun, G., & Lee, S. S. (2005). A systematic RNAi screen for longevity genes in C. elegans. *Genes Dev, 19*(13), 1544-1555. doi:10.1101/gad.1308205

Hansson, A., Hance, N., Dufour, E., Rantanen, A., Hultenby, K., Clayton, D. A., . . . Larsson, N. G. (2004). A switch in metabolism precedes increased mitochondrial biogenesis in respiratory chain-deficient mouse hearts. *Proc Natl Acad Sci U S A, 101*(9), 3136-3141. doi:10.1073/pnas.0308710100

Harman, D. (1956). Aging: a theory based on free radical and radiation chemistry. *J Gerontol, 11*(3), 298-300.

Harper, J. E., Miceli, S. M., Roberts, R. J., & Manley, J. L. (1990). Sequence specificity of the human mRNA N6-adenosine methylase in vitro. *Nucleic Acids Res, 18*(19), 5735-5741.

Harrison, D. E., Strong, R., Fernandez, E., & Miller, R. A. (2009). Rapamycin fed late in life extends lifespan in genetically heterogeneous mice. *Nature, 460*(7253), 392-395. doi:10.1038/nature08221

Hartl, F. U. (1996). Molecular chaperones in cellular protein folding. *Nature, 381*(6583), 571-579. doi:10.1038/381571a0

Havugimana, P. C., Hart, G. T., Nepusz, T., Yang, H., Turinsky, A. L., Li, Z., . . . Emili, A. (2012). A census of human soluble protein complexes. *Cell, 150*(5), 1068-1081. doi:10.1016/j.cell.2012.08.011

Hayakawa, M., Torii, K., Sugiyama, S., Tanaka, M., & Ozawa, T. (1991). Age-associated accumulation of 8-hydroxydeoxyguanosine in mitochondrial DNA of human diaphragm. *Biochem Biophys Res Commun, 179*(2), 1023-1029.

Heaton, G. M., Wagenvoord, R. J., Kemp, A., Jr., & Nicholls, D. G. (1978). Brown-adipose-tissue mitochondria: photoaffinity labelling of the regulatory site of energy dissipation. *Eur J Biochem, 82*(2), 515-521.

Heitman, J., Movva, N. R., & Hall, M. N. (1991). Targets for cell cycle arrest by the immunosuppressant rapamycin in yeast. *Science, 253*(5022), 905-909.

Hempenstall, S., Page, M. M., Wallen, K. R., & Selman, C. (2012). Dietary restriction increases skeletal muscle mitochondrial respiration but not mitochondrial content in C57BL/6 mice. *Mech Ageing Dev, 133*(1), 37-45. doi:10.1016/j.mad.2011.12.002

Hendrick, J. P., & Hartl, F. U. (1993). Molecular chaperone functions of heat-shock proteins. *Annu Rev Biochem, 62*, 349-384. doi:10.1146/annurev.bi.62.070193.002025

Holzenberger, M., Dupont, J., Ducos, B., Leneuve, P., Geloen, A., Even, P. C., . . . Le Bouc, Y. (2003). IGF-1 receptor regulates lifespan and resistance to oxidative stress in mice. *Nature, 421*(6919), 182-187. doi:10.1038/nature01298

Hongay, C. F., & Orr-Weaver, T. L. (2011). Drosophila Inducer of MEiosis 4 (IME4) is required for Notch signaling during oogenesis. *Proc Natl Acad Sci U S A, 108*(36), 14855-14860. doi:10.1073/pnas.1111577108

Houthoofd, K., Braeckman, B. P., Lenaerts, I., Brys, K., De Vreese, A., Van Eygen, S., & Vanfleteren, J. R. (2002). No reduction of metabolic rate in food restricted Caenorhabditis elegans. *Exp Gerontol, 37*(12), 1359-1369.

Houtkooper, R. H., Mouchiroud, L., Knott, G., Williams, R. W., & Auwerx, J. (2013). Mitonuclear protein imbalance as a conserved longevity mechanism. *Nature, 497*(7450), 451-457. doi:10.1038/nature12188

Hu, D., Cao, P., Thiels, E., Chu, C. T., Wu, G. Y., Oury, T. D., & Klann, E. (2007). Hippocampal long-term potentiation, memory, and longevity in mice that overexpress mitochondrial superoxide dismutase. *Neurobiol Learn Mem, 87*(3), 372-384. doi:10.1016/j.nlm.2006.10.003

Hunter, W. S., Croson, W. B., Bartke, A., Gentry, M. V., & Meliska, C. J. (1999). Low body temperature in long-lived Ames dwarf mice at rest and during stress. *Physiol Behav, 67*(3), 433-437.

Jang, Y. C., Perez, V. I., Song, W., Lustgarten, M. S., Salmon, A. B., Mele, J., . . . Richardson, A. (2009). Overexpression of Mn superoxide dismutase does not increase life span in mice. *J Gerontol A Biol Sci Med Sci, 64*(11), 1114-1125. doi:10.1093/gerona/glp100

Jia, G., Fu, Y., Zhao, X., Dai, Q., Zheng, G., Yang, Y., . . . He, C. (2011). N6-methyladenosine in nuclear RNA is a major substrate of the obesity-associated FTO. *Nat Chem Biol, 7*(12), 885-887. doi:10.1038/nchembio.687

Jia, G., Yang, C. G., Yang, S., Jian, X., Yi, C., Zhou, Z., & He, C. (2008). Oxidative demethylation of 3-methylthymine and 3-methyluracil in single-stranded DNA and RNA by mouse and human FTO. *FEBS Lett, 582*(23-24), 3313-3319. doi:10.1016/j.febslet.2008.08.019

Jia, K., Chen, D., & Riddle, D. L. (2004). The TOR pathway interacts with the insulin signaling pathway to regulate C. elegans larval development, metabolism and life span. *Development, 131*(16), 3897-3906. doi:10.1242/dev.01255

Kapahi, P., Zid, B. M., Harper, T., Koslover, D., Sapin, V., & Benzer, S. (2004). Regulation of lifespan in Drosophila by modulation of genes in the TOR signaling pathway. *Curr Biol, 14*(10), 885-890. doi:10.1016/j.cub.2004.03.059

Kennedy, E. P., & Lehninger, A. L. (1949). Oxidation of fatty acids and tricarboxylic acid cycle intermediates by isolated rat liver mitochondria. *J Biol Chem, 179*(2), 957-972.

Kenyon, C., Chang, J., Gensch, E., Rudner, A., & Tabtiang, R. (1993). A C. elegans mutant that lives twice as long as wild type. *Nature, 366*(6454), 461-464. doi:10.1038/366461a0

Kim, D. H., Sarbassov, D. D., Ali, S. M., King, J. E., Latek, R. R., Erdjument-Bromage, H., . . . Sabatini, D. M. (2002). mTOR interacts with raptor to form a nutrient-sensitive complex that signals to the cell growth machinery. *Cell, 110*(2), 163-175.

Kim, I., Rodriguez-Enriquez, S., & Lemasters, J. J. (2007). Selective degradation of mitochondria by mitophagy. *Arch Biochem Biophys, 462*(2), 245-253. doi:10.1016/j.abb.2007.03.034

Kim, Y. E., Hipp, M. S., Bracher, A., Hayer-Hartl, M., & Hartl, F. U. (2013). Molecular chaperone functions in protein folding and proteostasis. *Annu Rev Biochem, 82*, 323-355. doi:10.1146/annurev-biochem-060208-092442

Kinney, B. A., Coschigano, K. T., Kopchick, J. J., Steger, R. W., & Bartke, A. (2001). Evidence that age-induced decline in memory retention is delayed in growth hormone resistant GH-R-KO (Laron) mice. *Physiol Behav, 72*(5), 653-660.

Kitada, T., Asakawa, S., Hattori, N., Matsumine, H., Yamamura, Y., Minoshima, S., . . . Shimizu, N. (1998). Mutations in the parkin gene cause autosomal recessive juvenile parkinsonism. *Nature, 392*(6676), 605-608. doi:10.1038/33416

Klass, M., & Hirsh, D. (1976). Non-ageing developmental variant of Caenorhabditis elegans. *Nature, 260*(5551), 523-525.

Klass, M. R. (1977). Aging in the nematode Caenorhabditis elegans: major biological and environmental factors influencing life span. *Mech Ageing Dev, 6*(6), 413-429.

Klass, M. R. (1983). A method for the isolation of longevity mutants in the nematode Caenorhabditis elegans and initial results. *Mech Ageing Dev, 22*(3-4), 279-286.

Klein, A. H., Jenkins, J. J., Reviczky, A., & Fisher, D. A. (1981). Thyroid hormone-sensitive brown adipose tissue respiration in the newborn rabbit. *Am J Physiol, 241*(6), E449-453. doi:10.1152/ajpendo.1981.241.6.E449

Ku, H. H., Brunk, U. T., & Sohal, R. S. (1993). Relationship between mitochondrial superoxide and hydrogen peroxide production and longevity of mammalian species. *Free Radic Biol Med, 15*(6), 621-627.

Kujoth, G. C., Hiona, A., Pugh, T. D., Someya, S., Panzer, K., Wohlgemuth, S. E., . . . Prolla, T. A. (2005). Mitochondrial DNA mutations, oxidative stress, and apoptosis in mammalian aging. *Science, 309*(5733), 481-484. doi:10.1126/science.1112125

Laplante, M., & Sabatini, D. M. (2013). Regulation of mTORC1 and its impact on gene expression at a glance. *J Cell Sci, 126*(Pt 8), 1713-1719. doi:10.1242/jcs.125773

Lapointe, J., & Hekimi, S. (2008). Early mitochondrial dysfunction in long-lived Mclk1+/- mice. *J Biol Chem, 283*(38), 26217-26227. doi:10.1074/jbc.M803287200

Laron, Z. (2004). Laron syndrome (primary growth hormone resistance or insensitivity): the personal experience 1958-2003. *J Clin Endocrinol Metab, 89*(3), 1031-1044. doi:10.1210/jc.2003-031033

Larsen, P. L. (1993). Aging and resistance to oxidative damage in Caenorhabditis elegans. *Proc Natl Acad Sci U S A, 90*(19), 8905-8909.

Larsson, N. G., Wang, J., Wilhelmsson, H., Oldfors, A., Rustin, P., Lewandoski, M., . . . Clayton, D. A. (1998). Mitochondrial transcription factor A is necessary for mtDNA maintenance and embryogenesis in mice. *Nat Genet, 18*(3), 231-236. doi:10.1038/ng0398-231

Lee, C. K., Klopp, R. G., Weindruch, R., & Prolla, T. A. (1999). Gene expression profile of aging and its retardation by caloric restriction. *Science, 285*(5432), 1390-1393.

Lee, S. S., Lee, R. Y., Fraser, A. G., Kamath, R. S., Ahringer, J., & Ruvkun, G. (2003). A systematic RNAi screen identifies a critical role for mitochondria in C. elegans longevity. *Nat Genet, 33*(1), 40-48. doi:10.1038/ng1056

Lee, S. Y., Mendecki, J., & Brawerman, G. (1971). A polynucleotide segment rich in adenylic acid in the rapidly-labeled polyribosomal RNA component of mouse sarcoma 180 ascites cells. *Proc Natl Acad Sci U S A, 68*(6), 1331-1335.

Lehman, J. J., Barger, P. M., Kovacs, A., Saffitz, J. E., Medeiros, D. M., & Kelly, D. P. (2000). Peroxisome proliferator-activated receptor gamma coactivator-1 promotes cardiac mitochondrial biogenesis. *J Clin Invest, 106*(7), 847-856. doi:10.1172/jci10268

Leone, T. C., Lehman, J. J., Finck, B. N., Schaeffer, P. J., Wende, A. R., Boudina, S., . . . Kelly, D. P. (2005). PGC-1alpha deficiency causes multi-system energy metabolic derangements: muscle dysfunction, abnormal weight control and hepatic steatosis. *PLoS Biol, 3*(4), e101. doi:10.1371/journal.pbio.0030101

Levavasseur, F., Miyadera, H., Sirois, J., Tremblay, M. L., Kita, K., Shoubridge, E., & Hekimi, S. (2001). Ubiquinone is necessary for mouse embryonic development but is not essential for mitochondrial respiration. *J Biol Chem, 276*(49), 46160-46164. doi:10.1074/jbc.M108980200

Levin, E. D., Brady, T. C., Hochrein, E. C., Oury, T. D., Jonsson, L. M., Marklund, S. L., & Crapo, J. D. (1998). Molecular manipulations of extracellular superoxide dismutase: functional importance for learning. *Behav Genet, 28*(5), 381-390.

Levin, E. D., Christopher, N. C., & Crapo, J. D. (2005). Memory decline of aging reduced by extracellular superoxide dismutase overexpression. *Behav Genet, 35*(4), 447-453. doi:10.1007/s10519-004-1510-y

Levin, E. D., Christopher, N. C., Lateef, S., Elamir, B. M., Patel, M., Liang, L. P., & Crapo, J. D. (2002). Extracellular superoxide dismutase overexpression protects against aging-induced cognitive impairment in mice. *Behav Genet, 32*(2), 119-125.

Li, H., Wang, J., Wilhelmsson, H., Hansson, A., Thoren, P., Duffy, J., . . . Larsson, N. G. (2000). Genetic modification of survival in tissue-specific knockout mice with mitochondrial cardiomyopathy. *Proc Natl Acad Sci U S A, 97*(7), 3467-3472.

Li, S., Crenshaw, E. B., 3rd, Rawson, E. J., Simmons, D. M., Swanson, L. W., & Rosenfeld, M. G. (1990). Dwarf locus mutants lacking three pituitary cell types result from mutations in the POU-domain gene pit-1. *Nature, 347*(6293), 528-533.

Lin, C. S., Hackenberg, H., & Klingenberg, E. M. (1980). The uncoupling protein from brown adipose tissue mitochondria is a dimer. A hydrodynamic study. *FEBS Lett, 113*(2), 304-306.

Lin, J., Wu, H., Tarr, P. T., Zhang, C. Y., Wu, Z., Boss, O., . . . Spiegelman, B. M. (2002). Transcriptional co-activator PGC-1 alpha drives the formation of slow-twitch muscle fibres. *Nature, 418*(6899), 797-801. doi:10.1038/nature00904

Lin, S. J., Kaeberlein, M., Andalis, A. A., Sturtz, L. A., Defossez, P. A., Culotta, V. C., . . . Guarente, L. (2002). Calorie restriction extends Saccharomyces cerevisiae lifespan by increasing respiration. *Nature, 418*(6895), 344-348. doi:10.1038/nature00829

Lindberg, O., de Pierre, J., Rylander, E., & Afzelius, B. A. (1967). Studies of the mitochondrial energy-transfer system of brown adipose tissue. *J Cell Biol, 34*(1), 293-310.

Linder, B., Grozhik, A. V., Olarerin-George, A. O., Meydan, C., Mason, C. E., & Jaffrey, S. R. (2015). Single-nucleotide-resolution mapping of m6A and m6Am throughout the transcriptome. *Nat Methods, 12*(8), 767-772. doi:10.1038/nmeth.3453

Lithgow, G. J., White, T. M., Hinerfeld, D. A., & Johnson, T. E. (1994). Thermotolerance of a long-lived mutant of Caenorhabditis elegans. *J Gerontol, 49*(6), B270-276.

Liu, J., Yue, Y., Han, D., Wang, X., Fu, Y., Zhang, L., . . . He, C. (2014). A METTL3-METTL14 complex mediates mammalian nuclear RNA N6-adenosine methylation. *Nat Chem Biol, 10*(2), 93-95. doi:10.1038/nchembio.1432

Maheshwari, H. G., Silverman, B. L., Dupuis, J., & Baumann, G. (1998). Phenotype and genetic analysis of a syndrome caused by an inactivating mutation in the growth hormone-releasing hormone receptor: Dwarfism of Sindh. *J Clin Endocrinol Metab, 83*(11), 4065-4074. doi:10.1210/jcem.83.11.5226

Martinus, R. D., Garth, G. P., Webster, T. L., Cartwright, P., Naylor, D. J., Hoj, P. B., & Hoogenraad, N. J. (1996). Selective induction of mitochondrial chaperones in response to loss of the mitochondrial genome. *Eur J Biochem, 240*(1), 98-103.

Masternak, M. M., Bartke, A., Wang, F., Spong, A., Gesing, A., Fang, Y., . . . Westbrook, R. (2012). Metabolic effects of intra-abdominal fat in GHRKO mice. *Aging Cell, 11*(1), 73-81. doi:10.1111/j.1474-9726.2011.00763.x

Masters, B. S., Stohl, L. L., & Clayton, D. A. (1987). Yeast mitochondrial RNA polymerase is homologous to those encoded by bacteriophages T3 and T7. *Cell, 51*(1), 89-99.

Mecocci, P., MacGarvey, U., Kaufman, A. E., Koontz, D., Shoffner, J. M., Wallace, D. C., & Beal, M. F. (1993). Oxidative damage to mitochondrial DNA shows marked age-dependent increases in human brain. *Ann Neurol, 34*(4), 609-616. doi:10.1002/ana.410340416

Menon, V., Zhi, X., Hossain, T., Bartke, A., Spong, A., Gesing, A., & Masternak, M. M. (2014). The contribution of visceral fat to improved insulin signaling in Ames dwarf mice. *Aging Cell, 13*(3), 497-506. doi:10.1111/acel.12201

Meyer, K. D., Patil, D. P., Zhou, J., Zinoviev, A., Skabkin, M. A., Elemento, O., . . . Jaffrey, S. R. (2015). 5' UTR m(6)A Promotes Cap-Independent Translation. *Cell, 163*(4), 999-1010. doi:10.1016/j.cell.2015.10.012

Meyer, K. D., Saletore, Y., Zumbo, P., Elemento, O., Mason, C. E., & Jaffrey, S. R. (2012). Comprehensive analysis of mRNA methylation reveals enrichment in 3' UTRs and near stop codons. *Cell, 149*(7), 1635-1646. doi:10.1016/j.cell.2012.05.003

Miller, R. A., Buehner, G., Chang, Y., Harper, J. M., Sigler, R., & Smith-Wheelock, M. (2005). Methionine-deficient diet extends mouse lifespan, slows immune and lens aging, alters glucose, T4, IGF-I and insulin levels, and increases hepatocyte MIF levels and stress resistance. *Aging Cell, 4*(3), 119-125. doi:10.1111/j.1474-9726.2005.00152.x

Miller, R. A., Harrison, D. E., Astle, C. M., Baur, J. A., Boyd, A. R., de Cabo, R., . . . Strong, R. (2011). Rapamycin, but not resveratrol or simvastatin, extends life span of genetically

heterogeneous mice. *J Gerontol A Biol Sci Med Sci, 66*(2), 191-201. doi:10.1093/gerona/glq178

Mitchell, P. (1961). Coupling of phosphorylation to electron and hydrogen transfer by a chemi-osmotic type of mechanism. *Nature, 191*, 144-148.

Mitchell, P. (1968). *Chemiosmotic coupling and energy transduction*: Bodmin (Cornwall).

Morozov, Y. I., Agaronyan, K., Cheung, A. C., Anikin, M., Cramer, P., & Temiakov, D. (2014). A novel intermediate in transcription initiation by human mitochondrial RNA polymerase. *Nucleic Acids Res, 42*(6), 3884-3893. doi:10.1093/nar/gkt1356

Moullan, N., Mouchiroud, L., Wang, X., Ryu, D., Williams, E. G., Mottis, A., . . . Auwerx, J. (2015). Tetracyclines Disturb Mitochondrial Function across Eukaryotic Models: A Call for Caution in Biomedical Research. *Cell Rep*. doi:10.1016/j.celrep.2015.02.034

Muller-Hocker, J. (1990). Cytochrome c oxidase deficient fibres in the limb muscle and diaphragm of man without muscular disease: an age-related alteration. *J Neurol Sci, 100*(1-2), 14-21.

Muller-Hocker, J., Schneiderbanger, K., Stefani, F. H., & Kadenbach, B. (1992). Progressive loss of cytochrome c oxidase in the human extraocular muscles in ageing--a cytochemical-immunohistochemical study. *Mutat Res, 275*(3-6), 115-124.

Munscher, C., Muller-Hocker, J., & Kadenbach, B. (1993). Human aging is associated with various point mutations in tRNA genes of mitochondrial DNA. *Biol Chem Hoppe Seyler, 374*(12), 1099-1104.

Munscher, C., Rieger, T., Muller-Hocker, J., & Kadenbach, B. (1993). The point mutation of mitochondrial DNA characteristic for MERRF disease is found also in healthy people of different ages. *FEBS Lett, 317*(1-2), 27-30.

Murakami, S., & Johnson, T. E. (1996). A genetic pathway conferring life extension and resistance to UV stress in Caenorhabditis elegans. *Genetics, 143*(3), 1207-1218.

Murakami, S., Salmon, A., & Miller, R. A. (2003). Multiplex stress resistance in cells from long-lived dwarf mice. *FASEB J, 17*(11), 1565-1566. doi:10.1096/fj.02-1092fje

Nakazato, H., & Edmonds, M. (1972). The isolation and purification of rapidly labeled polysome-bound ribonucleic acid on polythymidylate cellulose. *J Biol Chem, 247*(10), 3365-3367.

Narayan, P., Ludwiczak, R. L., Goodwin, E. C., & Rottman, F. M. (1994). Context effects on N6-adenosine methylation sites in prolactin mRNA. *Nucleic Acids Res, 22*(3), 419-426.

Narendra, D., Kane, L. A., Hauser, D. N., Fearnley, I. M., & Youle, R. J. (2010). p62/SQSTM1 is required for Parkin-induced mitochondrial clustering but not mitophagy; VDAC1 is dispensable for both. *Autophagy, 6*(8), 1090-1106. doi:10.4161/auto.6.8.13426

Narendra, D., Tanaka, A., Suen, D. F., & Youle, R. J. (2008). Parkin is recruited selectively to impaired mitochondria and promotes their autophagy. *J Cell Biol, 183*(5), 795-803. doi:10.1083/jcb.200809125

Ngo, H. B., Kaiser, J. T., & Chan, D. C. (2011). The mitochondrial transcription and packaging factor Tfam imposes a U-turn on mitochondrial DNA. *Nat Struct Mol Biol, 18*(11), 1290-1296. doi:10.1038/nsmb.2159

Nisoli, E., Tonello, C., Cardile, A., Cozzi, V., Bracale, R., Tedesco, L., . . . Carruba, M. O. (2005). Calorie restriction promotes mitochondrial biogenesis by inducing the expression of eNOS. *Science, 310*(5746), 314-317. doi:10.1126/science.1117728

Nobes, C. D., Brown, G. C., Olive, P. N., & Brand, M. D. (1990). Non-ohmic proton conductance of the mitochondrial inner membrane in hepatocytes. *J Biol Chem, 265*(22), 12903-12909.

Nohl, H., & Hegner, D. (1978). Do mitochondria produce oxygen radicals in vivo? *Eur J Biochem, 82*(2), 563-567.

Nojima, A., Yamashita, M., Yoshida, Y., Shimizu, I., Ichimiya, H., Kamimura, N., . . . Minamino, T. (2013). Haploinsufficiency of akt1 prolongs the lifespan of mice. *PLoS One, 8*(7), e69178. doi:10.1371/journal.pone.0069178

Ojaimi, J., Masters, C. L., Opeskin, K., McKelvie, P., & Byrne, E. (1999). Mitochondrial respiratory chain activity in the human brain as a function of age. *Mech Ageing Dev, 111*(1), 39-47.

Page, M. M., Salmon, A. B., Leiser, S. F., Robb, E. L., Brown, M. F., Miller, R. A., & Stuart, J. A. (2009). Mechanisms of stress resistance in Snell dwarf mouse fibroblasts: enhanced antioxidant and DNA base excision repair capacity, but no differences in mitochondrial metabolism. *Free Radic Biol Med, 46*(8), 1109-1118. doi:10.1016/j.freeradbiomed.2009.01.014

Pagliarini, D. J., & Rutter, J. (2013). Hallmarks of a new era in mitochondrial biochemistry. *Genes Dev, 27*(24), 2615-2627. doi:10.1101/gad.229724.113

Palacino, J. J., Sagi, D., Goldberg, M. S., Krauss, S., Motz, C., Wacker, M., . . . Shen, J. (2004). Mitochondrial dysfunction and oxidative damage in parkin-deficient mice. *J Biol Chem, 279*(18), 18614-18622. doi:10.1074/jbc.M401135200

Pelham, H. R. (1986). Speculations on the functions of the major heat shock and glucose-regulated proteins. *Cell, 46*(7), 959-961.

Perier, C., Tieu, K., Guegan, C., Caspersen, C., Jackson-Lewis, V., Carelli, V., . . . Vila, M. (2005). Complex I deficiency primes Bax-dependent neuronal apoptosis through mitochondrial oxidative damage. *Proc Natl Acad Sci U S A, 102*(52), 19126-19131. doi:10.1073/pnas.0508215102

Perry, R. P., & Kelley, D. E. (1974). Existence of methylated messenger RNA in mouse L cells. *Cell, 1*(1), 37-42.

Perry, R. P., Kelley, D. E., Friderici, K., & Rottman, F. (1975). The methylated constituents of L cell messenger RNA: evidence for an unusual cluster at the 5' terminus. *Cell, 4*(4), 387-394.

Peters, T., Ausmeier, K., & Ruther, U. (1999). Cloning of Fatso (Fto), a novel gene deleted by the Fused toes (Ft) mouse mutation. *Mamm Genome, 10*(10), 983-986.

Pharaoh, G., Pulliam, D., Hill, S., Sataranatarajan, K., & Van Remmen, H. (2016). Ablation of the mitochondrial complex IV assembly protein Surf1 leads to increased expression of the UPR(MT) and increased resistance to oxidative stress in primary cultures of fibroblasts. *Redox Biol, 8*, 430-438. doi:10.1016/j.redox.2016.05.001

Pickering, A. M., Lehr, M., Gendron, C. M., Pletcher, S. D., & Miller, R. A. (2017). Mitochondrial thioredoxin reductase 2 is elevated in long-lived primate as well as rodent species and extends fly mean lifespan. *Aging Cell, 16*(4), 683-692. doi:10.1111/acel.12596

Pickering, A. M., Lehr, M., Kohler, W. J., Han, M. L., & Miller, R. A. (2014). Fibroblasts From Longer-Lived Species of Primates, Rodents, Bats, Carnivores, and Birds Resist Protein Damage. *J Gerontol A Biol Sci Med Sci*. doi:10.1093/gerona/glu115

Pickering, A. M., Lehr, M., & Miller, R. A. (2015). Lifespan of mice and primates correlates with immunoproteasome expression. *J Clin Invest, 125*(5), 2059-2068. doi:10.1172/jci80514

Piko, L., Bulpitt, K. J., & Meyer, R. (1984). Structural and replicative forms of mitochondrial DNA in tissues from adult and senescent BALB/c mice and Fischer 344 rats. *Mech Ageing Dev, 26*(1), 113-131.

Piko, L., Hougham, A. J., & Bulpitt, K. J. (1988). Studies of sequence heterogeneity of mitochondrial DNA from rat and mouse tissues: evidence for an increased frequency of deletions/additions with aging. *Mech Ageing Dev, 43*(3), 279-293.

Ping, X. L., Sun, B. F., Wang, L., Xiao, W., Yang, X., Wang, W. J., . . . Yang, Y. G. (2014). Mammalian WTAP is a regulatory subunit of the RNA N6-methyladenosine methyltransferase. *Cell Res, 24*(2), 177-189. doi:10.1038/cr.2014.3

Powers, R. W., 3rd, Kaeberlein, M., Caldwell, S. D., Kennedy, B. K., & Fields, S. (2006). Extension of chronological life span in yeast by decreased TOR pathway signaling. *Genes Dev, 20*(2), 174-184. doi:10.1101/gad.1381406

Preston, C. C., Oberlin, A. S., Holmuhamedov, E. L., Gupta, A., Sagar, S., Syed, R. H., . . . Jahangir, A. (2008). Aging-induced alterations in gene transcripts and functional activity of mitochondrial oxidative phosphorylation complexes in the heart. *Mech Ageing Dev, 129*(6), 304-312. doi:10.1016/j.mad.2008.02.010

Puigserver, P., Wu, Z., Park, C. W., Graves, R., Wright, M., & Spiegelman, B. M. (1998). A cold-inducible coactivator of nuclear receptors linked to adaptive thermogenesis. *Cell, 92*(6), 829-839.

Richter, C., Park, J. W., & Ames, B. N. (1988). Normal oxidative damage to mitochondrial and nuclear DNA is extensive. *Proc Natl Acad Sci U S A, 85*(17), 6465-6467.

Robida-Stubbs, S., Glover-Cutter, K., Lamming, D. W., Mizunuma, M., Narasimhan, S. D., Neumann-Haefelin, E., . . . Blackwell, T. K. (2012). TOR signaling and rapamycin influence longevity by regulating SKN-1/Nrf and DAF-16/FoxO. *Cell Metab, 15*(5), 713-724. doi:10.1016/j.cmet.2012.04.007

Rubio-Cosials, A., Sidow, J. F., Jimenez-Menendez, N., Fernandez-Millan, P., Montoya, J., Jacobs, H. T., . . . Sola, M. (2011). Human mitochondrial transcription factor A induces a U-turn structure in the light strand promoter. *Nat Struct Mol Biol, 18*(11), 1281-1289. doi:10.1038/nsmb.2160

Rudman, D., Feller, A. G., Nagraj, H. S., Gergans, G. A., Lalitha, P. Y., Goldberg, A. F., . . . Mattson, D. E. (1990). Effects of human growth hormone in men over 60 years old. *N Engl J Med, 323*(1), 1-6. doi:10.1056/nejm199007053230101

Salmon, A. B., Murakami, S., Bartke, A., Kopchick, J., Yasumura, K., & Miller, R. A. (2005). Fibroblast cell lines from young adult mice of long-lived mutant strains are resistant to multiple forms of stress. *Am J Physiol Endocrinol Metab, 289*(1), E23-29. doi:10.1152/ajpendo.00575.2004

Salvatori, R., Hayashida, C. Y., Aguiar-Oliveira, M. H., Phillips, J. A., 3rd, Souza, A. H., Gondo, R. G., . . . Levine, M. A. (1999). Familial dwarfism due to a novel mutation of the growth hormone-releasing hormone receptor gene. *J Clin Endocrinol Metab, 84*(3), 917-923. doi:10.1210/jcem.84.3.5599

Salway, K. D., Gallagher, E. J., Page, M. M., & Stuart, J. A. (2011). Higher levels of heat shock proteins in longer-lived mammals and birds. *Mech Ageing Dev, 132*(6-7), 287-297. doi:10.1016/j.mad.2011.06.002

Sanchez-Pulido, L., & Andrade-Navarro, M. A. (2007). The FTO (fat mass and obesity associated) gene codes for a novel member of the non-heme dioxygenase superfamily. *BMC Biochem, 8*, 23. doi:10.1186/1471-2091-8-23

Schatz, G., Haslbrunner, E., & Tuppy, H. (1964). DEOXYRIBONUCLEIC ACID ASSOCIATED WITH YEAST MITOCHONDRIA. *Biochem Biophys Res Commun, 15*(2), 127-132.

Schibler, U., Kelley, D. E., & Perry, R. P. (1977). Comparison of methylated sequences in messenger RNA and heterogeneous nuclear RNA from mouse L cells. *J Mol Biol, 115*(4), 695-714.

Schriner, S. E., Linford, N. J., Martin, G. M., Treuting, P., Ogburn, C. E., Emond, M., . . . Rabinovitch, P. S. (2005). Extension of murine life span by overexpression of catalase targeted to mitochondria. *Science, 308*(5730), 1909-1911. doi:10.1126/science.1106653

Schwartz, S., Agarwala, S. D., Mumbach, M. R., Jovanovic, M., Mertins, P., Shishkin, A., . . . Regev, A. (2013). High-resolution mapping reveals a conserved, widespread, dynamic mRNA methylation program in yeast meiosis. *Cell, 155*(6), 1409-1421. doi:10.1016/j.cell.2013.10.047

Sehgal, S. N., Baker, H., & Vezina, C. (1975). Rapamycin (AY-22,989), a new antifungal antibiotic. II. Fermentation, isolation and characterization. *J Antibiot (Tokyo), 28*(10), 727-732.

Selman, C., Partridge, L., & Withers, D. J. (2011). Replication of extended lifespan phenotype in mice with deletion of insulin receptor substrate 1. *PLoS One, 6*(1), e16144. doi:10.1371/journal.pone.0016144

Selman, C., Tullet, J. M., Wieser, D., Irvine, E., Lingard, S. J., Choudhury, A. I., . . . Withers, D. J. (2009). Ribosomal protein S6 kinase 1 signaling regulates mammalian life span. *Science, 326*(5949), 140-144. doi:10.1126/science.1177221

Sharp, Z. D., & Bartke, A. (2005). Evidence for down-regulation of phosphoinositide 3-kinase/Akt/mammalian target of rapamycin (PI3K/Akt/mTOR)-dependent translation regulatory signaling pathways in Ames dwarf mice. *J Gerontol A Biol Sci Med Sci, 60*(3), 293-300.

Sheldon, R., Jurale, C., & Kates, J. (1972). Detection of polyadenylic acid sequences in viral and eukaryotic RNA(polu(U)-cellulose columns-poly(U) filters-fiberglass-HeLa cells-bacteriophage T4). *Proc Natl Acad Sci U S A, 69*(2), 417-421.

Shimura, H., Hattori, N., Kubo, S., Mizuno, Y., Asakawa, S., Minoshima, S., . . . Suzuki, T. (2000). Familial Parkinson disease gene product, parkin, is a ubiquitin-protein ligase. *Nat Genet, 25*(3), 302-305. doi:10.1038/77060

Shokolenko, I. N., & Alexeyev, M. F. (2017). Mitochondrial transcription in mammalian cells. *Front Biosci (Landmark Ed), 22*, 835-853.

Short, K. R., Bigelow, M. L., Kahl, J., Singh, R., Coenen-Schimke, J., Raghavakaimal, S., & Nair, K. S. (2005). Decline in skeletal muscle mitochondrial function with aging in humans. *Proc Natl Acad Sci U S A, 102*(15), 5618-5623. doi:10.1073/pnas.0501559102

Shutt, T. E., Lodeiro, M. F., Cotney, J., Cameron, C. E., & Shadel, G. S. (2010). Core human mitochondrial transcription apparatus is a regulated two-component system in vitro. *Proc Natl Acad Sci U S A, 107*(27), 12133-12138. doi:10.1073/pnas.0910581107

Silva, J. P., Kohler, M., Graff, C., Oldfors, A., Magnuson, M. A., Berggren, P. O., & Larsson, N. G. (2000). Impaired insulin secretion and beta-cell loss in tissue-specific knockout mice with mitochondrial diabetes. *Nat Genet, 26*(3), 336-340. doi:10.1038/81649

Simmons, D. M., Voss, J. W., Ingraham, H. A., Holloway, J. M., Broide, R. S., Rosenfeld, M. G., & Swanson, L. W. (1990). Pituitary cell phenotypes involve cell-specific Pit-1 mRNA translation and synergistic interactions with other classes of transcription factors. *Genes Dev, 4*(5), 695-711.

Snell, G. D. (1929). DWARF, A NEW MENDELIAN RECESSIVE CHARACTER OF THE HOUSE MOUSE. *Proc Natl Acad Sci U S A, 15*(9), 733-734.

Sohal, R. S., & Dubey, A. (1994). Mitochondrial oxidative damage, hydrogen peroxide release, and aging. *Free Radic Biol Med, 16*(5), 621-626.

Sohal, R. S., & Sohal, B. H. (1991). Hydrogen peroxide release by mitochondria increases during aging. *Mech Ageing Dev, 57*(2), 187-202.

Sohal, R. S., Svensson, I., & Brunk, U. T. (1990). Hydrogen peroxide production by liver mitochondria in different species. *Mech Ageing Dev, 53*(3), 209-215.

Sohal, R. S., Svensson, I., Sohal, B. H., & Brunk, U. T. (1989). Superoxide anion radical production in different animal species. *Mech Ageing Dev, 49*(2), 129-135.

Sologub, M., Litonin, D., Anikin, M., Mustaev, A., & Temiakov, D. (2009). TFB2 is a transient component of the catalytic site of the human mitochondrial RNA polymerase. *Cell, 139*(5), 934-944. doi:10.1016/j.cell.2009.10.031

Soong, N. W., Hinton, D. R., Cortopassi, G., & Arnheim, N. (1992). Mosaicism for a specific somatic mitochondrial DNA mutation in adult human brain. *Nat Genet, 2*(4), 318-323. doi:10.1038/ng1292-318

Sorensen, L., Ekstrand, M., Silva, J. P., Lindqvist, E., Xu, B., Rustin, P., . . . Larsson, N. G. (2001). Late-onset corticohippocampal neurodepletion attributable to catastrophic failure of oxidative phosphorylation in MILON mice. *J Neurosci, 21*(20), 8082-8090.

Soukas, A. A., Kane, E. A., Carr, C. E., Melo, J. A., & Ruvkun, G. (2009). Rictor/TORC2 regulates fat metabolism, feeding, growth, and life span in Caenorhabditis elegans. *Genes Dev, 23*(4), 496-511. doi:10.1101/gad.1775409

Stanley, B. A., Sivakumaran, V., Shi, S., McDonald, I., Lloyd, D., Watson, W. H., . . . Paolocci, N. (2011). Thioredoxin reductase-2 is essential for keeping low levels of H(2)O(2) emission from isolated heart mitochondria. *J Biol Chem, 286*(38), 33669-33677. doi:10.1074/jbc.M111.284612

Starling, R. C., Hammer, D. F., & Altschuld, R. A. (1998). Human myocardial ATP content and in vivo contractile function. *Mol Cell Biochem, 180*(1-2), 171-177.

Stichel, C. C., Zhu, X. R., Bader, V., Linnartz, B., Schmidt, S., & Lubbert, H. (2007). Mono- and double-mutant mouse models of Parkinson's disease display severe mitochondrial damage. *Hum Mol Genet, 16*(20), 2377-2393. doi:10.1093/hmg/ddm083

Suen, D. F., Narendra, D. P., Tanaka, A., Manfredi, G., & Youle, R. J. (2010). Parkin overexpression selects against a deleterious mtDNA mutation in heteroplasmic cybrid cells. *Proc Natl Acad Sci U S A, 107*(26), 11835-11840. doi:10.1073/pnas.0914569107

Sun, L., Sadighi Akha, A. A., Miller, R. A., & Harper, J. M. (2009). Life-span extension in mice by preweaning food restriction and by methionine restriction in middle age. *J Gerontol A Biol Sci Med Sci, 64*(7), 711-722. doi:10.1093/gerona/glp051

Sun, L. Y., Spong, A., Swindell, W. R., Fang, Y., Hill, C., Huber, J. A., . . . Bartke, A. (2013). Growth hormone-releasing hormone disruption extends lifespan and regulates response to caloric restriction in mice. *Elife, 2*, e01098. doi:10.7554/eLife.01098

Tatar, M., Kopelman, A., Epstein, D., Tu, M. P., Yin, C. M., & Garofalo, R. S. (2001). A mutant Drosophila insulin receptor homolog that extends life-span and impairs neuroendocrine function. *Science, 292*(5514), 107-110. doi:10.1126/science.1057987

Tauchi, H., & Sato, T. (1968). Age changes in size and number of mitochondria of human hepatic cells. *J Gerontol, 23*(4), 454-461.

Torii, K., Sugiyama, S., Takagi, K., Satake, T., & Ozawa, T. (1992). Age-related decrease in respiratory muscle mitochondrial function in rats. *Am J Respir Cell Mol Biol, 6*(1), 88-92. doi:10.1165/ajrcmb/6.1.88

Trifunovic, A., Hansson, A., Wredenberg, A., Rovio, A. T., Dufour, E., Khvorostov, I., . . . Larsson, N. G. (2005). Somatic mtDNA mutations cause aging phenotypes without affecting reactive oxygen species production. *Proc Natl Acad Sci U S A, 102*(50), 17993-17998. doi:10.1073/pnas.0508886102

Trifunovic, A., Wredenberg, A., Falkenberg, M., Spelbrink, J. N., Rovio, A. T., Bruder, C. E., . . . Larsson, N. G. (2004). Premature ageing in mice expressing defective mitochondrial DNA polymerase. *Nature, 429*(6990), 417-423. doi:10.1038/nature02517

Tsang, W. Y., Sayles, L. C., Grad, L. I., Pilgrim, D. B., & Lemire, B. D. (2001). Mitochondrial respiratory chain deficiency in Caenorhabditis elegans results in developmental arrest and increased life span. *J Biol Chem, 276*(34), 32240-32246. doi:10.1074/jbc.M103999200

Twig, G., Elorza, A., Molina, A. J., Mohamed, H., Wikstrom, J. D., Walzer, G., . . . Shirihai, O. S. (2008). Fission and selective fusion govern mitochondrial segregation and elimination by autophagy. *Embo j, 27*(2), 433-446. doi:10.1038/sj.emboj.7601963

van Buul-Offers, S. C., Bloemen, R. J., Reijnen-Gresnigt, M. G., van Leiden, H. A., Hoogerbrugge, C. M., & Van den Brande, J. L. (1994). Insulin-like growth factors-I and -II and their binding proteins during postnatal development of dwarf Snell mice before and during growth hormone and thyroxine therapy. *J Endocrinol, 143*(1), 191-198.

van der Hoeven, F., Schimmang, T., Volkmann, A., Mattei, M. G., Kyewski, B., & Ruther, U. (1994). Programmed cell death is affected in the novel mouse mutant Fused toes (Ft). *Development, 120*(9), 2601-2607.

Vergara, M., Smith-Wheelock, M., Harper, J. M., Sigler, R., & Miller, R. A. (2004). Hormone-treated snell dwarf mice regain fertility but remain long lived and disease resistant. *J Gerontol A Biol Sci Med Sci, 59*(12), 1244-1250.

Vezina, C., Kudelski, A., & Sehgal, S. N. (1975). Rapamycin (AY-22,989), a new antifungal antibiotic. I. Taxonomy of the producing streptomycete and isolation of the active principle. *J Antibiot (Tokyo), 28*(10), 721-726.

Walker, W. H., & Singer, T. P. (1970). Identification of the covalently bound flavin of succinate dehydrogenase as 8-alpha-(histidyl) flavin adenine dinucleotide. *J Biol Chem, 245*(16), 4224-4225.

Wang, M., & Miller, R. A. (2012a). Augmented autophagy pathways and MTOR modulation in fibroblasts from long-lived mutant mice. *Autophagy, 8*(8), 1273-1274. doi:10.4161/auto.20917

Wang, M., & Miller, R. A. (2012b). Fibroblasts from long-lived mutant mice exhibit increased autophagy and lower TOR activity after nutrient deprivation or oxidative stress. *Aging Cell, 11*(4), 668-674. doi:10.1111/j.1474-9726.2012.00833.x

Wang, X., Lu, Z., Gomez, A., Hon, G. C., Yue, Y., Han, D., . . . He, C. (2014). N6-methyladenosine-dependent regulation of messenger RNA stability. *Nature, 505*(7481), 117-120. doi:10.1038/nature12730

Wang, X., Zhao, B. S., Roundtree, I. A., Lu, Z., Han, D., Ma, H., . . . He, C. (2015). N(6)-methyladenosine Modulates Messenger RNA Translation Efficiency. *Cell, 161*(6), 1388-1399. doi:10.1016/j.cell.2015.05.014

Wang, Y., Li, Y., Toth, J. I., Petroski, M. D., Zhang, Z., & Zhao, J. C. (2014). N6-methyladenosine modification destabilizes developmental regulators in embryonic stem cells. *Nat Cell Biol, 16*(2), 191-198. doi:10.1038/ncb2902

Weitzel, J. M., Radtke, C., & Seitz, H. J. (2001). Two thyroid hormone-mediated gene expression patterns in vivo identified by cDNA expression arrays in rat. *Nucleic Acids Res, 29*(24), 5148-5155.

Wilson, D. B., & Wyatt, D. P. (1986a). Immunocytochemistry of TSH cells during development of the dwarf mutant mouse. *Anat Embryol (Berl), 174*(2), 277-282.

Wilson, D. B., & Wyatt, D. P. (1986b). Ultrastructural immunocytochemistry of somatotrophs and mammotrophs in embryos of the dwarf mutant mouse. *Anat Rec, 215*(3), 282-287. doi:10.1002/ar.1092150311

Wredenberg, A., Wibom, R., Wilhelmsson, H., Graff, C., Wiener, H. H., Burden, S. J., . . . Larsson, N. G. (2002). Increased mitochondrial mass in mitochondrial myopathy mice. *Proc Natl Acad Sci U S A, 99*(23), 15066-15071. doi:10.1073/pnas.232591499

Wu, J. J., Liu, J., Chen, E. B., Wang, J. J., Cao, L., Narayan, N., . . . Finkel, T. (2013). Increased mammalian lifespan and a segmental and tissue-specific slowing of aging after genetic reduction of mTOR expression. *Cell Rep, 4*(5), 913-920. doi:10.1016/j.celrep.2013.07.030

Wu, Z., Puigserver, P., Andersson, U., Zhang, C., Adelmant, G., Mootha, V., . . . Spiegelman, B. M. (1999). Mechanisms controlling mitochondrial biogenesis and respiration through the thermogenic coactivator PGC-1. *Cell, 98*(1), 115-124. doi:10.1016/s0092-8674(00)80611-x

Yen, T. C., Chen, Y. S., King, K. L., Yeh, S. H., & Wei, Y. H. (1989). Liver mitochondrial respiratory functions decline with age. *Biochem Biophys Res Commun, 165*(3), 944-1003.

Yen, T. C., Su, J. H., King, K. L., & Wei, Y. H. (1991). Ageing-associated 5 kb deletion in human liver mitochondrial DNA. *Biochem Biophys Res Commun, 178*(1), 124-131.

Yokoyama, K., Fukumoto, K., Murakami, T., Harada, S., Hosono, R., Wadhwa, R., . . . Ohkuma, S. (2002). Extended longevity of Caenorhabditis elegans by knocking in extra copies of hsp70F, a homolog of mot-2 (mortalin)/mthsp70/Grp75. *FEBS Lett, 516*(1-3), 53-57.

Yoneda, T., Benedetti, C., Urano, F., Clark, S. G., Harding, H. P., & Ron, D. (2004). Compartment-specific perturbation of protein handling activates genes encoding mitochondrial chaperones. *J Cell Sci, 117*(Pt 18), 4055-4066. doi:10.1242/jcs.01275

Zhang, C., & Darnell, R. B. (2011). Mapping in vivo protein-RNA interactions at single-nucleotide resolution from HITS-CLIP data. *Nat Biotechnol, 29*(7), 607-614. doi:10.1038/nbt.1873

Zhang, H., Ryu, D., Menzies, K. J., & Auwerx, J. (2016). NAD(+) repletion improves mitochondrial and stem cell function and enhances life span in mice. *Science, 352*(6292), 1436-1443. doi:10.1126/science.aaf2693

Zhao, Q., Wang, J., Levichkin, I. V., Stasinopoulos, S., Ryan, M. T., & Hoogenraad, N. J. (2002). A mitochondrial specific stress response in mammalian cells. *Embo j, 21*(17), 4411-4419.

Zheng, G., Dahl, J. A., Niu, Y., Fedorcsak, P., Huang, C. M., Li, C. J., . . . He, C. (2013). ALKBH5 is a mammalian RNA demethylase that impacts RNA metabolism and mouse fertility. *Mol Cell, 49*(1), 18-29. doi:10.1016/j.molcel.2012.10.015

Zhong, S., Li, H., Bodi, Z., Button, J., Vespa, L., Herzog, M., & Fray, R. G. (2008). MTA is an Arabidopsis messenger RNA adenosine methylase and interacts with a homolog of a sex-specific splicing factor. *Plant Cell, 20*(5), 1278-1288. doi:10.1105/tpc.108.058883

Zhou, J., Wan, J., Gao, X., Zhang, X., Jaffrey, S. R., & Qian, S. B. (2015). Dynamic m(6)A mRNA methylation directs translational control of heat shock response. *Nature, 526*(7574), 591-594. doi:10.1038/nature15377

Zhou, Y., Xu, B. C., Maheshwari, H. G., He, L., Reed, M., Lozykowski, M., . . . Kopchick, J. J. (1997). A mammalian model for Laron syndrome produced by targeted disruption of the mouse growth hormone receptor/binding protein gene (the Laron mouse). *Proc Natl Acad Sci U S A, 94*(24), 13215-13220.